LABORATOIRE EUROPEEN POUR LA PHYSIQUE DES PARTICULES
CERN EUROPEAN LABORATORY FOR PARTICLE PHYSICS

CERN/SPSC 99-8
SPSC/P 310
17 March 1999

TOF

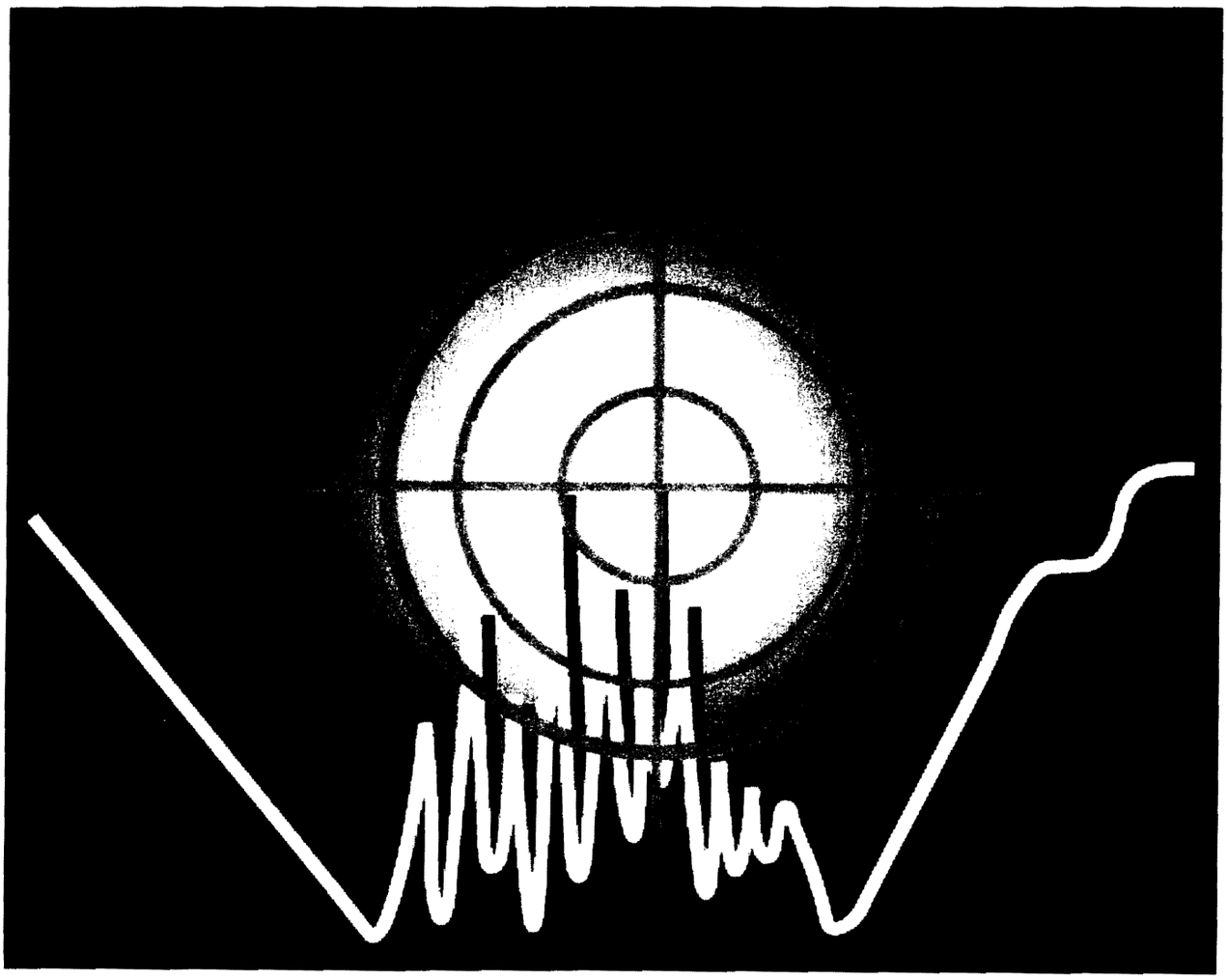

PROPOSAL FOR A NEUTRON TIME OF FLIGHT FACILITY

LABORATOIRE EUROPEEN POUR LA PHYSIQUE DES PARTICULES
CERN EUROPEAN LABORATORY FOR PARTICLE PHYSICS

CERN/SPSC 99-8
SPSC/P 310
17 March 1999

PROPOSAL

EUROPEAN COLLABORATION FOR HIGH-RESOLUTION MEASUREMENTS OF NEUTRON CROSS SECTIONS BETWEEN 1 eV AND 250 MeV.

THE TOF COLLABORATION

S. Abramovich[36], J. Andrejewsky[21], S. Andriamonje[9], A. Angelopoulos[2], A. Apostolakis[2], P. A. Assimakopoulos[18], G. Badurek[42], P. Baumann[37], M. Bernas[29], A. Billebaud[17], A.J.J. Bos[11], V. Bunakov[13],F. Calvino[5], D. Cano[22], P. Cennini[15], G. Charpak[30], V. Chepel[10], N. Colonna[6], F. Corvi[14], J. Derré[34], I. Duran[35], S. David[17], R. Del Moral[9], D. dos Santos[10], C. A. Eleftheriadis[38], M. Embid[22], F. Farget[29], A. Ferrari[15], R. Ferreira-Marques[10], E. Fomushkin[36], W. Furman[12], B. Fursov[27], A. Gadea[41], R. Gallino[39],E. N. Gazis[3], Y. Giomataris[32], A. Giorni[17], Yu. Gledenov[12], E.M. Gonzalez-Romero[22], P.B. Gossiaux[24], I. Goulas[15], A. Goverdovsky[27], O. Grudzevich[27], F. Gunsing[33], H.H. Gutbrod[24], S. Harissopoulos[1], E. Henry[20], D. Heuer[17], R.W. Hollander[11], K. G. Ioannides[18], S. Isaev[27], E. Jericha[42], Y. Kadi[15], F. Kaeppeler[19], A. Kagalenko[27], C. Kalfas[1], D. Karamanis[9, 18], A. Karydas[1], L. Kasakov[27], V. Ketlerov[27], T. Kirchner[24], G. Kitis[38], P.E. Koehler[26], N. Kolachevsky[23], V. Konovalov[12], S. Kossionides[1], V. Lacoste[9], H. Leeb[42], A. Leprêtre[33], J.M. Loiseaux[17], M. Lopes[10], R. Lougheed[20], A. Lychagin[27], A. Mengoni[8], O. Meplan[17], R. Meunier[28], P. Milazzo[40], V. Mitrofanov[27], S. Niemeyer[20], V. Nikolenko[12], N. Nikolis[18], H. Oberhummer[42], S. Oberstedt[16], A. A. Pakou[18], C. T. Papadopoulos[3], T. Paradelis[1], S. Parzhithki[12], V. Patticchio[6], P. Pavlopoulos[7,*], L. Perrot[17], V. Piksaaikin[27], J. Pinston[17], A. Plompen[14], A. Policarpo[10], Yu. Popov[12], Yu. Prokofichev[12], E. Radermacher[15], T. Rauscher[7], C.Rubbia[15,31], B. Rubio[41], G. Rudolf[37], P. Rullhusen[14], E. Sabbidis[38], L. Sakeliou[2], F. Saldana[15], G. Samosvat[12], B. Samylin[27], D. M. Santos[4], P. Sedysshev[12], V. Skoy[12], V. Sorokin[23], G. Souliotis[1], C. Stephan[29], J. L. Tain[41], L. Tassan-Got[29], R. Terchychnyi[27], C. Tsabaris[3], T. Tsirliganis[38],A. Tzima[15, 38], C.W.E. van Eijk[11], D. Villamarin[22], V. Vlachoudis[9,15], R. Vlastou[3], N. Vodinas[3], F. Voss[19], V. Vtyurin[12], H. Weigmann[14], M. Wiescher[25], K. Wisshak[19], K. Yuasa-Nakagawa[37], Yu. Zamyatnin[12], B. Zhuravlev[27]

---

* Spokesperson

1 National Research Centre for Physical Sciences "Demokritos", Institute of Nuclear Physics, Athens, Greece
2 University of Athens, Division of Nuclear Physics, Athens, Greece
3 Technical University of Athens, Division of Physics, Athens, Greece
4 Universidade de Aveiro, Aveiro, Portugal
5 SCN-FEN, Universitad Politecnica de Catalunya, Barcelona, Spain
6 Università di Bari e Sezione dell' INFN, Bari, Italy
7 Department of Physics and Astronomy, University of Basel, Basel, Switzerland
8 ENEA, Bologna, Italy
9 CEN, Bordeaux-Gradignan, France
10 Universidade de Coimbra, Coimbra, Portugal
11 Delft University of Technology, Delft, The Netherlands
12 Joint Institute for Nuclear Research, Frank Laboratory of Neutron Physics, Dubna, Moscow region, Russia
13 Petersburg Nuclear Physics Institute, Gatchina (St. Petersburg), Russia
14 IRMM, European Commission Joint Research Centre, Geel, Belgium
15 CERN, Geneva, Switzerland
16 ILL, Grenoble, France
17 ISN, IN2P3/CRNS & University J. Fourier Grenoble, France
18 University of Ioánnina, Nuclear Physics Laboratory, Ioánnina, Greece
19 Institut für Kernphysik III, FZK Karlsruhe, Germany
20 Lawrence Livermore National Laboratory, Analytical and Nuclear Chemistry Division, Livermore, USA
21 University of Lódz, Lódz, Poland
22 CIEMAT, Madrid, Spain
23 P. N. Lebedev Institute of Physics (FIAN), Optical Division, Russian Academy of Sciences, Moscow, Russia
24 SUBATECH UMR 6547, Nantes, France, (Ecole des Mines de Nantes, IN2P3/ CNRS & University of Nantes)
25 University of Notre Dame, Notre Dame, USA
26 Oak Ridge National Laboratory, Oak Ridge, USA
27 Institute of Physics and Power Engin.,Division of Nuclear and Neutron Physics, Obninsk, Kaluga reg., Russia
28 CSNSM, Orsay, France
29 IPN, Orsay, France
30 Ecole Supérieure de Physique et Chimie Industrielle (ESPCI), Paris, France
31 Università di Pavia e Sezione dell' INFN, Pavia, Italy
32 DSM/DAPNIA/SED, CEA, Saclay, France
33 DSM/DAPNIA/SPhN, CEA, Saclay, France
34 DSM/DAPNIA/SPP, CEA, Saclay, France
35 Universidad de Santiago de Compostela, Spain
36 All-Russia Scientific Research Institute of Experimental Physics, Sarov, Nizhnii Novgorod region, Russia
37 IReS, Strasbourg, France
38 Aristotle University of Thessaloníki, Department of Physics, Thessaloníki, Greece
39 Università di Torino e Sezione dell' INFN, Torino, Italy
40 Università di Trieste e Sezione dell' INFN, Trieste, Italy
41 Instituto de Física Corpuscular, Universidad de Valencia, Valencia, Spain
42 Institut für Kernphysik, Technische Universität Wien, Wien, Austria

EXECUTIVE SUMMARY

We consider a spallation driven TOF facility at the PS with an unprecedented neutron flux density in the broad energy range between 1 eV and 250 MeV and with very high energy resolution. The spallation process at high energies (24 GeV) is extremely neutron rich. This opens the way to new brand of neutron sources for cross section measurements through time of flight. The figure of merit of a TOF source is the actual neutron flux which can be achieved at the detector position for a given energy resolution. At a distance L, the energy resolution in turn is propotional to the effective relative longitudinal source size $\Delta\lambda$, namely $(\Delta E/E)_{mod} = 2\Delta\lambda/(\lambda+L)$, where $\lambda<<L$ is the equivalent neutron path in the target (calculated for the final neutron energy), with a fluctuation $\Delta\lambda$.

Classic TOF sources make use of a tiny neutron generation volume. The main draw-backs of such compact sources are the neutron yield, N_O~0.05 n/e and the large γ-contamination. The spallation cascade of an high energy beam inside a large lead block is more prolific and with much lower γ contamination (γ/n), but it is also extended over a much larger volume. Therefore the improvements of the neutron yield due to spallation could, in principle, be compromised by a greater detector distance required by the larger $(\Delta\lambda)^2$. The appropriate mechanism, based on the TARC experiment, "synchronises" different histories of spallation neutrons and hence reduces $\Delta\lambda$ to the order of 1.7 cm, though the longitudinal extent of the source is λ = 5.7 m (compression factor = 335). Such rich initial source offers, at a measuring station located at the distance L, a flux of $10^5/L^2$(km) n/cm^2/pulse with an energy resolution $\Delta E/E = 3.5 \times 10^{-5}/L$ [km].

We have organised a Joint CERN, GEDEON, (CEA+CNRS+EDF) and NEA (OCDE) Workshop in September 1998 at CERN inviting many already interested experimental groups to elaborate the physics programme. Various experimental programmes and ideas have been proposed by teams from almost all European countries, regarding the opportunities offered by the CERN Neutron TOF Facility. These proposals have been concentrated mainly in four research fields, i.e. Nuclear Astrophysics, Dosimetry and Nuclear Technology, and fundamental Nuclear Physics. In response to the request of the SPSC, we elaborated an Addendum of our Letter of Intent on the physics interests of the proposed TOF facility and, in collabration with the PS and TIS Divisions, a Feasibility Study of the implementation and costs which have been approved by the SPSC on the 3rd of November 1998.

The interested groups formed the present "European TOF Collaboration" and have elaborated the main research lines presented in this proposal to the SPSC. We intend initially to perform the necessary measurements with well established neutron detectors, already successfully used for the neutron flux measurements at CERN in the experiment PS211 (TARC and FEAT) and in the experimental program at the GELINA Facility, in order to determine the parameters and characteristics of the neutron beam. The neutron flux at the higher energies will be explored by the standard liquid scintillation GEEL detectors (NE-213) and the CERN ^{232}Th, ^{237}Np and ^{238}U fission gas detectors.

In the scope of our proogramme we propose for the year 2000 to start with measurements on fission and capture reactions which are well known, in order to check the reliability of the whole installation. In the neutron energy domain between 1 eV to few 100 keV, we intend to take advantage from the well known fission cross sections of ^{235}U and ^{239}Pu using fission gas detectors by directly counting the Fission Fragments. The prompt gamma detection technique with C_6D_6 or Moxon-Rae type gamma counters, standardly used at GEEL and FZK Karlsruhe, will allow to exploit the neutron capture cross sections of well-known elements, for instance ^{197}Au, ^{18}F, ^{27}Al and ^{nat}Ag with different Γ_γ/Γ_n ratios.

Given the experience from the above measurements, we propose in the fall of 2000 to start the first measurements of the cross sections for (n,γ), (n,f) and (n,xn) reactions on elements related to Astrophysics and ADS. With the foreseen development of more dedicated and powerful detectors, the TOF Collaboration will in the next stage be able to measure the more difficult cross sections of radioactive targets, thus exploiting fully the advantages of the CERN TOF facility. More elaborated work is required for the complexity and required precision for the experiments on fundamental Nuclear Physics.

1 - INTRODUCTION.

The experimental determination of neutron cross sections, elastic and inelastic across the whole Mendeleiev Table has always been of primary importance in Nuclear Physics. Many of the salient features of nuclear levels can be determined from the resonant structure of such cross sections and of their decay schemes. These cross sections have many different channels and exhibit a complex phenomenology with very many resonances over a very wide energy spectrum, extending from a fraction of eV to many MeV of neutron kinetic energy.

In addition to such a primary interest, recent developments at CERN and elsewhere have raised the practical need for better known cross sections aimed specifically at the design and understanding of the behaviour of ADS. In such devices, a charged particle beam is used to produce intense neutron fluxes.

These practical studies make massive use of Montecarlo techniques in order to predict ADS behaviour in a variety of possible configurations and running conditions. The relatively high energies involved require that not only neutron capture and fission, but also a larger variety of channels, like for instance (n,2n), (n,3n), (n,np), etc. should be taken into consideration. The presence of a high energy cascade implies extending the exploration to higher energies ($\approx$ 250 MeV for our programme). The design of innovative Accelerator-Driven Systems (ADS) for incineration of nuclear waste [1.1], energy production (EA) [1.2] and radio-isotope activation [1.3] for medical applications as well as many other subjects in Nuclear Physics, requires a knowledge as complete and as precise as possible of cross sections for neutron induced processes.

A fundamental pre-requisite of any computing method is the availability of reliable cross section data for many channels and at the appropriate energies. Unfortunately, the available Compilation Databases [1.4] — in general based on a mix of experimental measurements and of theoretical prejudices — present many "holes" and substantial differences amongst them, most likely due to the different fitting procedures used and the reliance on different theoretical models. They cannot be considered today as a totally reliable basis for planning in detail for instance the Energy Amplifier (EA) [1.5] prototype unit and simulating with the required accuracy the behaviour of the machine with a variety of different fuels, as required for instance when planning the incineration of radioactive waste from LWR's. Indeed, while the Thorium and Uranium related cross

sections are relatively well known, there are sometimes gigantic differences between Databases [1.4] when it comes to Americium and Curium, or more generally to higher Actinides.

The comprehensive elimination of LWR Waste implies consideration for the transmutation of several long-lived Fission Fragments into stable species as well. For such elements, the information is even more lacunary and in many important cases, like for instance ^{90}Sr, there are orders of magnitude discrepancies in the experimental data [1.6], mostly confined to the region of thermal or epi-thermal neutrons. Instead, the most promising transmutation method, the TARC [1.7] requires precise information on the resonances and specifically their widths.

Existing data are coming from compilations of many different experiments, often not in perfect agreement and generally each dedicated to specific energy domains and elements. They are currently mostly performed in association with a time of flight (TOF) measurement of the incoming neutron. This technique has been generally limited by the strength of the primary neutron source used which conditions the length of the flight-path and therefore the energy resolution vs. counting rate.

As a result of the studies reported in a first paper [1.8] and an addendum [1.9] we propose here a time of flight facility (TOF) at the CERN PS - delivering a maximum proton intensity of 3×10^{13} ppp at a kinetric energy of 24 GeV - which allows to study systematically and with excellent resolution neutron cross sections of almost any element using targets of very modest mass (even few milligrams), as needed for unstable or otherwise expensive materials, like for instance transuranics, in the interval from 1 eV to 250 MeV. In this facility we make use of the spallation mechanism as a strong source for neutrons by using a lead target and a flight path of 230 m.

2 – THE NEUTRON SOURCE AND THE TOF SPECTROMETER.

The spallation mechanism [1.8, 1.9] is a remarkably powerful source of neutrons: in a lead spallation target, one 24 GeV proton may produce as many as 760 neutrons. Furthermore lead has a high transparency for neutrons of energy ≤ 1 MeV. The CERN PS accelerator is capable of accelerating $2 \div 3 \times 10^{13}$ ppp, resulting in as many as 2×10^{16} neutrons at each pulse. This extraordinarily prolific source can be concentrated in short time pulses which are typically of the order of about 7 ns r.m.s. length, offering the added feature of a tremendous potential accuracy in the time of flight (TOF) determination of the neutron energy.

To the very small time uncertainty of the source one has to add the fluctuations in the moderating time needed to produce a wide initial neutron spectrum capable of covering the full extent of the energy domain in which cross sections need to be measured. It is a fortunate circumstance that the moderation in a high A material (the spallation target) occurs in a large number of steps in which the energy loss is small (≤ 1%). Hence the time fluctuations in the slowing-down process are also small, since the moderation time is strongly correlated with the energy of the outgoing neutron.

These features, already exploited in the TARC experiment, permit a very accurate TOF measurement of the incoming neutron energy. The operation of the CERN-PS like for antiproton production with an intensity of 2.5×10^{13} ppp and an energy of 24 GeV on a lead spallation target produces $24 \times 30 \times 2.5 \times 10^{13} = 1.8\ 10^{16}$ neutrons/pulse. The rich initial source strength of 1.43×10^{15} n/ster/pulse offers a flux of $2.8 \times 10^5/L^2$(km) n/cm^2/pulse at a measuring station located at a distance L.

With a flight-path of 230 m the TOF energy resolution ΔE for a neutron of kinetic energy E due to a beam time uncertainty Δt is given in fig. 2.1. The energy resolution is, as expected, quite good over the whole energy interval. It should be however remarked that this is only the contribution due to the beam time uncertainty. Additional contributions have to be added due to the thermalisation process and the detector resolution.

2.A.– THE PROTON BEAM AND THE SPALLATION TARGET.

2.A.1 – THE PROTON BEAM

The idea is to extract at 24 GeV/c proton bunches ($N_b \approx 0.7 \times 10^{13}$ p/bunch, r.m.s. length ≈ 7 ns) onto a lead target. The neutrons produced by spallation are canalised to an experimental area located 230 m downstream throughout a vacuum pipe making use of the existing TT2A tunnel about 7 m below the ISR tunnel (see Fig. 2.2).

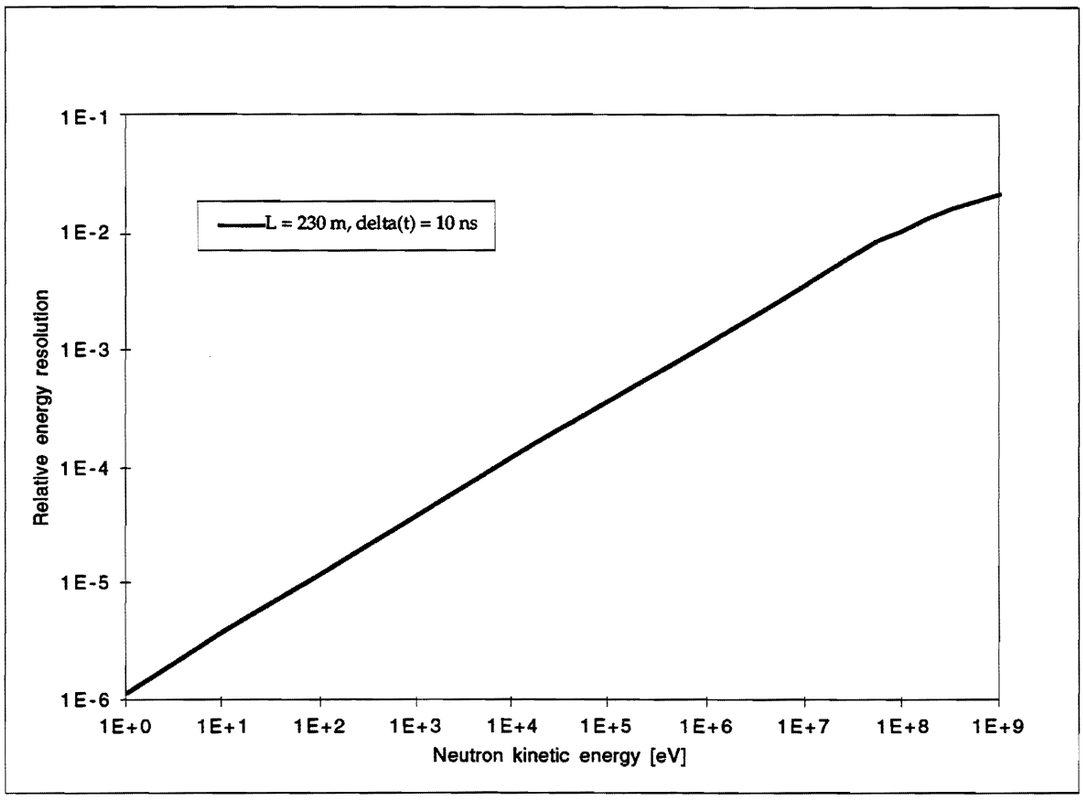

Figure 2.1: Neutron energy relative uncertainty after 230 m of flight path due to 10 ns beam time spread.

We report here only about the initial phase of the project, the so-called "1st year test phase" which differs from the "final phase" essentially in the proton beam intensity requirements. In the "1st year test phase" only one bunch of 0.5-0.7 x 10^{13} p/bunch will be extracted at 24 GeV/c (or 19 GeV/c). In the "final phase" four bunches with total intensity of 2-3x10^{13} p/pulse will be extracted, one every 50 ms, at 24 GeV/c. More details about this phase can be found in [2.1]. The initial phase does not require any modification in the PS machine itself, while the final phase requires important modifications in the power supplies of the fast

extraction elements (septum magnet, bumps, etc.) as well as a more refined cooling system for the lead target.

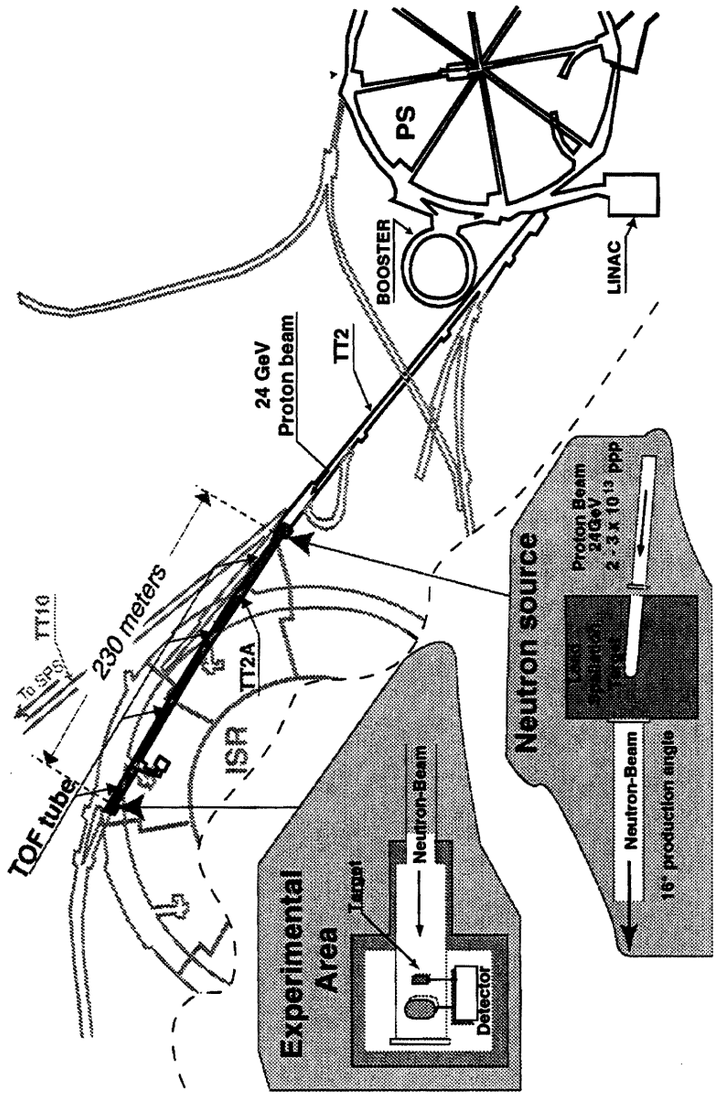

Figure 2.2: General layout of the experiment. The proton beam is extracted via the TT2 transfer line and hits the lead target. At the end of the TOF tunnel (TT2A) neutrons are detected about 230 m from the primary target.

The single bunch will be obtained by accelerating the beam in only one of the four PS Booster rings working with a RF harmonic number h = 1. The estimated longitudinal emittance will be $\varepsilon_l \approx 1.6$ eVs. Injection will take place at 1.4 GeV into the PS machine with a RF at h = 8, filling only one bucket. The incoherent space charge tune shift will be $\Delta Q_x \approx -0.2$ and $\Delta Q_y \approx -0.3$. These can be considered acceptable values as some transverse emittance blow-up, of about 20-

30%, can be tolerated. Transverse head-tail instabilities will be controlled with chromaticity tuning (negative below and positive above transition), transverse feedback, octupoles and x-y coupling. A controlled longitudinal blow-up with the 200 MHz cavity system will be adjusted to minimise longitudinal instabilities. The expected resulting longitudinal beam parameters at 24 GeV/c (V_{RF} = 200kV, h = 8) will be:

ε_l ~3 eVs $\qquad$ σ_t ~14 ns $\qquad$ σ_p/p ~0.8×10^{-3}

A bunch compression with a phase jump gymnastics will reduce, just before the extraction, the r.m.s. bunch length to the required value of $\sigma_t \approx 7$ ns. The corresponding increase of the r.m.s. momentum spread to $\sigma_p/p \approx 1.6 \times 10^{-3}$ will be still acceptable by the transfer line total momentum acceptance of $\approx 8 \times 10^{-3}$. Recent preliminary tests have already produced bunches with parameters close to the required ones (see Fig. 2.3a,b).

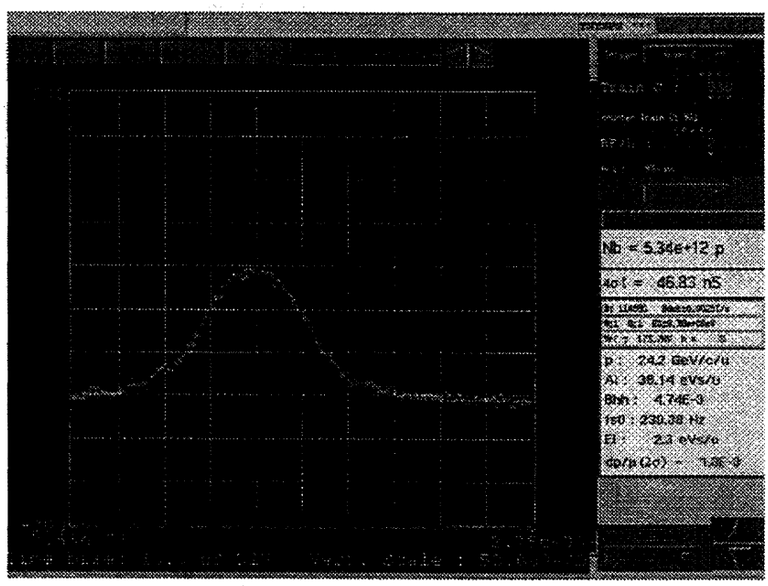

Figure 2.3a: A proton bunch of 0.5 10^{13} p/bunch at 24 GeV/c before bunch rotation. The r.m.s. bunch length is ~12 ns and ε_l =2.3 eVs (time base: 10 ns/div.).

In order to deviate the proton beam onto the lead target a new transfer line will be connected to the FT12 transfer line just downstream of the QDE380 quadrupole, see fig. 2.4. The proton beam is bent by 6 degrees to the right of the dump D3. Such a deflection is sufficient to avoid the dump. The position of the lead target is foreseen in front of the door separating the TT2 transfer line and TT10. The deflection will be produced by mean of three MCA bending dipoles, each providing a 2 degrees bending angle. A QFS quadrupole will be installed

downstream of the bending magnets. It will provide the necessary focalisation to the beam and it will be connected in series with the string of focusing quadrupoles already present in the TT2 line. Further downstream, two beam stoppers will be installed for an overall length of 3.2 m. The vacuum pipe will be terminated just in front of the lead target by means of a 100μm thick aluminium window.

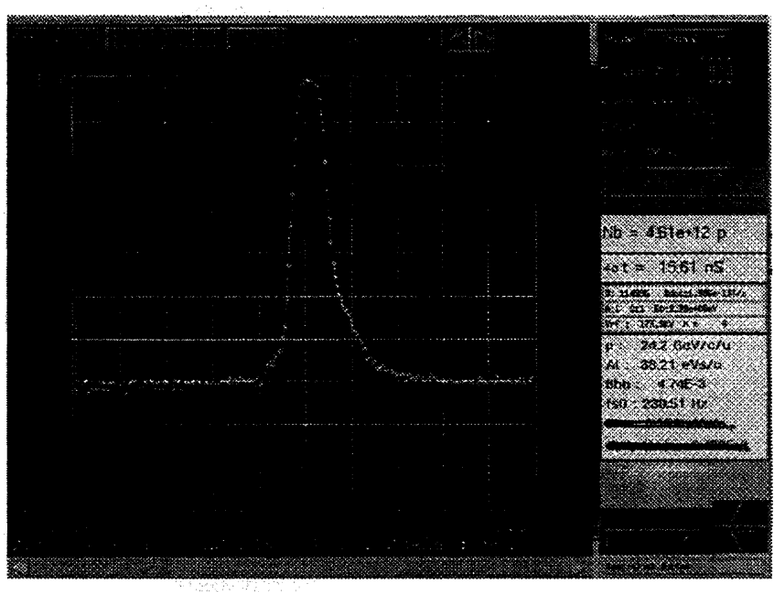

Figure 2.3b: The proton bunch after the bunch rotation in phase space. The r.m.s. bunch length is ~4 ns (time base: 10 ns/div).

In order to deviate the proton beam onto the lead target a new transfer line will be connected to the FT12 transfer line just downstream of the QDE380 quadrupole, see fig. 2.4. The proton beam is bent by 6 degrees to the right of the dump D3. Such a deflection is sufficient to avoid the dump. The position of the lead target is foreseen in front of the door separating the TT2 transfer line and TT10. The deflection will be produced by mean of three MCA bending dipoles, each providing a 2 degrees bending angle. A QFS quadrupole will be installed downstream of the bending magnets. It will provide the necessary focalisation to the beam and it will be connected in series with the string of focusing quadrupoles already present in the TT2 line. Further downstream, two beam stoppers will be installed for an overall length of 3.2 m. The vacuum pipe will be terminated just in front of the lead target by means of a 100μm thick aluminium window.

To monitor the proton beam intensity a beam current transformer similar to the one installed in the FT12 line, should be installed between the quadrupole

and the beam stoppers as well as a scintillation screen just in front of the lead target block. A wide band resistive wall pick-up should provide a bunch shape monitor.

Standard beam optics is used as starting point for the fast extracted LHC-type beam delivered by the PS [2.2]. The final trimming of the beam size on the lead target will be obtained by using the strength of the QFO375 quadrupole and the position of the additional quadrupole installed in the new transfer line. In Table 1 are reported the beam parameters used for the computation of the beam envelope, together with the beam size on the target.

Table 2.1 : Beam parameters used for beam envelope computation and beam size on the target (including the emittance blow-up due to multiple Coulomb scattering).

Transverse Parameters		**Longitudinal Parameters**		**Beam size on target**	
$\varepsilon_H(1\sigma)$ [μm]	0.5	σ_p/p	2×10^{-3}	$4\sigma_H$ [mm]	10
$\varepsilon_V(1\sigma)$ [μm]	0.5			$4\sigma_V$ [mm]	25

2.A.2. – THE SPALLATION TARGET.

An overall optimisation of the layout made of a lead spallation target of length h , diameter R followed by a water moderator of thickness W has been performed for the neutron emission angle of 16° from the proton beam direction, as set by the configuration of Ref. [1.8]. As result of a general trade-off between neutron flux and $\Delta\lambda$ resolution, we have chosen the parameters h = 80 cm , R = 40 cm and W = 5 cm.

Detailed calculations show that the power dissipation in the target gives rise to an increased temperature and requires therefore a cooling. In fact, about half of the 2 kW "initial phase" beam power will dissipate into the block and will require an air cooling (closed circuit). The temperature in the centre will reach 60 ^{0}C. Immediately behind and as close as possible to the lead target is mounted the 5 cm water moderator enclosed in a carbon fibre container which constitutes the window of the TOF tube. The complete target, once activated, can be removed with its support on rails and closed into a concrete blockhouse.

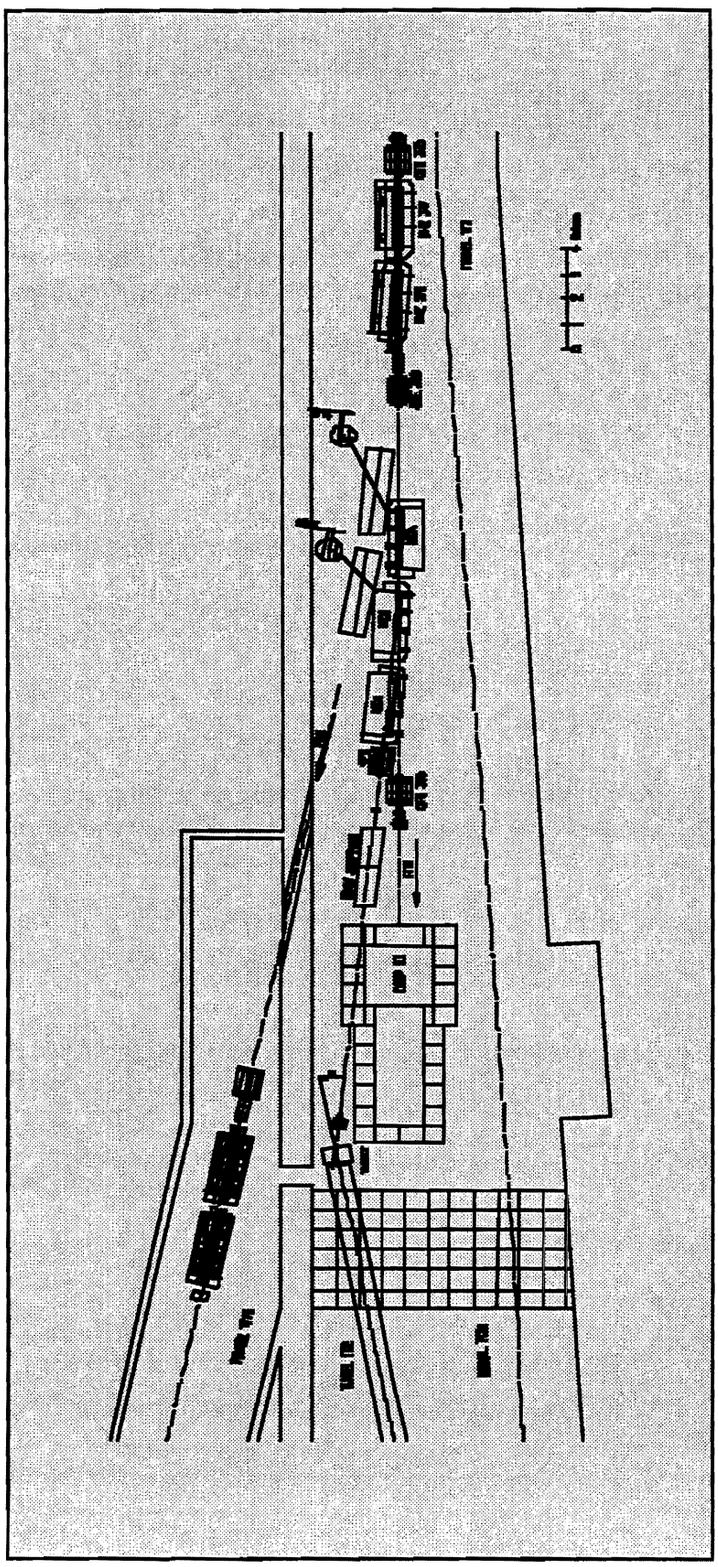

Figure 2.4: *Layout of the new transfer line to be installed in the TT2 tunnel.*

2.B – THE TOF TUNNEL AND THE MEASURING STATIONS.

The 230 m long beam pipe starting with a diameter of 80 cm, see fig. 2.5, will be at 16 degrees with respect to the proton beam direction in order to minimise the collection of unwanted secondary particles. Between the beam pipe and the output face of the lead target there is a gap of ≈ 1 cm of air to facilitate the installation of the target. The window of the stainless steel vacuum tube will serve at the same time as moderator, i. e. a 5 cm thick water volume enclosed in 2 carbon fibre windows of 3 mm will close the 80 cm TOF tube. The 230 m long stainless steel 304L pipe is made of several sectors connected by vacuum flanges. Each sector is made of various pieces welded together. Along the 230 m (fig. 2.5) the diameter varies as shown in Table 2.

Table 2.2: Mechanical dimensions of the various sectors of the vacuum chamber.

sector number	length [m]	ext. diam. [mm]	thickness [mm]
1	10	812.8	8.0
2	40	609.6	6.0
3	150	408.0	4.0
4a	27	812.8	8.0
4b	3	812.8	8.0

At the place where the diameter is changing from 60 cm to 40 cm an additional measuring station can be inserted.

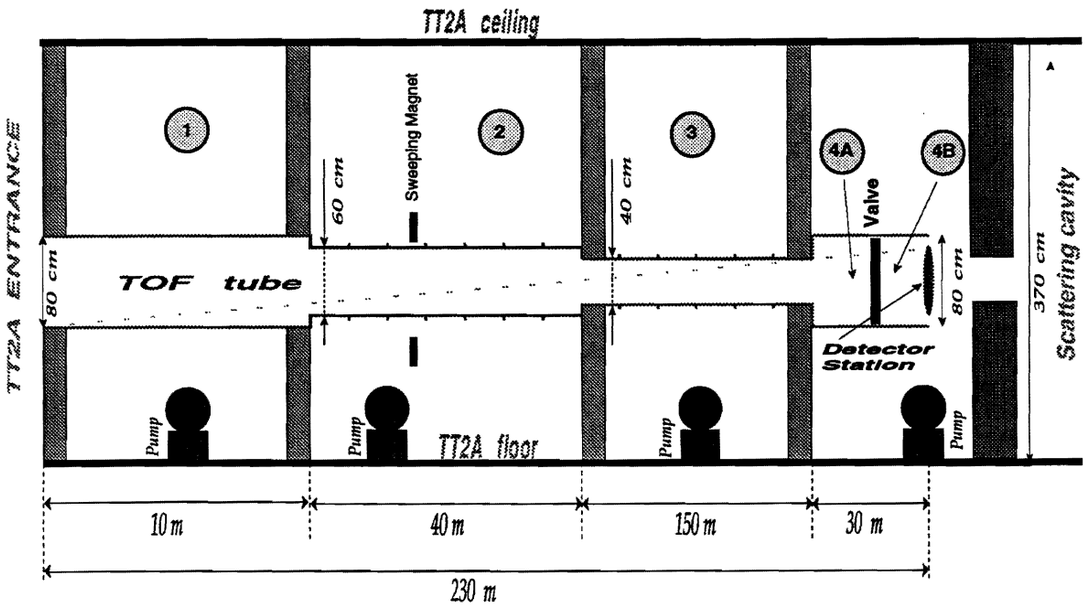

Figure 2.5: Schematic view of the TOF tube.

A DN800 vacuum valve will be installed between Sectors 4a and 4b. The "last window" at the end of sector 4b will be a fast open vacuum door to install the sample under study (neutron capture, fission, etc.) with associated detectors and electronics. 15 m downstream of the measuring stations a variable collimator will be installed to define the diameter of the beam together with the appropriate shielding.

In Sector 2 a bending magnet, with an integrated field of ≈ 1Tm, will eliminate the secondary charged particles coming from the lead target.

After the detection station, a special area of ≈ 8 m length with concrete shielding and neutron chicanes is foreseen for trapping the neutrons and protect the detection station from back-scattered neutrons.

The required vacuum pressure of 1 millibar will be obtained in ~10 hours, by installing in each of the first five Sectors, 1 to 4a, a single stage 16 m^3/h primary pump. In the last Sector 4b, a 500 m^3/h pump will reduce the pumping time to few minutes, to minimise waiting time and beam time.

2.C – THE NEUTRON BEAM AND BACKGROUNDS.

2.C.1 – NEUTRON MODERATION WITH A SMALL TIME SPREAD.

A time of flight selection of the neutron energy requires the shortest initial neutron pulse, in principle of duration of the order of the precision timing of the detectors used to observe the reactions, which is currently of several nanoseconds. As we have already pointed out, the accelerator is generating a sharp initial pulse, for which however one has to add the moderation time in the absorber. The spallation source of a large A material has the remarkable property, already exploited in the TARC experiment [1.7] of sharply correlating the slowing down time and energy of the resulting neutrons. An Uranium target would give about a factor 2 higher neutron yield, but at the price of a higher activation and considerable complications because of safety requirements. Although this factor could be recovered with a future construction of a properly engineered Uranium target, at this point we are prepared to accept the loss in flux as a trade-off for a better safety, easiness of operation and much lower cost.

It is a fortunate circumstance that, for high A, moderation introduces a relatively small time spread, once the energy of the outgoing neutron is defined.

This has been explored in great detail by the TARC experiment [1.7], where it has been shown that a sharp correlation exists between the time of moderation t and the kinetic energy E of the neutron. This correlation is valid only in the energy region in which elastic scattering dominates ($E \leq 10^4$ eV). More precisely, for a large block of lead, energy E and moderation time t are directly correlated [2.3]. The energy spread ΔE for a given time of moderation has been calculated [2.4]. The distribution around the mean speed v for a fixed moderation time is in a very good approximation a gaussian, with a r.m.s. spread Δv and essentially energy independent [8]. For lead the r.m.s. energy spread is

$$\frac{2\Delta v}{v} = \frac{\Delta E}{E} \approx 0.114\left[1+\frac{2}{E(eV)}\right]^{1/2}$$

Such time spread has been currently measured in the TARC experiment [1.7] and found to be essentially energy independent and in excellent agreement with the above formula. Such a time spread induces an apparent source length $\Delta\lambda$ in the direction of the flight-path which is also energy independent for E >> 2 eV and t >> 0.4 μs.

To conclude, in the region in which the elastic scattering dominates the slowing-down process accounts for an artificial lengthening of the path length of about 5.7 metres, corresponding to an extra time evaluated at the speed of the outgoing neutron. But, because of the strong energy-time correlation, the corresponding gaussian spread is reflected in a (energy independent) longitudinal uncertainty of the flight path of a mere ≈ 33 cm r.m.s. again.

The energy uncertainty due to the thermalisation process can be easily evaluated with the help of λ and of its variance $\Delta\lambda$ [1.8]. The thermalisation time is replaced by a displacement of a "virtual" neutron source which emits the neutron already at the final energy. The source is located on a plane parallel to the outer face of the spallation target (normal to the TOF direction) at a distance λ and with an uncertainty $\Delta\lambda$ from it:

$$\left.\frac{\Delta E}{E}\right|_{TOF} = 2\frac{\Delta t}{t} = 2\frac{\Delta\lambda}{\lambda + L}$$

Setting for instance L = 230 m, λ = 5.7 m, $\Delta\lambda$ = 0.33 m valid for E < 10^4 eV we find $\Delta E/E|_{TOF} = 2.8 \times 10^{-3}$, energy independent.

2.C.2 - OPTIMISATION CRITERIA FOR THE NEUTRON PRODUCING TARGET.

The specific geometry of the spallation target and the subsequent neutron moderation are application dependent, as a compromise between neutron flux in the energy domain under study and uncertainties in the moderation path fluctuations, $\Delta\lambda$. For instance in our main paper [1.8] the described geometry of the lead target has been optimised in order to provide a neutron spectrum as close as possible to the one of the Energy Amplifier (EA), i.e. peaked at about 450 keV with a mean energy of about 500 keV, for which a vast measuring campaign is anticipated. In these conditions, the neutron flux at 230 m is as large as 7×10^6 neutron/ cm^2/pulse, but with $\Delta\lambda \approx 35$ cm, i.e. relatively large, but sufficient to resolve the majority of resonances in the relevant cross sections at the prescribed measuring distance and with adequate counting rates (10^3 - 10^5 ev/pulse/gram of target, depending on the element.

It should be pointed out that in the evaluation of the neutronic characteristics of the EA with a Montecarlo method, the utilisation of measured cross sections do not require resolving all resonances. An "effective" cross section can be directly derived from the experimental data, provided that the energy steps of the measurement are much smaller than the "lethargic" energy loss in the moderator. As shown in the main paper [1.8], such a spectrum ensures for instance a uniform "illumination" of the major fission cross sections for transuranic elements, relevant to the projected transmutation programme.

In the case of Actinides and long-lived Fission Products, resonances are concentrated in the relatively low energy domain between 0.1 and 10^4 eV. Therefore a substantial improvement of the energy resolution of TOF may be welcome, which in turn means a much smaller value of $\Delta\lambda$, since, as we have already pointed out, the beam time uncertainties are masked by the fluctuations in $\Delta\lambda$.

A much smaller $\Delta\lambda$ can be indeed obtained, but at the price of a lower average energy spectrum, as suitable for the measurements at lower energies. To such an effect, the spallation target is to be followed by a thin 5 cm Hydrogen (water) moderation. The physical idea is that if at the exit of the lead (spallation) target, the neutron speed v is abruptly reduced by a large factor, for instance with a hydrogen rich moderator slab, also the value of $\Delta\lambda = v\Delta t$ will be correspondingly reduced. Note that the time fluctuations Δt of the moderation process are essentially unchanged because of the small thickness of the hydrogen layer. *There is evidently a trade-off between energy resolution and kinetic energy of the TOF neutrons.* For instance, if the speed v is reduced by a factor 20 (energy

of a factor 400), the value of $\Delta\lambda$ will be reduced by a corresponding factor, from 35 cm to about 1.75 cm.

This method is well applicable in our case, since the initial neutron energies are generally high, in view of the high incident proton beam energy and of the generally large longitudinal boost in the collision processes. *This method will be particularly useful whenever cross sections between 0.1 and 10^4 eV* have to be studied in detail.

An overall optimisation of the layout made of the lead spallation target led to the target geometry defined in 2.A.2. The resulting spectrum is given in fig. 2.6. We also show for comparison the energy spectrum obtained with the lead configuration of Ref. [1.8], with and without a water layer of 5 cm. One can see that the general drop of the integrated flux — from 7×10^6 n/ cm^2/pulse without hydrogen post-moderation to 2.7×10^6 n/ cm^2/pulse for the optimal parameters — is accompanied with a substantial increase in the flux at lower energies and an almost exact iso-lethargic behaviour.

2.C.3 - FLUXES VS. RESOLUTION.

The resulting uncertainty in $\Delta\lambda$ is shown in fig. 2.7, for the same exemplar configurations of fig. 2.6. It is evident that values of $\Delta\lambda \leq 1.5$ cm can be attained for neutron energies $\leq 10^3$ eV, with an improvement of over a factor 20 in the ultimate resolution. This extra factor can be used, for instance, (1) either to improve the resolution of the measurement or (2) to increase the flux at a constant resolution, by nearing the counting station by about a factor 20 in distance. This would increase the flux by the fantastic factor of 400, bringing it to $2.7 \times 10^6 \times 400 = 1.1 \times 10^9$ n/ cm^2/pulse or about 10^{12} n/pulse over a target surface of 1000 cm^2, as foreseen in Ref. [1.8]. It is doubtful that the detector station might operate in such an incredible flux !

The very high instantaneous flux is also of considerable interest in the study of radio-active targets. Reducing the TOF length implies reducing the corresponding time window in which counting is performed and therefore it means reducing the accidental background. In addition for a given number of events/pulse, the target mass can be reduced correspondingly. Therefore the signal/background is reduced by the factor $1/400 \times 1/20 = 1/8000$, which is considerable.

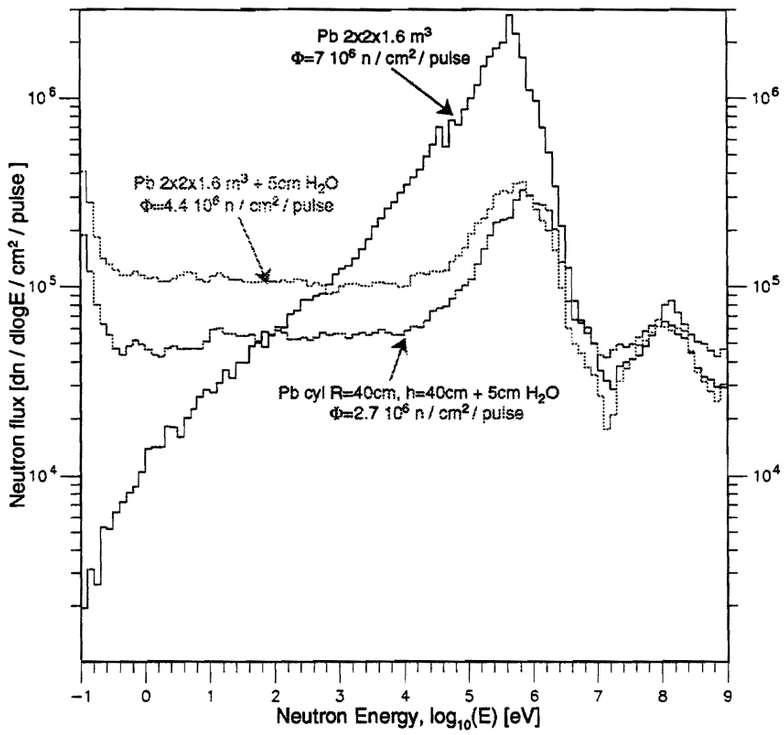

Figure 2.6: Neutron energy spectrum for various lead target configuration, with and without a 5 cm water moderator. The TOF path is 230 m.

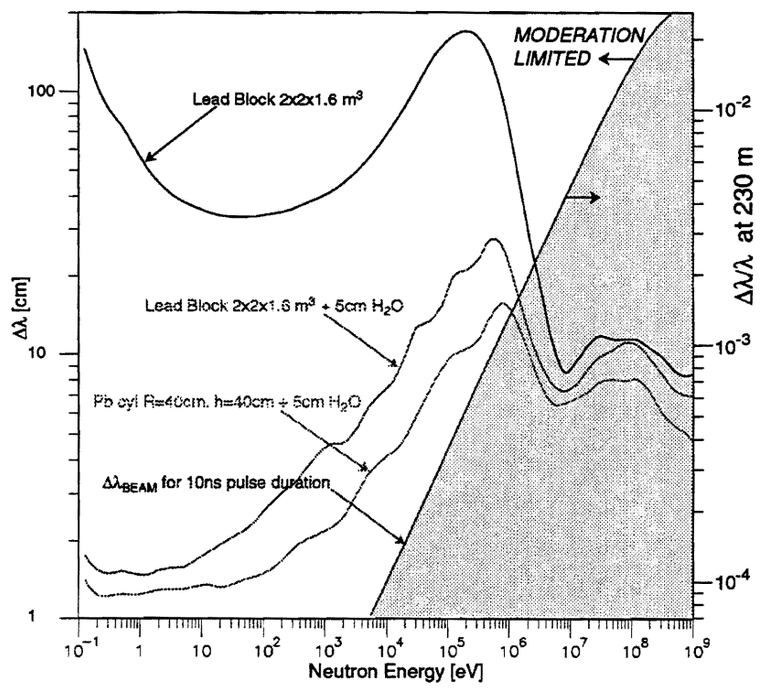

Figure 2.7: The uncertainty in the path $\Delta\lambda$ as a function of neutron energy for various target configurations. The reflected $\Delta\lambda$ uncertainty due to the CERN-PS pulse duration is also shown.

Let us consider for instance the case of ^{243}Cm ($t_{1/2}$ = 28 y) which has an activity of 51.6 Ci/g = 1.9×10^9 Bq/mg. The fission rate is (Ref. [1.8] appendix 2) is of the order of 10^2 ev/mg/pulse. The time window corresponding to 10 eV at 250 m is 6.5 ms (correspondingly less for shorter distances). In this time window, the spontaneous α-decays are 1.2×10^7 /mg, out of which one has to identify the fission signal. Hence the detector must provide a rejection of the order of 10^5 against natural background. Making use of the improvement in $\Delta\lambda$ and the corresponding factor 1/8000, the initial signal to background ratio is reduced to 1/12.5 which can be trivially separated out.

2.C.4 - THE BACKGROUND

The neutron environmental background is very sensitive to the geometry of the TOF tube and the beam apertures, as well as to the place of the detector room. By ignoring for instance the background introduced by the neutrons scattered on the target, there are mainly two kind of contributions i) neutrons leaking through the shielding concrete walls in the detector station and ii) neutrons entering the detector station through a scattering on the TOF tube walls .

The neutrons with small azimuthal angles after a certain flight in the tube would collide with the TOF tube and start a random path inside the tunnel. These neutrons introduce a significant background ~1% in the detector station, only if their collision take place 20 - 30 m before or after the detector station. The evident solution to avoid this type of background is the appropriate enlargement of the radius of the TOF tube, such that even the most divergent neutrons cross the TOF tube only 30 m after the detector station. Moreover, neutrons scattered on the TOF tube or leaking through the shielding can be reflected back and found with random incident angles in the detector station. Therefore, it it necessary to divide the tunnel, by concrete walls 2 - 3 m thick, into several compartments (used as neutron traps) starting at the position where the tube is enlarged and also before and after the detector station (Figs. 2.8 and 2.9). By such a geometry it is possible to reduce the contribution of this background to levels $<10^{-5}$ for a detector station at small distances ~80 m and near to zero inside our statistics for the detector station at large distances ~200 m.

The direct neutrons from the beam going straight will hit, passing through the target, the end of the TOF beam pipe and will reenter by backscatterings in the detector station. The mean free path in air (assuming a total cross section of about 10 b) is about ~20 m, thus a few meters of air is enough to introduce a backscatter background of the order of 1-2 %. With the appropriate simulations we have

concluded that at least 8 m of vacuum are necessary after the detector station, in order to eliminate this effect of backscattering of the straight traveling neutrons, mainly on oxygen. By using a compartment geometry the background from backscattered neutrons can be totally eliminated (Fig. 2.10).

In the compartment geometry, another important contribution to the background arises from the neutrons scattering on concrete and entering through the neutron-tube in the detector station. In order to avoid these neutrons entering the detector station an additional concrete shielding of ~5 m around the neutron tube in the direction away from the detector station, is required.

In both cases, the shape of the energy spectrum of the background neutrons is almost the same and only the neutron flux is reduced by a factor 10^{-5} or below. The energy spectrum of the neutrons in the different areas is shown in figure 2.11 and the neutron flux along the TOF beam line is shown in figure 2.12. The only major difficulty arises for the detector station at small distances ~80m concerning the component of the fast neutrons. The fast neutrons continue to generate other secondary neutrons either by spallation or by other mechanisms, requiring thicker concrete shielding.

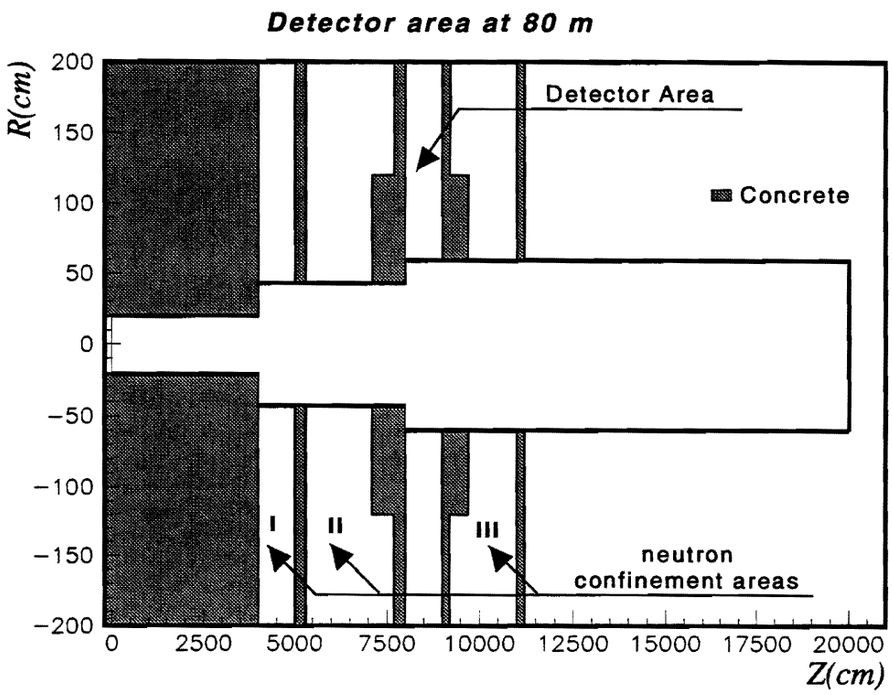

Figure 2.8: Schematic view of the TOF tube geometry and neutron traps before and after the detector station.

To reduce the radius of the neutron beam, the use of collimators is necessary. The introduction of a collimator inside the neutron tube, creates a halo in the neutron profile, which is larger as we are approaching smaller flight paths. At small distances (80m), in order to minimise this halo, we must use more than one collimators, with a substantial reduction of the neutron flux. At large distances (200m), only one collimator is necessary, producing a sharper beam profile (Fig. 2.12), leaving the neutron flux almost unaltered.

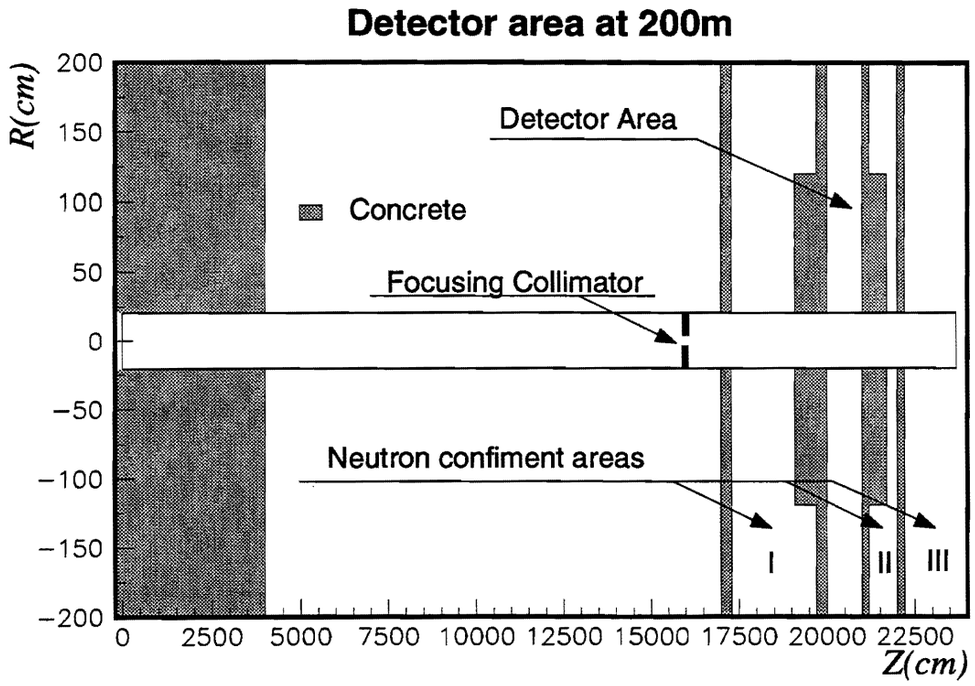

Figure 2.9: Schematic view of the TOF tube geometry and neutron traps before and after the detector station.

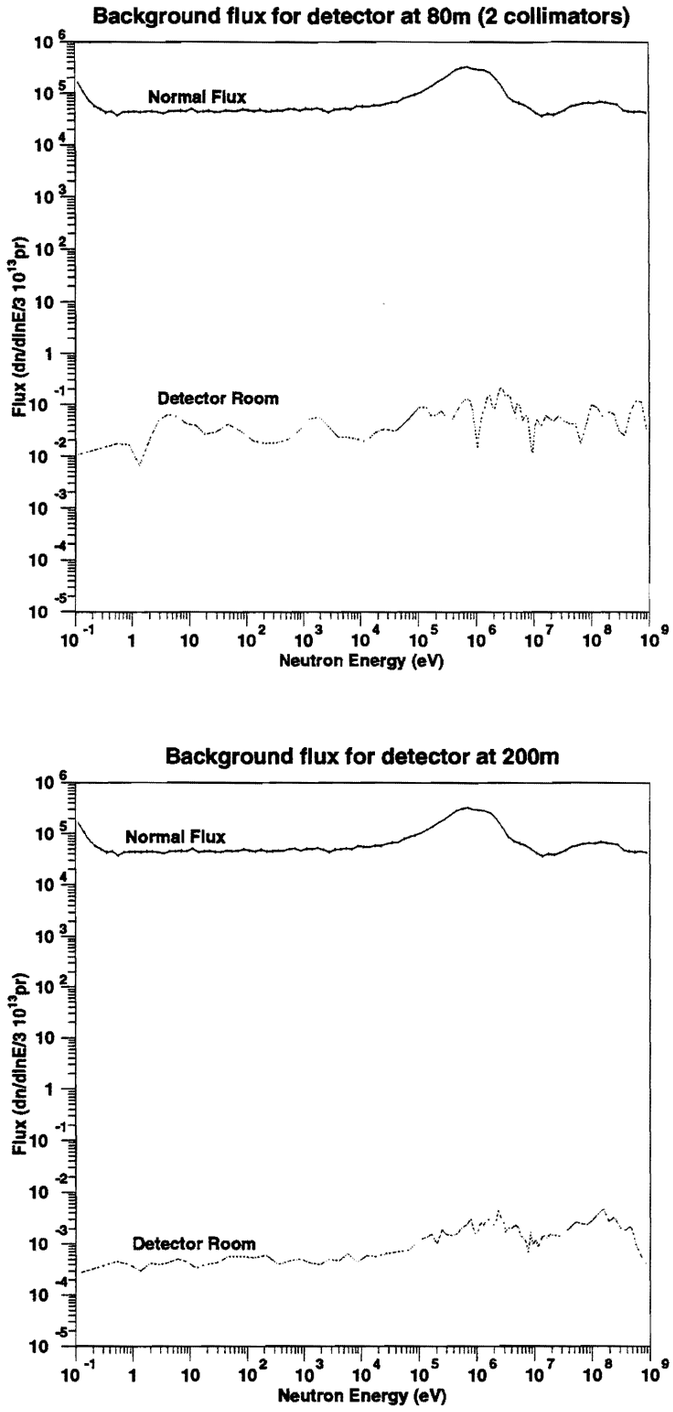

Figure 2.10: Energy of neutrons inside the detector station at 80 m. The spectra at 200 m have the same shape.

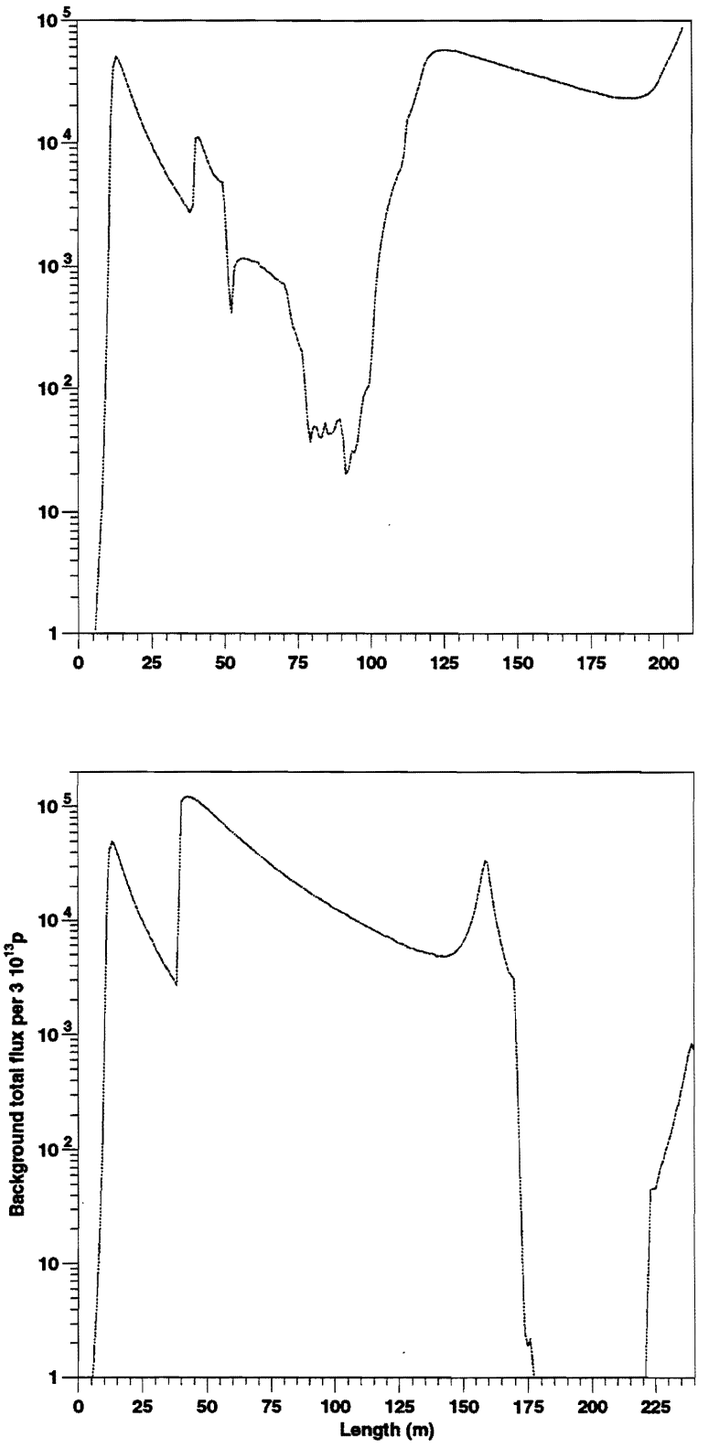

Figure 2.11 : The neutron flux along the TOF beam axis for the 80 m and 200 m target station. The flux in the beam tube amounts for the 80 m distance to 1.7×10^7 *and for the 200 m distance to* 2.7×10^6 *neutrons per* cm^2 *per high intensity pulse.*

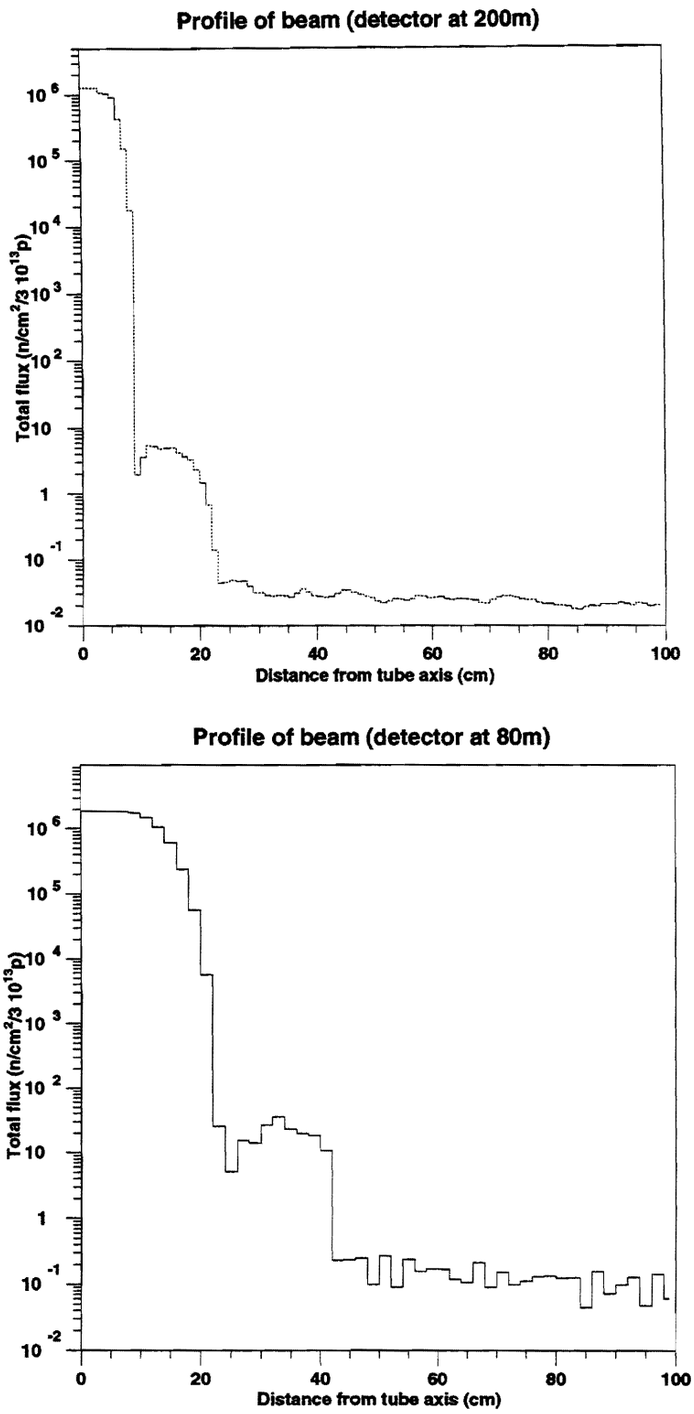

Figure 2 .12 :The neutron profile versus the distance of the neutron-tube axis. The halo is evident in the case of 80m with the use of 2 collimators, where in the 200m, the profile is more sharp, even with the use of a single collimator.

3 – THE PHYSICS MOTIVATION AND GOALS.

Neutrons play a specific role in Nuclear Physics research. Together with protons they are the main constituents of nuclei. They are electrically neutral and are not affected by the strong Coulomb repulsion in the vicinity of nuclei. Therefore, capture reactions as well as emission processes from the nuclei are not hampered by the Coulomb barrier and can occur also at low energies with reasonable probabilities. It is this property which makes the importance of neutron induced reactions for the development of nuclear technologies but also for the evolution of the universe. In fact these two topics are the main subject of the planned activities at the CERN TOF Facility.

The neutron-nucleon and the neutron-nucleus interaction is dominated by the strong force and is therefore of short range. The absence of the Coulomb force simplifies in many cases the theoretical description of scattering experiments and thus the analysis of scattering data. Hence experiments with neutrons can provide very clear information about the properties of the strong interaction. This aspect has been taken into account in the present proposal which includes some fundamental few-nucleon experiments. Making use of the unique high flux of neutrons at the CERN TOF facility novel aspects can be studied.

The neutron is also affected by the weak and the electromagnetic interaction. Although the weak interaction plays a minor role in most nuclear collisions, it is of great importance in neutron physics because it determines the beta-decay as well as the half-life of the neutron itself. The reaction chains of nucleosynthesis represent a delicate balance between capture reactions, which are subject of this proposal, and beta decays. Another interesting aspect in this context is parity violation. In the first phase of the TOF facility, however, dedicated experiments on this topic are too early because it requires neutron polarization option and are not discussed here. The electromagnetic interaction couples to the neutron mainly via its anomalous magnetic moment. This feature is of great importance for the use of scattering techniques with thermal or cold neutrons in condensed matter physics. In the energy regime of the TOF facility the cross sections are sensitive to the charge distribution of the neutron. Thus electromagnetic structure constants of the neutron, i.e. the charge radius and the electric polarizability can be studied.

The novel features of the spallation driven TOF facility at the CERN-PS attracted physicists with different scientific interests and experience. We elaborate

on the physics potential of the following areas of interest expressed by the collaborating Institutes :

(1) Cross sections relevant to Nuclear Astrophysics;
(2) Cross sections relevant to Nuclear Waste Transmutation and other fields in Technology.
(3) Neutrons as a probe for fundamental Nuclear Physics;

Substantial funding for the experimental programme related to technological applications will be requested from the 5th EC Framework Programme, from which we have received a preliminary, but favourable indication.

3.A – NEUTRON REACTIONS FOR STELLAR NUCLEOSYNTHESIS.

The to-date evolution of the Universe can, from our Earthly perspective, be divided into a few main stages: Big Bang, primordial nucleosynthesis and atomic formation, galactic condensation, stellar and explosive nucleosynthesis, and formation of the Solar System. What is now called the Standard Model of the hot Big Bang cosmology includes an overall framework based on the General theory of Relativity, nuclear and particle properties and some extrapolations based on reasonable hypotheses. When the temperature of the Universe had decreased to about 10^{10} °K about 1 second after the Big Bang, weak interactions froze out and the currently observed ratio of neutrons and protons (about 13% n and 87% p) was established. As the nucleosynthesis chain began with the formation of deuterium, it was delayed past the point where the temperature had fallen below the deuterium binding energy, which is 10^9 °K, when the Universe was about 200 seconds old. After that a wealth of nuclear reactions could occur and lead to the production of ^{2}H, ^{3}He, ^{4}He and ^{7}Li. The input data to the stellar models must yield abundance results in agreement with observations, the primary ones being the relative amounts of these light isotopes produced during the earliest epoch of element formation. The observed abundances can then put severe constraints on the fundamental processes that occured during the formation epoch.

The hot mix of H, He, and Li continued expanding and cooling. After about $3x10^5$ years the atomic nuclei could combine with the free electrons to form atoms but only after 30 million years, at a temperature of 100 °K, the force of gravity began to take over and lead to the formation of galaxies and stars. Most of the light elements up to Fe that we see in nature were produced in massive stars

(say 10 to 100 times the mass of our sun) and in the supernova explosions that mark the end of their life. Understanding the relative abundances of these elements and isotopes has been a great puzzle for astronomy over the last 60 years, and the answer depended greatly on nuclear physics demanding an ever increasing body of nuclear data.

The difficult task is to understand the formation of the more heavy elements following fusion reactions and neutron captures in stellar interiors. Not only is the nuclear physics complicated but also the mechanisms and thermodynamics are not completely understood yet. The observational evidence consists of astronomical observations, not only with ground-based telescopes, but recently also with X-, γ-, and particle spectrometers carried in orbiting spacecraft. Furthermore, microanalysis studies of meteorites have become an increasingly important source of information. Also in the latter cases, nuclear reaction data from terrestrial laboratories are essential to determine fundamental limits on the involved processes and conditions, and thus on the nature and especially on the evolution of stars.

The synthesis of most of the heavy elements with $A > 60$ has been attributed primarily to neutron-capture processes. Recent "phenomenological" studies have succeeded in pinpointing the required conditions for such a nucleosynthesis. A combination of sites providing those conditions has been suggested. Promising candidates range from the interior of red giant stars to the low-density, high-entropy bubble just inside of an expanding core-collapse supernova shock wave. Advances in our understanding of these processes and of the astrophysical sites where they occur, require advances in laboratory measurements of neutron cross sections. The goal in modeling these processes is to understand not only the detailed way in which heavy elements are synthesized, but also the conditions of the astrophysical sites where these syntheses occur. An overwhelming majority of cross section measurements, which comprise the crucial input for astrophysical models of heavy element nucleosynthesis, is proposed to be performed at the TOF facility, uniquely suited, not only in Europe but also worldwide, to enable further advances in our understanding of heavy element nucleosynthesis. An active experimental nuclear astrophysics programme to measure neutron reactions of importance to nuclear astrophysics is presented.

Neutron reactions are responsible for the formation of all elements heavier than iron. In astrophysical scenarios, the heavy elements can only be produced by neutron capture reactions and subsequent beta decays. Fusion of charged particles

no longer contributes in this mass range, since the Coulomb barriers are becoming too high and the binding energies per nucleon are decreasing beyond A~60. For explaining the observed abundance distribution between iron and the actinides, essentially three processes must be invoked (Figure 3.1). In the slow neutron capture process (s-process), neutron captures occur much slower than beta decays and the reaction flux stays close to the line of beta stability. Under explosive conditions in neutron-rich environments, neutron capture can become much faster than all but the most short-lived beta decays. Thus, the reaction path can move far off stability and create a different abundance pattern. A few proton-rich stable isotopes are shielded from the s- as well as from the r-process. Another process has to be invoked to account for them, which is called p-process for historical reasons. The p-process is much less understood than the s- and r-processes and is mostly thought to occur via photodisintegration reactions at high temperatures in supernova explosions. Despite some problems with this scenario, the r-process is usually attributed to nucleosynthesis in the high entropy bubble behind the shock front in type II supernova explosions.

s- process	Red Giant stars, (α,n) reactions, Fe-Bi, resulting abudances directly determined by (n,γ) cross sections, E_n=0.3-300 keV, reaction path in stability valley.
r- process	Supernova at mass cut, neutronized matter, Fe-U, (n,γ) cross sections for freeze-out, E_n=0.3-300 keV, reaction path close to neutron drip line.
p- process	Supernova in O/Ne shell, (γ,n) reactions, Fe-Bi, (n,γ) cross sections for freeze-out and for estimating the inverse rates, E_n up to 1 MeV, reaction path in proton rich region.

***Table 3.1** : Scenarios for the origin of the heavy elements [3.1].*

So far, laboratory studies have concentrated on the s-process, which operates in or near the valley of β-stability. This process associated with stellar helium burning is characterized by relatively low neutron densities. This implies neutron capture times of the order of several months, much longer than typical beta decay half-lives. Therefore, the s-process reaction path follows the stability valley as indicated by the solid line in the N-Z-plane of figure 3.1. The developing s-abundances are determined by the respective (n,γ) cross sections averaged over the stellar neutron spectrum, such that isotopes with small cross sections are built up to large abundances. This holds in particular for nuclei with closed neutron shells N = 50, 82, and 126, giving rise to the sharp s-process maxima in the abundance distribution around A = 88, 140, and 208. This process has produced about half of the elemental abundances between Fe and Bi, the resulting

abundance distribution being essentially determined by an almost linear relation to the stellar (n, γ) cross sections.

The accuracy of (n, γ) cross section data for the s-process has an immediate impact on the resulting abundances. The quantitative interpretation of the s-abundances represents sensitive tests for models of stellar He-burning [3.2], of the mixing mechanisms to the stellar atmosphere [3.3], and of the grain formation in circumstellar envelopes leading to the isotopic anomalies in presolar meteoritic inclusions [3.4].

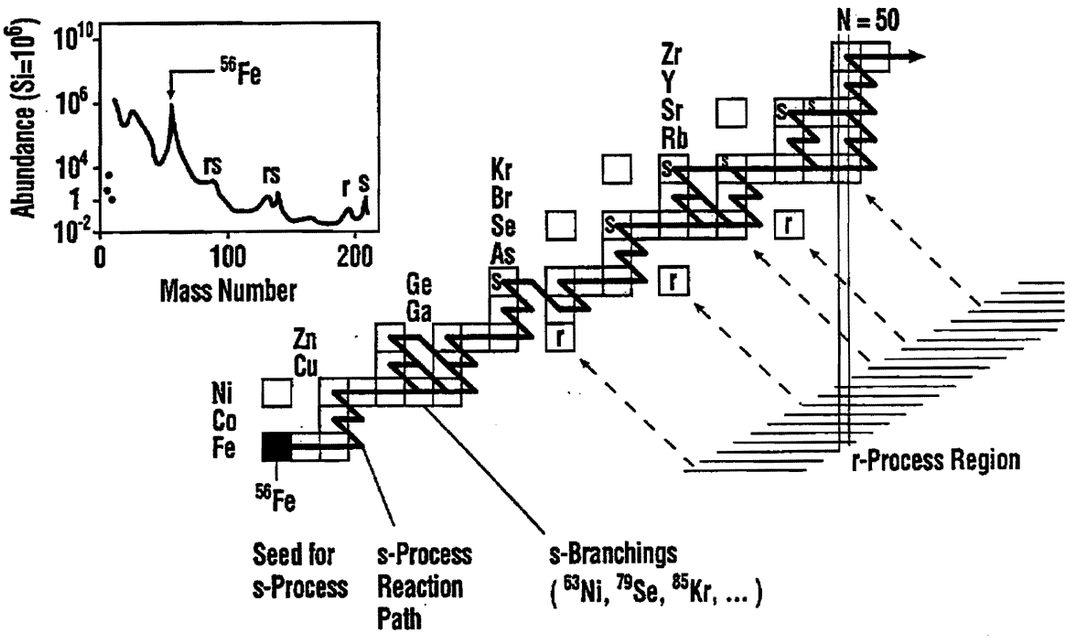

Figure 3.1: An illustration of the neutron capture processes responsible for the origin of the elements between iron and the actinides. The observed abundance distribution in the inset shows characteristic twin peaks. These result from the nuclear properties at magic neutron numbers under typical s- and r-process conditions, an obvious example for the intimate correlation between the observed abundances and the physical conditions during nucleosynthesis.

Numerous new measurements helped to resolve discrepancies between older data sets, but more reliable data are still needed, particularly for even-even nuclei in the region from Mo to Pd, where large uncertainties persist despite the recent improvements of the data bases. It is also very important to measure such cross sections on isotopes produced only in the s-process (the "s-only isotopes"), especially for those elements with two or more such isotopes (Kr, Sr, Te, Xe, Ba, Sm, Gd, and Os), because they are used to precisely normalize the s-process contributions to all elements, and because the ratios of these isotopic abundances

can be compared to extremely precise measurements from meteorites. In some cases, experimental data are still completely missing, i.e. for isotopes of Ge and Se as well as for the important s-only nuclei as ^{128}Xe, ^{130}Xe, and ^{192}Pt. In fact, the high precision of new abundance measurements of *s-only isotopes*, primarily in meteorites, is a strong motivation for new, precise measurements of neutron capture cross sections.

Additionally, detailed analysis of s-process branch point nuclei - light and intermediate mass isotopes where both neutron capture and beta decay occur - provide the most sensitive probe of the astrophysical environments (temperatures and neutron densities) where the s-process occurs. These s-process branchings include the unstable isotopes ^{85}Kr, $^{134\text{-}135}$Cs, ^{147}Nd, $^{147\text{-}148}$Pm, ^{151}Sm - ^{152}Eu, ^{153}Gd, ^{163}Dy, $^{163\text{-}164}$Ho, ^{169}Er, ^{170}Tm, ^{176}Lu and ^{185}W-^{186}Re. With the same motivation the cross sections of thermally-excited low-lying states for some 30 nuclei in the mass region 150<A<190 e.g. for ^{187}Os and ^{189}Os are important. For determining the endpoint of the s-process, neutron capture measurements are needed on the long-lived radioactive ^{210}Bi in its ground and isomeric state and the ground state of ^{210}Po.

Given the range of temperatures from 100 to 300 x10^6 ^{o}K, which are characteristic for He burning scenarios, differential neutron data are needed between 0.3 and 300 keV, mostly for stable nuclei, but also for a significant number of radioactive isotopes with half-lives comparable to the typical neutron capture times of a few months. These cases are important, because the competition between neutron capture and β-decay causes the reaction path to split, resulting in very particular abundance patterns which are reflecting the stellar neutron density and temperature. Therefore, these branchings represent sensitive tests of the yet uncertain stellar models for the He burning stages of evolution.

A satisfactory database for s-process studies should, therefore, contain experimental information over a sufficiently wide energy range, and with uncertainties of about 5%. Beside these general requirements, data with typical uncertainties of 1% are needed for (i) the s-only nuclei, which are important as normalisation points of the s-abundance distribution and for defining the s-process branchings, and (ii) for the interpretation of isotopic anomalies in meteoritic inclusions. The cross sections of neutron magic nuclei and of the abundant light isotopes, which represent the major neutron poisons, should be

known to better than 5% despite the persisting difficulties in the investigation of these small cross sections.

Explosive scenarios are affected by neutron reactions during the freeze-out phase and require predominantly cross sections of radioactive nuclei. At traditional facilities, measurements on this species are difficult because of the limited neutron fluxes. In this respect, spallation sources offer a new and promising approach for a variety of experiments on hitherto inaccessible nuclei [3.1]. Neutron capture data are also important for the explosive r- and p-process scenarios, particularly during the freeze-out phase, where they lead to significant modifications of the primary reaction yields. These scenarios occurring far from stability, imply reactions on rather short-lived isotopes, which are much more difficult to study experimentally. Modelling the r-process nucleosynthesis requires neutron binding energies and beta-decay lifetimes for thousands of nuclei close to the drip line. This necessarily requires the use of nuclear models, which are pushed to their limits when predicting nuclear properties near the drip line. In fact, recent work looking at systematics of r-process abundances has been used to correct inconsistencies in nuclear models; such use of astrophysical r-process abundances to check nuclear microscopic models may be expanded in the future. However, such work is possible only with very accurate s- process abundances: the intimate link between studies of the s- and the r-process is that the r-process abundances, to which calculated abundances are compared, are determined by subtracting calculated s-process abundances from the observed abundances; these r-process abundances are sometimes referred to as residual abundances. Advanced r-process studies therefore require precise s-process studies, and the precision of these studies rely on accurate (n,γ) cross section measurements.

From r-process scenarios comes a further motivation to study neutron induced reactions close to stability. In order to investigate freeze-out effects, huge reaction networks are required, including several thousand reactions. So far, the respective reaction rates have been exclusively obtained by statistical model calculations. Nuclear properties are also an essential input for these theoretical predictions far off stability. The theoretical models have to be tested against as many isotopic chains as possible. Furthermore, it could prove important to include additional effects in the rate calculations (see next section). These have to be studied thoroughly close to stability in order to provide a more secure base for extrapolation.

TOF techniques are most suitable for measurements on practically all stable nuclei, yielding differential cross sections $\sigma(E_n)$ for calculating the stellar average:

$$\langle\sigma\rangle_{kT} = \frac{2}{\sqrt{\pi}} \frac{\int_0^\infty \sigma(E_n) \times E_n \times \exp(-E_n/kT) dE_n}{\int_0^\infty E_n \times \exp(-E_n/kT) dE_n}$$

In this type of experiments, capture events are detected simultaneously over the whole neutron energy range via the prompt γ-rays emitted in the reaction, where the neutron energy is tagged by TOF. The best identification of neutron capture events is provided by the total energy of the capture γ-cascade. This requires a detector that operates as a calorimeter with a γ-ray efficiency better than 90% in the entire energy range below 10 MeV. The high efficiency and the good resolution in gamma ray detection together with the high TOF resolution, are essential for achieving the required accuracy of 1%. Although spallation neutron sources have not often been used for astrophysically motivated measurements so far, their huge fluxes allow to reduce the sample mass by a factor of 1000 compared to the traditional facilities. This aspect becomes essential in dealing with radioactive samples, where high intensity, low repetition spallation sources provide excellent signal-to-background ratios.

Neutron capture studies on radioactive targets are hampered by the background from the sample activity, but also because suited samples are only available at limited quantities. The discussion of experimental possibilities for measurements on short-lived branch-point nuclei showed that a number of these cases can be studied with 1000 times smaller samples of about 100 micrograms using the much higher flux at spallation sources and neutron capture integrated cross sections over quasi-stellar neutron spectra extracted with the very sensitive activation technique [3.5]. However, the activation technique is restricted to cases, where neutron capture produces an unstable nucleus, and it yields the stellar rate only for certain thermal energies.

3.A.1 – NEUTRON CAPTURE CROSS SECTIONS FOR THE S-PROCESS.

3.A.1.A – UNSTABLE TARGETS.

The very high neutron fluxes make spallation neutron sources a unique place to study the stellar neutron capture rates of a number of unstable nuclei

which act as branching points in the reaction path of the s-process. These data on branch point isotopes are urgently required to interpret the abundance pattern of these branchings, which can be analyzed in terms of the stellar neutron density, temperature, and pressure. These parameters help to characterize the He-burning zones, where the s-process takes place and, hence, represent important constraints for the yet uncertain stellar models. Also the cross sections at the termination of the s-process path at Pb and Bi provide important clues for the recycling of the reaction flow and the resulting isotopic lead abundances.

From an extensive list of isotopes, which could be measured at such a source, the highest priority should be given to the important branch points ^{79}Se, ^{147}Pm, ^{151}Sm, ^{163}Ho, ^{170}Tm, ^{171}Tm, ^{179}Ta, ^{204}Tl, and ^{205}Pb. These cases are of immediate relevance to s-process analyses and should not present unexpected experimental problems.

Given the experience with this first set of measurements, further studies could then be carried out on ^{60}Fe, ^{63}Ni, ^{81}Kr, ^{85}Kr, ^{135}Cs, ^{154}Eu, ^{153}Gd, ^{185}W, ^{210m}Bi, and ^{210}Po. This second group of nuclei would benefit from the optimization of the setup, e.g. as far as backgrounds are concerned.

It has to be pointed out, however, that such studies require the capability for preparing samples of these unstable nuclei in sufficient quantities and with sufficient purity.

3.A.1.B – STABLE TARGETS.

For a large number of stable isotopes, the high neutron flux at a spallation source would allow to measure the cross sections which are very difficult to obtain at other facilities. Provided that backgrounds can be sufficiently reduced, this concerns nuclei with very small cross sections:

- Nuclei at or near magic neutron numbers, which act as bottlenecks in the s -process reaction flow from Fe to Bi ^{86}Kr, ^{87}Rb, ^{88}Sr, ^{89}Y, ^{90}Zr at N=50, and ^{138}Ba, ^{139}La, ^{140}Ce at N=82);
- Abundant light isotopes below Fe, which may consitute crucial neutron poisons for the s -process, in particular ^{16,18}O and ^{22}Ne;
- Light isotopes which were found to exhibit isotopic anomalies, including the stable isotopes of oxygen, neon, magnesium, silicon, calcium, titanium and zirconium;
- Nuclides where the direct capture process accounts for a significant fraction of the astrophysical reaction rate. For example, as much as 2/3 of

the $^{208}Pb(n,\gamma)$ reaction rate at s-process temperatures is due to direct capture. A TOF measurement of the direct capture component should be feasible using a high efficiency germanium detector. Additional cases where direct capture contributes significantly to the reaction rate are ^{14}C, ^{16}O, ^{88}Sr, and ^{138}Ba.

3.A.2 – NEUTRON CAPTURE CROSS SECTIONS FOR THE r-PROCESS.

Nucleosynthesis in explosive scenarios occurs off the stability valley (on the far neutron rich side in the r-process and on the proton rich side in the p-process) and requires huge reaction networks including several thousand reactions. So far, the respective reaction rates have been exclusively obtained by statistical model calculations, which could only be tested by experimental data for stable nuclei. In order to verify the necessary extrapolation to the region of unstable nuclei, experimental data for as many unstable isotopes as possible would, therefore, be highly desirable.

- **FREEZE-OUT:** Experimental TOF data may even have a direct impact during the freeze-out phase, where they contribute to smoothen the pronounced odd-even effects predicted for the primary yields. In this context, the following nuclei could be studied : ^{90}Sr, ^{123}Sn, ^{126}Sn, ^{127m}Te, ^{182}Hf, ^{210}Pb, ^{226}Ra, ^{227}Ac, and several higher actinides.

- **GIANT DIPOLE RESONANCE (GDR) :** Essential for the prediction of nuclear reaction rates for unstable nuclei is the knowledge of the low-energy tail of the GDR. It is well known that the low-energy dependence of the GDR is stronger than given by the standard Lorentzian. Furthermore, a non-zero limit for E_γ has to be assumed. Recently, an indication of so-called *pygmy* resonances in the low-energy tail of the GDR could be found in some experiments on heavy, neutron-rich nuclei. These resonances depend on the formation of a neutron-skin and the introduction of an additional vibrational mode of the skin-neutrons against the core built from protons and remaining neutrons. Pygmy resonances enhance considerably the capture cross sections of very neutron-rich nuclei but various theoretical models exist to predict the resonance properties far from stability. Such an enhanced neutron capture would heavily impact the r-process path and the r-process freeze-out.
  High resolution neutron capture measurements between thermal energies and 1 MeV can probe the behavior of the low-energy tail of the

GDR as well as test different predictions of neutron capture enhancement by pygmy resonances. Of interest are γ -ray spectra as well as neutron capture cross sections. Among others, interesting targets include ^{93}Nb, ^{105}Pd, ^{126}Sn, ^{143}Nd, ^{166}Ho, ^{176}Lu, ^{182}Hf, ^{197}Au, and a number of isotopes from Os to Pb. Of special interest is ^{210}Pb, a very neutron-rich isotope for which capture cross section enhancements of a factor 5–10 have been predicted.

- NEUTRON INDUCED FISSION : Fission enters into the r-process path in several ways: It can terminate the r-process path at Z~92, during freeze-out, it can alter the resulting abundances of the long-lived heavy isotopes ^{232}Th, ^{235,238}U and ^{244}Pu, which are used to determine the duration of nucleosynthesis in our galaxy and the galactic age as well as the age of the Universe. Finally, in environments with a long duration of neutron exposure, *fission cycling* can determine the total abundance of heavy nuclei. This is relevant for primordial nucleosynthesis in neutron-rich zones of an inhomogeneous big bang.
  However, the r-process path is located in the region of highly neutron-rich nuclei with short β-decay half-lives. Because of β-decay Q values of the order of 13-15 MeV, β-decay will populate highly excited states above the fission barrier and, consequently, β-delayed fission plays a more important role than neutron-induced fission. The only available experimental tests for theoretical predictions of β-delayed fission comes from the analysis of abundances in the products of nuclear explosions. Therefore, the prediction of fission barrier properties (height and curvature) is essential for the astrophysical applications. Neutron-induced fission can support calculations by providing test cases for theoretical barrier models and resulting predicted cross sections.

- INDIRECT REACTION RATE DETERMINATIONS : The high neutron flux at this facility provides the opportunity for a novel approach to derive information on nuclear reaction rates. In nuclear astrophysics, frequent use is made of reaction network calculations in order to determine final stellar yields of nuclei. Such calculations could also be utilized to analyze abundances from an artificially produced *miniature- r-process* in the extreme neutron flux inside the lead spallation target. After exposure and decay of highly unstable reaction products, the resulting abundances can be analyzed and compared to a calculation with a limited network code.

Such studies should provide valuable information on integral cross sections which can be used for testing the nuclear structure parameters needed in the cross section calculations. The feasibility of this idea has to be further investigated by studying different target materials. Similar network calculations will also prove important for Accelerator Driven Systems, ADS.
Hence, a corresponding irradiation channel should be considered in the design of the lead spallation target where these irradiations can be performed. This channel must be equipped with a rabbit system and a hot cell for sample handling.

3.A.3 – NEUTRON CAPTURE CROSS SECTIONS FOR THE p-PROCESS.

The requests for neutron capture data for the p-process are based on similar arguments with those made before with respect to the r-process. Also in this case, experimental TOF data would clearly improve the description of freeze-out effects in the p-process, where neutrons are liberated by (γ,n) reactions during the explosive burning of the Ne/O shell. The strong impact of the subsequent neutron capture reactions on the final abundance distribution has already been demonstrated by Rayet et al. (1990). Furthermore, (n,γ) cross sections of proton rich nuclei would be most useful in determining the inverse rates by detailed balance. Feasible cases at a spallation source include ^{53}Mn, ^{55}Fe, ^{57}Co, ^{59}Ni, ^{91}Nb, ^{92}Nb, ^{93}Mo, ^{97}Tc, ^{109}Cd, ^{137}La, ^{139}Ce, ^{143}Pm, ^{145}Pm, ^{145}Sm, ^{146}Sm, ^{148}Gd, ^{150}Gd, ^{154}Dy, ^{159}Dy, ^{157}Tb, ^{159}Dy, ^{172}Hf, ^{195}Au, ^{194}Hg, ^{202}Pb.

Apart from radioactive nuclei, there are a number of stable targets, which can also improve the data bases for p-process studies. This group consists of the rare stable p nuclei, where only small samples of isotopically enriched materials are available, comprising of 32 isotopes between ^{74}Se and ^{196}Hg, most of which have not yet been studied at astrophysically relevant energies. Though all of these isotopes are important in order to check and to improve statistical model calculations for p-process nucleosynthesis, the cases to start with may be chosen from mass regions near magic neutron numbers.

3.A.4 – NEUTRON CROSS SECTIONS FOR PRIMORDIAL NUCLEOSYNTHESIS.

Some of the neutron capture cross sections mentioned in the previous sections are also required in primordial nucleosynthesis calculations. In

particular, it has been recently realized that to test the production of some of the light nuclei in standard big-bang scenarios a number of neutron capture cross sections and reaction rates are necessary. These include neutron capture on ^{6}Li, ^{7}Li, ^{8}Li, ^{7}Be, ^{9}Be, ^{10}Be, ^{10}B, ^{11}B. In particular, the capture cross section of the Lithium isotopes may influence the primordial abundance of ^{7}Li and ^{6}Li. The production (and destruction) rates of these two isotopes provide an important test of consistency of the big-bang nucleosynthesis as well as on the baryon density of the universe.

It is important to notice here that some of the nuclei involved in the primordial nucleosynthesis networks are being investigated for their exotic structure properties. For example, the ground-state of ^{11}Be is one of the most clear examples of neutron halo nuclei. Its structure can be investigated in the ^{10}Be $(n,\gamma)^{11}$Be channel as well as in the Coulomb dissociation process (the latter being an important reaction mechanism widely employed in experiments with radioactive ion beams). The neutron capture by ^{10}Be may therefore provide an important test of the neutron halo structure of ^{11}Be.

The reaction network requested in non-standard big-bang models such as that for the inhomogeneous big-bang cosmology, is even more extended. For these kinds of investigations, the capture cross sections requested include the following stable and unstable targets: ^{12}C, ^{13}C, ^{14}C, as well as several nitrogen and oxygen isotopes. In this case the neutron capture rates directly influence the production of the light elements up to mass number A ~ 40.

Because of their extremely small (n,γ) cross sections, all these cases represent an experimental challenge. Nevertheless, successful measurements appear feasible with the very high neutron flux provided by the CERN-PS spallation source, at least for some stable and long-lived isotopes.

3.A.5 – IMPROVEMENT OF THE STATISTICAL MODEL

- EXTRAPOLATION TO UNSTABLE NUCLEI : A number of nuclear properties have to be known for statistical model calculations. Far from stability, such properties have to be taken from theoretical predictions. In order to test and improve the parametrizations and predictions, nuclear information (cross sections, strength functions, level densities) has to be obtained over a wide range of masses and energies, including unstable

nuclei. Especially at neutron shell closures, neutron strength functions and level densities are still not well-known and also hard to predict. A high-flux facility can be used to determine the relevant information also at low count rates, which are due to the low capture cross sections at neutron magic numbers. Likewise, a high energy resolution is useful to study the interplay between compound capture and direct capture, which is important for nuclei with low level densities. A similar interplay proves important in the r-process path, close to the (experimentally unaccessible) neutron dripline. Unstable nuclei around N=50 include ^{85m}Kr, ^{89}Sr, ^{91}Nb, ^{92m}Nb, ^{93m}Mo; around N=82 ^{137}Cs, ^{37}La, ^{45}Pm, ^{45}Sm.

- EXPERIMENTS ON ISOMERS : The experiments listed above include already a number of isomeric targets, e.g. the branch point ^{210m}Bi or cases related to explosive nucleosynthesis such as ^{127m}Te. An important nucleus is ^{180}Ta, which occurs naturally as an isomer and which is part of a branching at A=179. There is a lot of astrophysical interest focused on this isotope, since it is yet completely unknown how it is produced in nature. With experimental neutron capture data, it would be possible to establish at least the s-process contribution in a reliable way. The problem here would be to produce an appropriate sample, since the best presently available enrichment is only 5%. Reactions in stellar and explosive environments proceed on thermally excited targets. This modification usually has to be included into the rate calculation by theoretical means and can give considerable contributions when low-lying target states are populated. In order to study the reliability of the stellar enhancement factors, capture data on isomeric targets can be used. In this way, the accuracy of the calculated transmission coefficients and the reliability of the neutron optical potentials for targets not being in the ground state can be tested, especially if the cross sections for the ground state and the isomer could be measured in the same isotope. Such a case may be studied in ^{93}Nb, where the isomer is preferentially produced via β–decay.

- NEUTRON CROSS SECTIONS OF (n,x) REACTIONS : Neutron reactions among the light elements below Fe have contributed to the abundances of some neutron-rich isotopes, e.g. to ^{36}S. In this mass region, (n,p) and (n,α) reactions are important in addition to neutron capture. In this context, the ^{39}Ar(n,α)^{36}S cross section is the only yet unmeasured s-process rate that

contributes to the ^{36}S abundance. This measurement would best be done with an implanted ^{39}Ar sample.

The importance of (n,p) reactions for stellar beta decay rates was emphasized by Aufderheide et al.[3.6]. The (n,p) reactions have been developed as a probe of the GT_+ strength (similar to an electron capture with neutrino emission). In the core of a pre-supernova star, the electrons are highly degenerate and are able to induce captures into these GT resonances. Because both the decay and capture rates are exponentially sensitive to the location of the GT_+ resonance, the experimental measurements of them are of extreme interest.

Neutron production in the s-process is mainly based on the $^{13}C(\alpha,n)^{16}O$ and $^{22}Ne(\alpha,n)^{25}Mg$ reactions, but $^{21}Ne(\alpha,n)^{24}Mg$ may also contribute to some extent. These cross sections are not yet directly measured in the relevant stellar energy range. The best way to improve the necessary extrapolation to the stellar energy range is to combine as many reaction channels as possible by an R-Matrix analysis. Accordingly, improved measurements of the (n,α) cross sections of ^{16}O, ^{24}Mg, and ^{25}Mg would provide a significant contribution to this problem.

A series of (n,α) measurements on intermediate to heavy mass targets would provide valuable constraints on nuclear models used to calculate (γ,α) and (α,p) reaction rates for studies of the nucleosynthesis occurring during novae and supernovae explosions. These (γ,α) and (α,p) rates are the largest nuclear physics uncertainty limiting the understanding of the yield of proton-rich isotopes resulting from these astrophysical explosions. Direct (γ,α) and (α,p) measurements are currently very difficult or impossible and the rates are, at present, very poorly constrained by theory. The main difficulty is thought to be the poorly understood α-nucleus potential in the statistical model used to calculate these rates. A series of (n,α) measurements could eliminate this uncertainty by providing data with which to constrain the statistical model calculations at astrophysically meaningful energies. The main experimental challenge will be to measure these small cross sections across a broad enough energy range. Measurements on as many as 30 nuclides across a range of masses from Sulfur to Hafnium should be possible.

- INELASTIC SCATTERING DATA : Inelastic scattering cross sections below about 500 keV neutron energy are required for describing the effect of thermally excited nuclear states. Similar to what has been said in the

context of measurements on isomeric states, also the inelastic channels are important for the calculation of stellar enhancement factors – including the case of superelastic scattering from a higher initial state to a lower final state, a process where neutrons gain energy. Such measurements should concentrate on the mass region $150 < A < 190$, where the stellar (n,γ) rates of some 30 nuclei are significantly influenced by this effect.

3.B – NEUTRON CROSS SECTIONS FOR CORNERSTONE APPLICATIONS.

Many applications, such as fusion, fission reactors, accelerator-based systems, transmutation of nuclear waste, energy production, dosimetry and radiotherapy require nuclear data that quantitatively and qualitatively go beyond the presently available traditional evaluation. For instance, one of the possible candidates for the neutron multiplying and tritium breeding zone of the fusion reactor is ^{9}Be. For this reason not only the accurate knowledge of all integral cross sections but also of the energy and angular distribution of the secondary neutrons is needed for fusion technology [3.7]. Up to now little experimental data exist for the cross section for the ^{9}Be(n,2n) reaction, which is mainly responsible for the emission of secondary neutrons. Nearly all reactions induced by neutrons with energies higher than the threshold for inelastic scattering lead to a decay of the compound system into two neutrons and two α particles.

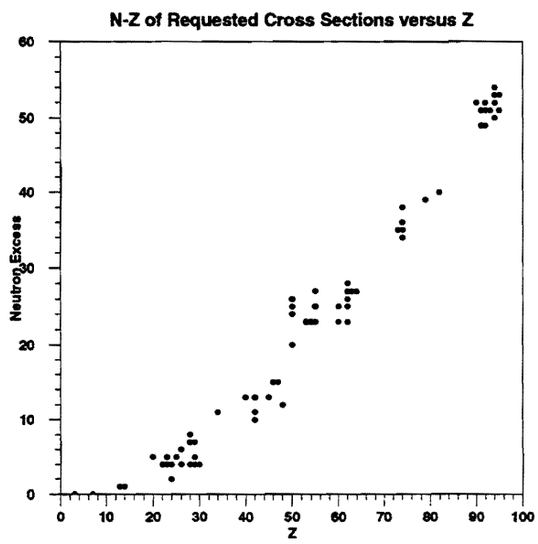

Figure 3.2: The requested isotopes in the OECD/NEA 1998 High Priority List [3.8] as function of the charge number and the neutron excess.

The Nuclear Energy Agency of OECD compiled these needs in the "High Priority Nuclear Data Request List". The purpose of the list is to provide a guide for those planning measurements, nuclear theory and evaluation programmes. The 1998 List includes more than 200 requests from 7 different countries [3.8] for Standards, Fusion, Fission, Dosimetry, Medical and Industrial applications (Figure 3.2).

3.B.1 – ADS AND WASTE TRANSMUTATION APPLICATIONS.

The present concern about a sustainable energy supply is characterised by a considerable uncertainty : the green house effect and foreseeable limits in fossil fuel resources on the one hand, the concern about the environmental impact of nuclear fission energy and the long term fusion research on the other hand, have led to the consideration of a variety of advanced strategies for the nuclear fuel cycle and related nuclear energy systems. The present research directories concern such strategies as the extension of the life span of presently operating reactors, the increase of the fuel burnup, the plutonium recycling, and in particular the incineration of actinides and long-lived fission products, the accelerator driven nuclear energy systems like the energy amplifier concept of C. Rubbia, and the possible use of the Thorium fuel cycle. The detailed feasibility study and safety assessment of these strategies requires the accurate knowledge of neutron nuclear reaction data. Both, higher fuel burnup and especially waste incineration options require improved and partly new data on minor actinides and long-lived fission products. Better data are also demanded for specific structural components of accelerator driven systems.

Evaluations performed on neutron induced reaction cross sections for neutron data libraries presently in use [3.9] are based on differential measurements. However, they rely to a large extent on theoretical model codes to complement the databases where data are lacking or inconsistent. Such model predictions are benchmarked against (i) crucial integral experiments and (ii) the available differential data, that are obtained under different conditions and in different neutron energy domains. Nevertheless, evaluated data files often show substantial differences amongst them due, on the one hand, to the lack of measurements and on the other hand to differences in fitting procedures and the use of different nuclear models ; this is the case for the minor actinides, long-lived fission products and other poorly measured nuclei. The detailed requirements for neutron nuclear data measurements are collected in "The NEA High Priority Nuclear Data Request List" which is edited by the working Party on

International Evaluation Co-operation of the OECD-NEA Nuclear Science Committee. Indeed, while thorium and uranium related cross sections could be considered as relatively well known, there are sometimes gigantic differences between databases when it comes to curium and americium, or more generally to minor actinides [3.9, 3.10]. Important minor actinides are ^{232,233}Pa (for the ^{232}Th-^{233}U fuel cycle), ^{237,238}Np, $^{241\text{-}244,242m,244m}$Am and $^{242\text{-}248}$Cm.

Despite the huge and well organised amount of neutron induced reaction data, the onset of new applications broadened the range of needed data beyond the canonical reactor-driven sets. For instance minor actinides, not critical for fission reactors, gained importance in Accelerator Driven Systems (ADS) for waste transmutation and energy production, as well as the unstable fission products. In particular, the concepts in Europe (ADS) and the U.S (ATW) envision transmuting the actinides (except uranium) from a light water reactor spent fuel in a subcritical assembly. The TARC experiment has directly demonstrated the success of the transmutation through adiabatic resonance crossing as an efficient incineration method in the examples of several long-lived fission fragments and actinides [3.11].

Nuclide	Half-life	Thermal $\sigma_{n,\gamma}$ (b)	Thermal $\sigma_{n,f}$ (b)	ENDF/B-VI Quality [Ref. 3.76]
^{237}Np	$2.1 \cdot 10^6$ y	176 ± 3	$(21.5 \pm 2.4)10^{-3}$	Good
^{238}Np	2.1 d	~ 300	2088 ± 30	Very weak
^{238}Pu	87.7 y	~605	17.1±0.4	Very weak
^{242}Pu	$3.7 \cdot 10^5$ y	18.7± 0.7	-	Weak
^{244}Pu	$8.1 \cdot 10^7$ y	1.6± 0.3	-	Very weak
^{241}Am	433 y	620 ± 13	3.2 ± 0.1	Reasonable
^{242m}Am	141 y	~2000	6328± 320	Very weak
^{243}Am	7370 y	75.1 ± 1.8	0.198 ± 0.004	Needs update
^{242}Cm	163 d	16 ± 5	< 5	Very weak
^{243}Cm	29.1 y	137.4± 9.6	633.3± 26.9	Very weak
^{244}Cm	18 y	15.2 ± 1.2	1.04 ± 0.20	Reasonable
^{245}Cm	8500 y	340± 20	2143± 58	Weak
^{246}Cm	470 y	1.22 ± 0.16	0.14 ± 0.05	Needs update
^{247}Cm	$1.6 \cdot 10^7$ y	57 ± 10	81.9 ± 4.4	Weak
^{248}Cm	$3.5 \cdot 10^5$ y	2.63 ± 0.26	0.37 ± 0.05	Needs update
^{232}Pa	1.3 d	700 ± 100	464 ± 95	None

Table 3.2: *Higher Actinides Transmutation candidates, heavily produced in a PWR. The cross sections are from Mughabghab [3.12] comments refer to ENDF/B-VI.*

The bulk of the charge in this accelerator driven assembly will consist of isotopes of Np, Pu, Am, and Cm. The neutron spectrum in the assembly will be quite hard, with half of the flux above approximately 0.2 MeV. Measurements of interest to this program include differential (n,γ) and (n,f) cross sections.

NEA Req. ID	(Z,A)	$\tau_{1/2}$ or Abundance [%]	Mass [mg]	(n,γ) events/ d	Req. country & Priority	Use
4.A.8	Cr-50	4.3 %			D	SM
4.A.10	Cr-52	83.8%			D	SM
4.A.12-16	Ni-nat	-			F1,Ja,USA	SM
4.D.12	Se-79	6.5×10^5 y	250	1.4×10^7	F2	FF
4.D.13	Zr-93	1.5×10^6 y	1000	7.3×10^6	F2/D	FF/SM
4.D.14	Mo-95	15.9 %			F1,UK1	FF
4.D.1/15	Tc-99	2.1×10^5 y	31	4.3×10^6	F,UK,Ru	FF
4.D.2/16	Rh-103	100 %			UK1,F2	FF
4.D.17	Pd-107	6.5×10^6 y	1000	4.6×10^7	F2	FF
4.C.2	Cd-nat	-			F1,UK2	AM
4.C.18	Sn-120	32.6 %			WPEC	SM
4.C.19	Sn-122	4.6 %			WPEC	SM
4.C.22	Sn-124	5.8 %			WPEC	Fusion
4.D.19	Sn-126	10^5 y	20	2.1×10^3	F2	FF
4.D.20	I-129	1.57×10^7 y	1000 (IF)	1.6×10^7	F2	FF
4.D.3	Xe-131	21.2 %			Ja	FF
4.D.4/21	Cs-133	100 %			F1,UK1,Ru	FF
4.D.5/22	Cs-135	2.3×10^6 y	0.37	8.1×10^3	F2,Ja,Ru	FF
4.D.23	Nd-143	12.2 %			F1,UK1	FF
4.D.24	Nd-145	8.3%			F2,UK1	FF
4.D.25	Sm-147	15 %			F2,UK1	FF
4.D.26	Sm-149	13.8 %			F1,UK1,Ja	FF
4.D.27	Sm-150	7.4 %			F2	FF
4.D.28	Sm-151	90 y			F1,UK1,Ja	FF
4.D.29	Sm-152	26.7 %			F1,UK1	FF
4.D.29	Eu-153	52.2 %			F1,UK1	FF
4.C.5	Gd-nat	-			F2,UK2	AM
4.D.29	Gd-155	14.8 %			F2,UK1	FF
4.C.6	Dy-nat	-			F2,UK2	AM

***Table 3.3** : Requested neutron capture cross sections for stable and radiactive Fission Fragments (FF), Structural (SM) and Absorber (AM) Materials according to Ref. [3.13]. The index of request and the requesting country with the priority given by the country are also presented.*

The production and destruction of minor actinides and fission fragments in the ADS assembly, along with their fission neutron multiplicity, help to

determine the neutron economy of the assembly and the evolution of the fuel composition. Regarding the transmutation of Actinides, data are required for nuclides important in the ^{232}Th-^{233}U energy production cycle and in burning ^{239}Pu, as well as for the higher actinides in fission reactor waste that would be introduced into the EA for destruction. A qualitative assessment of evaluated data in the ENDF/B-VI file for important higher Actinides is given in Table 3.2, including thermal cross sections from Mughabghab' s compilation [3.12]. There is presently no evaluation in the ENDF/B-VI file for ^{232}Pa while the evaluations concerning ^{238}Np, ^{242}Am and ^{247}Cm are regarded as weak.

The comprehensive elimination of PWR waste implies consideration for the transmutation of several long-lived Fission Fragments into stable species as well. For such elements, the information is even more lacunary and in many important cases as ^{90}Sr (with a half-life of 28.8yrs which is very important for the calculation of reactor neutronics), ^{129}I and ^{135}Cs there are orders of magnitude discrepancies in the experimental data, which are mostly confined to the region of thermal or epithermal neutrons. A list of the more important long-lived fission products that are transmutation candidates is given in Table 3.3, together with a selected summary of the requests by NEA/OCDE.

In addition to the fission fragments, in ADS systems interest is focused to the target, beam and structural materials. All these materials are exposed to both the direct beam protons and the secondary neutrons, ranging in energy from the primary beam energy down to thermal energies. Target materials under current consideration are Pb and Pb-Bi eutectic. The structural materials (C, Al, Si, P, Cr, Fe, Mn, Ni, Zr, Mo, Sn) and liquid metal coolant (Pb, Bi) are irradiated by neutrons from (p,xn) reactions with a significant hard component near the target, which becomes a slightly moderated fission spectrum further into the subcritical core region. Transmutation/activation cross sections are required for all nuclides that are products of spallation, fission, absorption, activation, (n,x), (n,xn) etc. reactions, including nuclides that are formed in isomeric states.

The (n,γ) and (n,f) reactions are the most important ones to develop transmutation projects, since they allow to transform long-lived radioactive isotopes into short-lived ones, but may also transform stable ones into radioactive ones. Charged particle producing reactions such as (n,p) and (n,α) reactions have generally much lower cross sections, usually below 100 mbarns. They are therefore of lesser importance in the energy production of Accelerator Driven systems (ADS). However, (n,n') and (n,xn) have cross sections which can

attain several barns and are of great interest in the conception of ADS projects, since they govern the neutron flux and a large part of the energy flux in reactors, but the experimental investigation of (n,X) reactions appears more complicated than that of (n,γ) or (n,f) ones.

In terms of nuclear reactions, the required data are neutron total, elastic and inelastic scattering, double differential (n,xn) and (n,xp), (n,γ), (n,f), (n,x) and (n,xγ) cross sections. Double differential cross sections with heavy products (α, etc.) would be also very useful for nuclear reaction modelling, while data on (n, $x\pi^{\pm o}$) at 600-1000 MeV even with a moderate resolution are very interesting since very scarce relevant data exist in this region. These data are of relevance for the determination of the transmutation rates, to the inventories in LWRs, LWR-MOX, LWR-MOX with multiple recycling, to the design and inventories of waste burners and to the calculations of the neutron multiplication factor, of radiation damages and of gas production in such systems.

The expertise in measuring keV neutron cross sections of stable and unstable isotopes, which was developed over more than two decades for astrophysical problems, can be of immediate interest for reactor and ADS applications. Already the presently available techniques allow for a number of accurate measurements, either for resolving discrepancies in existing data or for exploring terra incognita, e.g. the urgently needed neutron nuclear data for ^{233}Pa and ^{233}U. A number of important nuclei for transmutation studies, such as stable, long- or medium-lived fission products (Table 3.3), are accessible to measurements with the techniques and detectors of the TOF Collaboration. Depending on the accessible resources, this could be achieved in a foreseeable period of time and with a moderate financial effort. The EC priority to ADS in the 5th Framework Programme is clearly stated and the requirement from the European Nuclear Industry for more complete and precise Nuclear Data has been generally adopted by EC.

Although it's always valuable to have precise nuclear data on all sort of elements, the expression "measurement campaign", lead us to try to define a program which answer, in a coherent approach, well identified questions. We present them below in three items :

1) The first question to answer through the measurement campaign concerns the nuclear data related to the thorium cycle, which is considered to be the most promising fuel to reduce the production of the long lived heavy element component of the waste. Problems related to

the future of nuclear energy and the role of ADS is organised around two main questions :

What is the optimal way for producing nuclear energy in the long run?

As shown by C.Rubbia et al and other studies, fast neutron ADS using thorium cycle is a very promising solution. It has been shown that it reduces radiotoxicity released by the fuel reprocessing by large factors compared to present solution or to the uranium based cycle. Sustainability for long term and massive production is provided, while the specific properties of ADS are improving the safety and the flexibility of such reactors which can burn a large variety of fuels.

What can be done with the already existing nuclear waste produced, or to be produced by present PWR reactors ?

Different scenario are presently studied. In one class of scenario, actinides (Pu and other heavy elements) are recycled in fast neutron reactors (critical or ADS reactors). In this case the heavy element component of the waste is used as fissile material. In the other class of scenario, a new generation of PWR reactors is operated, coupled to fast neutron reactors (fully or partly based on ADS) in order to burn and to reduced significantly the amount of waste to be put in repository. Thermal ADS reactors using molten salt fuel are also proposed to reduce the Plutonium inventory.

In the thorium cycle (^{232}Th–^{233}U) the fissile element is ^{233}U and the regeneration process of the fissile element is ^{232}Th(n,γ)^{233} Pa -> ^{233}U + β. The ^{232}Th(n,γ) and ^{233}U(n,f) reactions are the basic cross sections and have to be known very precisely. An important cross section (but very difficult to measure) is the ^{233}Pa(n,γ) (τ= 30d) reaction. In the uranium cycle (^{238}U-^{239}Pu) the main fissile element is ^{239}Pu, and the regeneration process of the fissile element is ^{238}U(n,γ)^{239}Np -> ^{239}Pu + β. Therefore, the ^{238}U(n,γ) and ^{239}Pu(n,f) reactions are the basic cross sections and have to be known precisely.

In fast neutron reactors the (n,n') inelastic scattering has also to be considered, since the ratio of fission over capture cross section is in some cases very dependent of the neutron energy spectrum. Therefore the ^{238}U (n,n') and ^{232}Th(n,n') cross sections have to be also determined.

The Long Lived Heavy Elements (LLHE) component of the waste comes from parasitic reactions which are produced on the different constituents

of the fuel. The important reactions for LLHE are well identified for each fuel cycle.

For the **Th-cycle the parasitic reactions** are $^{233}U(n,2n)^{232}U$, $^{232}Th(n,2n)^{231}Th \rightarrow \beta^- + ^{231}Pa$ and $^{231}Pa(n,\gamma)^{232}Pa \rightarrow \beta^- + ^{232}U$ leading to the production of ^{232}U, which is responsible for a large part of the short term (few centuries) radiotoxicity, and ^{231}Pa responsible for the long term radiotoxicity.

For the **U cycle the parasitic reactions** produce LLHE :

$^{238}U(n,2n)^{237}Np$, $^{235}U(n,\gamma)^{236}U(n,\gamma)^{237}U$ (6 days) $\rightarrow$ **^{237}Np** and

$^{239}Pu\ (n,\gamma)^{240}Pu\ (n,\gamma)^{241}Pu\ (n,\gamma)^{242}Pu(n,\gamma)^{243}Pu$ (5 hours) $\rightarrow$ **^{243}Am**

where $^{241}Pu \rightarrow$ **$^{241}Am(n,\gamma)^{242}Am$** and $^{242}Am \rightarrow {}^{242}Cm(n,\gamma)^{243}Cm(n,\gamma)$ **^{244}Cm**

$^{243}Am(n,\gamma)^{244}Am$ (10 hours) $\rightarrow$ **^{244}Cm**

$^{242}Cm \rightarrow \alpha +$ **^{238}Pu** and $^{237}Np(n,\gamma)^{238}Np \rightarrow$ **^{238}Pu**

From these parasitic reactions, it is rather obvious that the LLHE production is driven by the (n,γ) reactions. These (n,γ) cross sections are very important but poorly known because of the difficulty to get precise experimental data. An important effort has to be made to measure this type of cross sections using the TOF facility.

2) The second question is related to the Long-Lived Fission Products (LLFP) transmutation in order to reduce their long term radiotoxicity. The LLFP production rate per Terawatt-hour-electric in a PWR reactor is presented below :

LLFP	Period in years	Production per TWh_e	LLFP/fission
^{79}Se	$7\ 10^4$	20 g	0,045 %
^{93}Zr	$1,5\ 10^6$	2.8 kg	5 %
^{99}Tc	$2,1\ 10^5$	3.2 kg	5,4 %
^{107}Pd	$6,5\ 10^6$	800 g	1,2 %
^{126}Sn	10^5	80 g	1,1 %
^{129}I	$1,57\ 10^7$	700 g	0,9 %
^{135}Cs	$2\ 10^6$	1.4 kg	0,17 %
^{151}Sm	93	60 g	0,066 %
^{90}Sr	28	1.9 kg	3,5 %
^{137}Cs	30	4.4 kg	5,4 %

Relatively large amount of such LLFP are produced in any fission nuclear reactor. This production is only slightly dependent on the fuel or the neutron energy spectrum.

The way to reduce the LLFP radiotoxicity is to transmute them by (n,γ) reactions which lead in general to stable or short lived nuclides. However, in most cases the neutron energy spectrum has to be well adapted to enhance the transmutation efficiency as demonstrated in the TARC experiment. So the (n,γ) cross sections for LLFP have to be precisely determined from the thermal region up to a few MeV. A good energy resolution is needed, because the resonance's energy region is very important for such transmutation processes.

3) In the target of an ADS or in its vicinity the spallation process produces high energy E>10 MeV neutrons which can induce (n,xn) reactions, but are also producing charged particles (mostly p and α). Cross-section measurements for target, structural materials around it, and even fuel materials irradiated by such a hard neutron component, are not only important to calculate precise neutronics characteristics, but also for radiation damage studies and evaluation of the gas induced production inside the material. We propose to start this program by studying (n,xn) and (n,p) reactions on Pb and Bi, as well as (n,p) and (n,α) reactions on Fe, Cr, Mn, Ni, Mo.

3.B.2 – DOSIMETRY IN RADIOLOGICAL PROTECTION AND THERAPY.

Accurate cross section evaluations for neutron induced reactions, including charged particle and gamma ray emission, are required for radiation transport calculations of any type of radioprotection and radiotherapy. The type, accuracy, and specificity of the needed information vary with the application. Similarly, the gamma rays produced by neutron interactions as well as energy and angular distributions for secondary neutrons are a major concern also for transport calculations, for instance, as a source of background in experimental nuclear and high energy physics.

Nuclear data are fundamental to our understanding of dosimetry in radiological protection (assessment of doses to aircraft crews for instance) and radiation therapy when energetic neutrons are used. Neutron dosimetry for

neutrons up to 14 MeV is underdeveloped compared to gamma dosimetry. There is an urgent need for materials sensitive to fast neutrons in order to comply with present (more strict) regulations. For neutrons above 14 MeV the necessity to develop new dosimetric methods is even more important. At present for higher than 14 MeV energies no dosimeters are known. So a serious effort is needed to develop high energy neutron dosemeters.

Neutron therapy dosimetry and more importantly neutron transport calculations for dosimetry demand detailed microscopic charged particle production information for prediction and interpretation of absorbed dose to the patient. The same need exists for advanced proton therapy facilities, where secondary neutrons are produced with energies as high as 250 MeV. Since data above few MeV are scarce, presently, only nuclear model calculations can provide some of the needed information. Measurements of neutron interaction cross sections for different elements, in a wide energy range, would allow to perform more accurate simulations of the moderation process for new materials being considered for accelerator-based therapies. In particular, the accurate determination of resonances of the cross section in the high-energy region could lead to the design of more efficient beam shaping assemblies, and to the setup of epithermal neutron beams of superior quality than the ones currently available in BNCT. Finally, reliable neutron interaction cross sections are necessary to determine with high accuracy the dose produced in the therapy by the epithermal neutron beams and therefore are of fundamental importance in the treatment planning for cancer therapy.

Table 3.4, shows the principal needs organised by dosimetry and transport. As for C, N and O, there is a scarcity of microscopic cross section information for the stated elements. A needed high priority measurement is charged particle emission spectra from neutron reactions on oxygen for wide range of emission angles. Besides C, N and O, Si and Ca require the most complete information of dosimetry. Detailed ejectile data are needed for Si to support applications in medical electronics. As bone is almost always present in the radiated field in Neutron Radiotherapy, Ca data are essential for accurate dosimetry. As P, K and N are present at less than a few percent in most tissues and dosimeters, less comprehensive data are required. For neutron transport calculations, Fe and W are the elements next in importance to C, N and O. Information about Si, Ca and N is required for transport calculations due to their presence in significant quantities in concrete and air.

Dosimetry					Transport		Importance[1]* [Ref. 3.77]
Element	p	α	d	recoil	Element	n, γ	
H	3				H	3	1
C	3	3	3	3	C	3	1
O	3	3	3	3	O	3	1
Si	3	3	3	3	Fe	3	2
Ca	3	(3)	(3)	3	W	3	2
P	3	(3)			Si	3	3
K	3	(3)			Ca	3	3
N	3	(3)			Pb	3	3
					N	3	3

Table 3.4: Required neutron cross section information for dosimetry and radiotherapy.

3.C – NEUTRONS AS PROBE FOR BASIC NUCLEAR PHYSICS.

3.C.1 – THE NUCLEON-NUCLEON INTERACTION.

3.C.1.A – NEUTRON-NEUTRON SCATTERING LENGTH : The question of charge symmetry of the nucleon-nucleon interaction is a longstanding problem in nuclear physics. Nowadays the violation of charge symmetry is well established and is explained as a consequence of the differences in the masses and the electric charges of the *d* and *u* quarks [3.14]. The quark mass difference manifests itself in the difference of the $^1S_0$ neutron-neutron (nn) and proton-proton (pp) scattering lengths a_{nn} and a_{pp}, respectively. Therefore measurements of a_{nn} and a_{pp} yield a direct experimental determination of the quark mass differences. Proton-proton scattering experiments provide the value a_{pp} although significant uncertainties arise in the analysis due to the Coulomb force. The best available value is

$$a_{pp} = -17.3 \pm 0.4 \text{ fm}$$

where the errors state the uncertainty due to the model dependence of the analysis [3.15]. The determination of a_{nn} requires a more sophisticated experiment

[1]Importance:
(1) Need best accuracy, most complete data, small neutron energy intervals.
(2) Need good accuracy, wider spacing of neutron energies.
(3) High accuracy is not needed; approximate data are required.

because neutron-neutron scattering experiments are not feasible until now. In principle the determination of a_{nn} has been performed via two reactions. One is the $^2H(\pi^-,\gamma)nn$ reaction with two strongly interacting particles in the exit channel. At the moment the best value of a_{nn} has been obtained from such a measurement [3.15],

$$a_{nn} = -18.5\pm0.05(stat)\pm0.44(syst)\pm0.3(theor)\ fm.$$

Most determinations of a_{nn} have been performed via the neutron induced deuteron breakup [3.16] at incident neutron energies between 10 and 130 MeV. However, these studies lead to rather large discrepancies in a_{nn} because of the use of non-realistic NN-potentials and our ignorance about the three-nucleon force.

To solve this problem in the nd-system new consistent measurements and analyses of the neutron induced deuteron breakup are required over a range of energy, where one has to choose the best kinematic situation from the theoretical point of view. It is the hope that such measurements can clarify the role of $\rho-\omega$ mixing to determine charge symmetry breaking effects [3.17].

The TOF Collaboration provides an ideal framework for this experimental program because it includes collaborations with the leading neutron source institutes in Europe. In the beginning phase measurements at several incident energies smaller than E_n=180 MeV could be performed at the TSL(Uppsala) neutron beam facility in Uppsala. These results would represent an excellent reference for the second phase when a transfer of this experiment to the TOF Facility at CERN is envisaged to cover systematically an extended energy range up to 250 MeV and beyond.

3.C.1.B – NEUTRON-PROTON BREMSSTRAHLUNG : In the late sixties and early seventies there has been a great effort to study the nucleon-nucleon (NN) bremsstrahlung process because it was hoped that it provides a crucial test for the off-shell behaviour of the NN interaction which cannot be extracted from elastic NN scattering data. Extensive calculations [3.18], mostly in non-relativistic potential models, and comparison with available experimental data indicated only a small sensitivity on the off-shell behaviour of the NN-interaction. As a consequence the effort on NN bremsstrahlung has been reduced. Only in the late eighties polarized bremsstrahlung data [3.19] became available and seem to indicate that off-shell effects might be important. Recent considerations give strong arguments that NN-bremsstrahlung cannot exhibit off-shell effects [3.20].

Today there is an increasing interest in NN bremsstrahlung data. Originally the revival was triggered by the observation of energetic photons produced in intermediate-energy heavy-ion collisions [3.21]. Calculations based on transport equations to describe the heavy-ion dynamics lead to photon cross sections which are in reasonable agreement with experimental data [3.22]. The basic ingredient in such calculations is the elementary np-bremsstrahlung process, while pp-bremsstrahlung plays a minor role. Unfortunately, there is still a scarcity of the np-bremsstrahlung data and therefore calculations must rely on theoretical models. In addition there are persisting inconsistencies in the description of bremsstrahlung from pd and pA collisions.

The NNγ cross sections are an indispensable input for disentangling dynamical effects and medium dependent radiative corrections in photon yields of heavy-ion collisions [3.23]. Therefore systematic measurements of np-bremsstrahlung cross sections in a wide kinematical regime from 90 MeV to 1 GeV are required [3.24]. Of particular importance are the measurements above the pion threshold, where the cross sections may deviate considerably from that of theoretical models. The inclusion of the corresponding inelasticites in the T-matrix is usually not considered in simple model estimates. In addition a significant increase of the effect of meson exchange currents may occur above the pion threshold. Triggered by recent measurements of the pp bremsstrahlung above pion threshold, the development of a proper theoretical description for this energy regime can be expected in the near future. Since in np bremsstrahlung, charged pion exchange gives a large contribution to the cross section at low energies, it seems to be an ideal process to investigate rather directly a possible enhancement of meson exchange currents. Thus the availability of high energy np bremsstrahlungs data will have a great impact on this theory.

Because of the high proton energy of 24 GeV used for spallation there will be a considerable flux of neutrons up to energies of 1GeV. Making use of this unique feature of the CERN neutron source complete measurements of the np-bremsstrahlung cross sections including the option of the determination of the analyzing will be considered in a later phase at the TOF Facility. At the beginning only preparatory works and first tests at the TSL neutron beam facility in Uppsala are foreseen within the collaboration.

3.C.1.C – MESON PRODUCTION IN NEUTRON-PROTON SCATTERING: The study of nucleon-nucleon inelastic collisions provides a powerful tool to

deepen our insight into the properties of the nucleon-nucleon interaction and baryonic resonances. Specifically, meson production close to the kinematical threshold, where the relative momenta between the final state particles are small, provides valuable information on the nucleon-nucleon interaction.

Recently, high precision measurements of the reactions $pp \Rightarrow pp\pi^0$ and $pp \Rightarrow pn\pi^+$ [3.25] have been performed near the threshold. In both reactions the isospin of the entrance channel is I=1. Single pion production in neutron-proton scattering is required to study the contribution of the I=0 entrance channel. Therefore in a recent experiment at CELSIUS (Uppsala) the quasi-free $pn \Rightarrow pp\pi^-$ in pd collisions at 320 MeV has been studied. The availability of a beam of high energy neutrons would allow measurements of the free process. Besides total cross data no other data of this process are available. Recently, measurements of the single pion production in np scattering have been started in parallel to bremsstrahlung measurements at Los Alamos. Such experiments on meson production are under consideration also at the CERN TOF facility which provides a considerable flux of high energy neutrons unprecedented at energies above 800 MeV. The available energy range would also allow measurements on the η-production in free np scattering which are of specific interest because of speculations on the existence of a quasi-bound state in the twonucleon system [3.26]. Recently, measurements of the quasi-free $np \Rightarrow d\eta$ reaction have been performed at CELSIUS [3.27]. However, we are still far from a complete understanding of the production mechanism and further experiments are required. The possibility of such experiments at the CERN TOF facility requires still investigation.

3.C.2 – NEUTRON-NUCLEUS SCATTERING.

3.C.2.A – OPTICAL POTENTIAL : Optical potentials play a key role in nuclear physics because they are an important ingredient of most reaction calculations [3.28]. Besides theoretical calculations which can only provide the basic structure [3.29], the optical potential is usually determined from elastic scattering data. However, the extraction of the optical potential from scattering data is ambiguous because cross section and polarization data at a single energy do not determine the S-matrix uniquely. The degree of ambiguity of the analysis becomes reduced if the total reaction cross section is known and scattering data over a range of energies are available. It must be emphasized that the determination of the total reaction cross section is of great importance because it

represents an upper bound of the so-called defect term in the generalized flux theorem and suppresses considerably the substitution of absorption by reflection and vice versa in the analysis.

Neutron-nucleus elastic scattering data at high energies (from a few MeV to several hundreds of MeV) are of particular interest for several reasons.

- They provide an important test of theoretical model calculations performed with both non-relativistic and relativistic formulations. With neutrons, these tests can be made without the complication of a strong, long-range Coulomb interaction, which leads to ambiguities in the interpretation of so-called Coulomb corrections.

- They allow a direct comparison with proton-nucleus scattering at a given target nucleus. Apart from the Coulomb interaction the main source of the difference is the isospin term V_t of the optical potential

$$V_t = V_0 \, (\mathbf{t} \cdot \mathbf{T}) \, / A \, ,$$

where A is the mass number of the target nucleus, **t** and **T** are the isospins of the incident particle and the target nucleus, respectively. The dependences of the strength V_0 is subject to investigation.

- The high energy neutron-nucleus optical potentials are also required for a number of applied science programs such as assessing the possibility of accelerator driven systems for transmutation of nuclear waste which is discussed in chapter 3.B.

At present there is a scarcity of neutron-nucleus data above 100 MeV [3.30]. It is one of the goals of the TOF collaboration to fill this gap. Although this collaboration will focus on nuclei relevant for accelerator driven systems, measurements of elastic cross sections of other nuclei for the determination of optical potentials will also be obtained. Together with the knowledge of the total cross sections it will provide a valuable data set which allows to determine global optical potentials over a large range of nuclei and energies. With the increase of the data base these global optical potentials gain in predictive power and allow more reliable estimates of reaction rates of experimentally non accessible nuclei. The inclusion of analyzing power would further improve this data basis.

At this point it is appropriate to remark that in general the availability of a polarization option would be of interest for many nuclear physics questions. To

include this option at the TOF facility requires still some studies and could only be considered for a later phase.

3.C.2.B – INELASTIC SCATTERING : Inelastic scattering that leads to low-lying collective states, or giant resonances, can provide important nuclear structure information on the neutron and proton contributions to these excitations. Specifically one can obtain neutron transition densities as well as the ratio of the relative coupling to the protons and neutrons of the target nucleus. Since no dedicated experiments in this direction are planned, we do not discuss this point in more detail.

3.C.3. – THE FISSION AS PROBE OF NUCLEAR MATTER.

The study of nuclear fission induced by resonance and low energy neutrons is proposed in the energy range from 0.01 eV to 5 MeV. This is an investigation of the interconnection between fission channels and modes, obtaining the complete information on the potential energy surface of highly deformed fissioning nuclei from the stage of second deformation well population up to descent to a scission point. These experiments include the measurements of fission fragment mass (charge) and total kinetic energy distribution as a function of the incident neutron energy. From this data it is possible to obtain information on the nuclear viscosity at the stage of descent from outer fission barrier.

3.C.3.A – STUDY OF VIBRATIONAL RESONANCES IN ^{232}TH AND ^{234}U : The hybrid macroscopic-microscopic method, suggested by Strutinsky [3.31], can explain the neutron induced fission process by introducing a double-humped fission barrier (DHB). A good agreement between experimental data and theoretical predictions exists for the light and heavy actinides. However, nuclei with $87<Z<92$ show an anomalous behaviour and question the validity of this model. In particular, experimental results on the nuclei ^{230}Th and ^{232}Th indicate a dominant second barrier, resulting in the creation of a shallow third well [3.32] roughly 1 MeV deep, just deep enough to accommodate some very deformed metastable states with a ratio of major to minor axis of order 3. This effect suggests the existence of the triple-humped fission barrier (THB), predicted by A. Bohr already in 1955 [3.33]. Blons et al [3.34] showed experimental evidence for the existence of this THB in the fissioning ^{231,233}Th nuclei. The level density of the second well is hardly known.

The high quality CERN TOF neutron spectrometer permits to reveal structures of vibration resonances, directly confirming the existence of the THB for these anomalous elements. The measurement of the angular distribution of the fission fragments with an energy resolution comparable to that of the fission cross section allows the determination of spin and parity of such substructures. The double differential cross section, $d^2\sigma/d\Omega dE$, measurement of the fission fragments of ^{233}Th and ^{235}U, will evidence the individual rotational components and extract the associated band parameters. The interesting neutron energy region lies below and above the fission threshold at 1.4 MeV for ^{232}Th. In other words, it is necessary to determine the quantum and dynamical properties of all separate fission valleys. To do this, we are going to use Bragg-spectroscopy with twin Frisch-grid ionization chamber which has been used in neutron physics for the past 3 years at the IPPE, Obninsk. The first stage of the project can start in 2000 with a high-purity ^{232}Th target. All calibration procedures will be done at the KG-2.5 accelerator of the IPPE.

EXPERIMENTAL METHOD	Bragg-spectroscopy and Frisch-grid ionization chamber with wave form digitizer
ENERGY REGION	0.2 MeV — 4 MeV
TARGETS	Circular layers of high-purity (99,999%) thorium and uranium (>98%) isotopes, 10-100 $\mu g/cm^2$ thick, covered with gold, 30 $\mu g/cm^2$ thick
ISOTOPES	^{232}Th, ^{234}U — available now
MONITOR	^{235}U; calibration with thermal neutron induced fission fragments
CALIBRATION	Preliminary measurements and calibration at IPPE, Obninsk, KG-2.5 and EG-1 accelerators with T(p,n) and D(d,n) neutron sources with energy up to 5 MeV; determination of main corrections like fission fragments energy losses inside fissile targets and backings

It should be pointed out that many other light actinides such as ^{227,228}Ra, ^{227}Ac, ^{230,234}Th and ^{232}Pa, show also a resonant behaviour just below the fission threshold. The excitation of these "resonances" is found to be a few MeV greater than the first barrier maximum. The high energy resolution offered by the CERN-PS TOF facility could lead to the acquisition of the required fine-structure data for these nuclei.

PERSPECTIVE EXPERIMENTS FOR THE SECOND STAGE : The experimental studies on nuclear matter through neutron induced fission reactions should address the following problems :

1) INVESTIGATION OF THE MECHANISM OF DEEP DAMPING OF SHELL EFFECTS IN FISSION PROCESSES : It requires the detailed study of fragment mass-energy spectra for high energy neutron induced fission of heavy nuclei. Neutron energies range from 20 to 500 MeV. Moreover, the data of these experiments will be used to generate a Nuclear Data Library of evaluated data on fission product yields for ADS applications.

2) SYSTEMATICAL STUDIES OF NUCLEAR VISCOSITY EFFECTS AND DETERMINATION OF THE FISSION TIME WITH THE «NEUTRON CLOCK» METHOD : It requires precise measurements on neutron multiplicities as a function of the fragment's mass and of their kinetic energy. Large neutron detectors like DEMON with an incorporated grid-ionization chamber are preferred at the high-collimated neutron beam of the CERN TOF facility.

3) MEASUREMENTS AND THEORETICAL ANALYSIS OF EXCITATION FUNCTIONS AND EMISSION SPECTRA IN (n,xp), (n,xn) and (n,xa) REACTIONS : The required neutron energies span from 20 to 150 MeV. These experiments are addressing a scientific and a practical problem : i) to get new information on the total level density of nuclei far from stability and the level density for large angular momentum nuclei; it consists in the observation of the damping of collective modes with the excitation energy; ii) to investigate in details the mechanism of multi-cascade non-equilibrium emission of neutrons, charge particles and gamma-rays. Determination of these parameters for the corresponding theoretical models is important for various applications.

3.C.4. – THE NUCLEAR PHYSICS INTEREST IN THE (n,X) REACTIONS.

Charged particle producing reactions such as (n,p) and (n,α) reactions have low cross sections, usually below 100 mb. They are, therefore, of less importance in the energy production of Accelerator Driven systems (ADS). However, apart from their own interest for the Nucleosynthesis, they allow to improve the models which are used in the cross sections calculations. Moreover, they are very interesting from the point of view of fundamental Nuclear Physics.

Cross sections over a wide energy range are needed to determine the optical model parameters used to predict the non-measurable cross sections. Some of these reactions are exothermic and are of direct interest for astrophysics.

The Strasbourg group stressed the particular interest of the charge-exchange reaction (n,p) at intermediate energies. They have provided in the past a powerful probe of the spin-isospin response in nuclei [3.35, 3.36]. For a small momentum transfer the response is dominated by Gamow-Teller (GT) transitions, corresponding to $\Delta J^{\pi} = 1^{+}$ ($\Delta L=0$, $\Delta S=1$), which are identified by the strong peaking of the reaction cross section at 0^{o}. The GT strength in both light and heavy nuclei is generally "quenched" from that expected using "free nucleon" GT operators and shell-model calculations [3.37, 3.38, 3.39, 3.40]. This quenching is seen in beta decays strengths [3.41], but also in (p,n) [3.42] and (n,p) [3.43] reaction studies. A similar reduction factor is found in the spin component of the M1 strength measured in (e,e') and (p,p') experiments [3.44]. Two different mechanisms have been proposed for this quenching of the total GT strength. One is the $\Delta(1232)$-isobar nucleon-hole admixture into the proton-particle neutron-hole GT state resulting in a part of the GT strength being moved from the low excitation region to the delta excitation region at around 300 MeV excitation. The other is due to the higher-order configuration mixing in which the energetically high-lying two-particle two-hole (2p-2h) state mixes with the low-lying 1p-1h GT state and shifts GT strength to the energy region beyond the GTGR. This quenching is generally discussed in the model-independant "3(N-Z)" sum rule of Ikeda [3.45]. In order to elucidate the different mechanisms new measurements should be done at the CERN TOF facility, using (n,p) reactions at $E_n > 100$ MeV

3.C.5. – TEST OF TIME REVERSAL INVARIANCE.

At present the study of the propagation of polarized neutrons through polarized targets seems to be the most convenient way to test T invariance in nuclei. Dynamical and resonance enhancement factors [3.46, 3.47] related to both, P and T violating interactions, cause an increase of the violation effects near the neutron p-wave resonances.

However, it has been suggested, that there are many fake effects related to the experimental designs which could mimic a true effect of T violation. The most serious effect is arising from the pseudomagnetic fields giving rise to a rotation of the neutron spin around the target polarization. It has been shown, also, that misalignments between the polarizer and the analyzer axis still leads to significant systematic effects [3.48].

The propagation of neutrons is described by the refractive index :

$$n = 1 + \frac{2\pi}{k^2} N_t f$$

where k is the neutron wave number, N_t is the target number density, and f is the forward scattering amplitude:

$$f = A + p_t B\vec{s}\cdot\vec{I} + C\vec{s}\cdot\vec{k} + p_t D\vec{s}\cdot\left[\vec{k}\times\vec{I}\right] + p_t E\vec{k}\cdot\vec{I}$$

where $\vec{s}$ is the neutron spin, $\vec{I}$ is the target spin, p_t is the target polarization, and $\vec{k}$ is the neutron wave vector. The coefficient B represents the combined effects of the external magnetic field, the spin-orbit interaction between the neutron and the nucleus, and the interactions of the neutron magnetic moment with the nuclear and electron magnetization. The coefficients C and E represent the parity violating interaction, and the coefficient D represents the parity and the T-odd scalar triple product (the so-called three-fold correlation coefficient). The real parts of all coefficients cause a precession of the neutron about the relevant axes and the imaginary parts lead to an attenuation, which depends on the neutron spin direction.

Let us take the neutron beam direction $\vec{k}$ along the z axis; the y axis is perpendicular to z and lies in the $\vec{I}-\vec{k}$ plane. The x axis direction is given by $\left[\vec{k}\times\vec{I}\right]$. The transmission of the polarized neutron beam after propagation through the polarized target would be [3.48]

$$T \approx T_0 + p_x \,\mathrm{Im}(D+BC) + p_y \,\mathrm{Im}(B+DC) + p_z \,\mathrm{Im}(C+BD),$$

where p_i are the components of the neutron polarization and T_0 is the neutron spin independent contribution. We see that, in general , the terms BC, B, and C mimic the true T violating term D. To avoid this problem, the groups of FLNP-JINR and the Lebedev Institute proposed [3.49, 3.50] a two stage scheme as shown in Fig. 3.3.

At first, one should measure the transmission difference of neutrons with opposite polarization directions $\pm\vec{p}$ passing through the target (Figure 3.3a).

$$\Delta T_1 = T_+ - T_- \approx 2p_x \,\mathrm{Im}(D+BC) + 2p_y \,\mathrm{Im}(B+DC) + 2p_z \,\mathrm{Im}(C+BD),$$

The second part consists of measuring of the polarization of the initially unpolarized beam after propagation through the target. It should be performed after rotation of the polarizer around the x -axis (axis of the effect) by 180^0 as shown in Fig. 3.3b. The components of the neutron polarization are transformed in this way (we assume an exact rotation by 180^0)

$$\vec{p} \rightarrow \vec{p}' = \left(p_x, -p_y, -p_z\right).$$

Besides this, the polarizer becomes an analyzer of the neutron polarization. Thus, the transmission in the second case would be [3.48, 3.49]:

$$\Delta T_2 = T'_+ - T'_- \approx 2p_x \,\mathrm{Im}(D - BC) - 2p_y \,\mathrm{Im}(B - DC) - 2p_z \,\mathrm{Im}(C - BD).$$

The sum of ΔT_1 and ΔT_2 gives

$$\Delta T_1 + \Delta T_2 = 2p_x \,\mathrm{Im}(D) + 2p_y \,\mathrm{Im}(DC) + 2p_z \,\mathrm{Im}(BD).$$

We see that all terms are proportional to the T violating amplitude D. Besides, we see that the T violation effect can be observed for any direction of the neutron polarization.

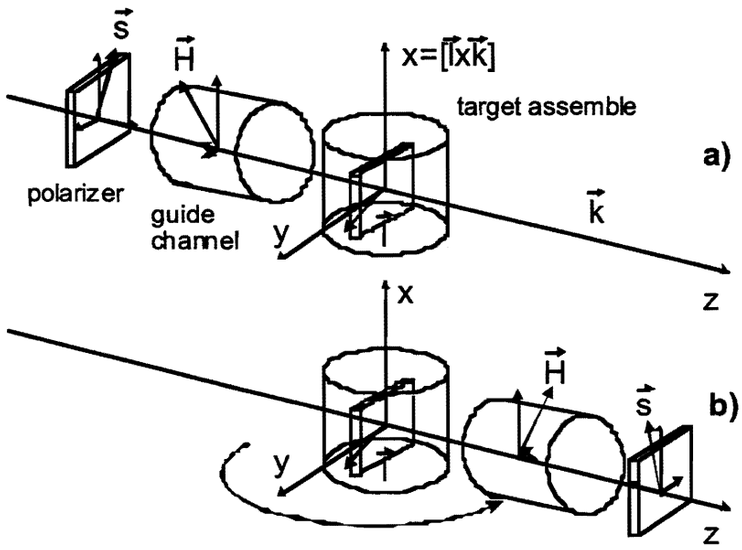

Figure 3.3 : Experimental setup

The measurement consists in the determination of the ratio:

$$R_{x,z} = \frac{\Delta T_1 + \Delta T_2}{2N_0} \approx \frac{\mathrm{Im}(D)}{\mathrm{Im}(B) + \mathrm{Re}(B)}$$

for the neutron polarization along the$x$ or z axis. Usually, the pseudomagnetic term $\mathrm{Re}(B) >> \mathrm{Im}(B) >> \mathrm{Im}(D)$. Thus, both ratios contain the suppression term. To compensate the "field" $\mathrm{Re}(B)$ one should use the external magnetic field H:

$$\mathrm{Re}(B) - H \approx 0,$$

or make the target with admixtures with opposite sign of $\mathrm{Re}(B_a)$:

$$\mathrm{Re}(B) + \mathrm{Re}(B_a) \approx 0.$$

If this condition is met, then the maximum magnitude of the effect would be [3.51]:

$$R_{\max} \approx \sqrt{\frac{\Gamma_p^n}{\Gamma_s^n}} \cdot \frac{v_{PT}}{d} \cdot \left(\frac{d}{\Gamma}\right)^2.$$

Here v_{PT} is the matrix element of the P - and T - violating interaction which mixes the s- and p-wave compound resonances of which the total width $\Gamma_s \approx \Gamma_p \approx \Gamma \approx 0.1\,eV$. The first term is the hindrance factor of order $kR \approx 10^{-3}$, the

second is the dynamical enhancement factor. It arises due to the complexity of the compound resonance structure. For heavy nuclei [3.47]:

$$\frac{v_{PT}}{d} \approx F_{PT} 10^3 ,$$

where F_{PT} is the ratio of the strengths for P - and T - violating and strong interaction. The neutron EDM result sets the limit $F_{PT} \leq 10^{-10}$ for the single meson change mechanism, whereas the limit on the QCD q - term from the neutron EDM gives $F_{PT} \leq 10^{-11}$. The last term is the resonance enhancement term - the magnitude of the symmetry breaking effect is proportional to the time $\tau \approx \hbar/\Gamma$ spent by the incident neutron in the weak - interaction field of the target. Thus, we see that

$$R_{\max}^{QCD} \leq 10^{-6} .$$

The ^{3}He-based neutron polarizer using laser pumping [3.52] can be the most appropriate device for this measurement, without requiring cooling and high magnetic fields. The achieved polarization for 1 eV neutrons is about 80% with a transmission probability near to 22% . These advantages make such a polarizer to be compact and light. Since the ^{3}He polarization mechanism does not require external magnetic fields for producing the level splitting, like the Dynamical Nuclear Polarization (DNP), the ^{3}He cell can be introduced inside the magnetic shield, avoiding thus any influence of an external magnetic field on the neutron polarization at the cell output.

With this experimental method one needs to rotate the polarizer about the $\left[\vec{k} \times \vec{I}\right]$. But with the DNP-based neutron polarizer, it is difficult to align a guide magnetic field and, therefore, the $\vec{I}$ direction is exactly perpendicular to $\vec{k}$. Thus, the direction of the above axis is known with some uncertainties. If the polarizer is ^{3}He - based, this is not important, because the polarization of ^{3}He nuclei does not change the direction under rotation about any axis if the surrounding fields are cancelled, say, by metal shields. As a result, the systematic effect will be proportional to the initial deviation of the laser beam (and neutron polarization) respectively to the direction perpendicular to $\vec{k}$. This deviation can be strongly reduced by using the interferometric technique.

The interaction of low - energy neutrons with ^{3}He is dominated by the presence of a $J^P = 0^+$ exited state of the ^{4}He compound nucleus. This resonance is located 650 keV below the n + ^{3}He threshold, but because it is 400 keV broad, it is easily exited by low energy neutrons. The 0^+ is unstable and decays to p + ^{3}H with a nearly 100% branching ratio. The cross section of the ^{3}He(n,p)^{3}H reaction is 850 b at 1 eV, compared to 3 b for elastic scattering.

The spin and parity of the 0^+ state dictate that it can only be exited when the neutron and ^{3}He spins are antiparallel. Thus, the neutron total cross section is highly spin - dependent, and the two spin states of the initially unpolarized beam will undergo unequal attenuation when transmitted through a polarized ^{3}He. The optical ^{3}He polarization consists of pumping of $5S_{1/2}$ Rb with 795 nm, circular polarized light to a polarized state. Under radiative decays, the state $m_s = -1/2$ Rb is excited to this metastable $5P_{1/2}$ state by the incoming photons. As governed by the polarization ratio, 1/3 of which return to their original state, the rest is sent to a $m_s = +1/2$ state. Most undergo non-radiative decay; they are first excited to the $P_{1/2}$ state, exhibit collision mixing, and return back to the $S_{1/2}$ state. Eventually, all end up in the $S_{1/2}$, $m_s = +1/2$ - spin state. Next, the polarized Rb electron interacts with the ^{3}He nucleus via spin exchange. This means that when encountered with a ^{3}He nucleus, whose spin is "antiparallel" to that of the Rb, the spin directions are exchanged. The present prototype facility (which was completed at September of 1998) produces the polarized ^{3}He via pumping by circular polarized laser light. The installation includes a magnetic guide system, a diode laser array, an alumosilicate glass cell with ^{3}He and small amounts of N_2 and Rb, an oven to produce the necessary Rb vapor number density, and a NMR measurement system. Now the ^{3}He polarization of 40 % is achieved for the Δ=10 mm cell and 7 % for Δ=40 mm. The group is working to improve the polarization technique. Figure 3.4 shows the time dependence of the ^{3}He polarization after the start of pumping.

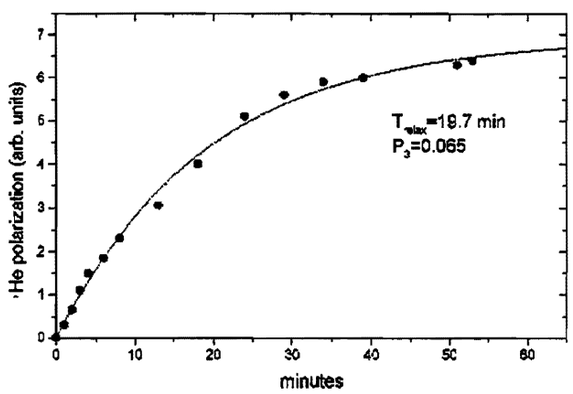

Figure 3.4: Time dependence of the ^{3}He - neutron polarizer prototype.

Nowadays there are two possible target designs for the proposed experiment. The first one is the DNP - based technique for polarization of ^{139}La nuclei, the $LaAlO_3$ compound [3.53]. It requires extra low temperatures and a high magnetic field. The second way is the optical polarization of ^{131}Xe exactly by the same manner as ^{3}He [3.54, 3.55, 3.56]. Besides, one can possibly use the^{129}Xe admixture to

compensate the pseudomagnetic field $\mathrm{Re}(B)$. It is intended to investigate the second way in the nearest future. Figure 3.5 shows the energy dependence of the expected effects $R_{x,z}$ near the p - wave resonances of ^{139}La (0.75 eV) and ^{131}Xe (3.22 eV). The curves are obtained for $v_{PT} = 3.3\times10^{-7}$ eV (QCD), $p_t = 0.5$. Also 95% - compensation of $\mathrm{Re}(B)$ is assumed for both nuclei.

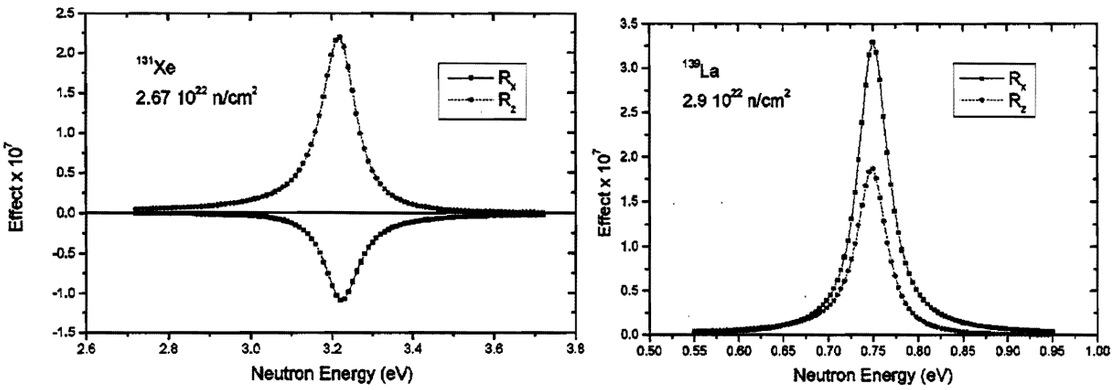

Figure 3.5 : The expected magnitudes of the P and T violation effects near the neutron p-wave resonances of ^{131}Xe and ^{139}La. See text for details.

To realize the proposed a experiment high neutron flux is required. On the other hand, the task is not very sensitive to the energy resolution. Thus, the flight path base of 50 m is suitable for this purpose. The other requirement is a low magnetic field environment to avoid the influence on the neutron polarization. Thus, the magnetic field measurements should be performed at the possible facility site before installation.

3.D – FUNDAMENTAL PROPERTIES OF THE NEUTRON.

The CERN PS TOF Facility provides unique possibilities for investigation in fundamental nuclear physics. The high intensity and precise energy resolution together with the regime of very low repetition rate ensure exclusive conditions for experiments in fundamental physics.

3.D.1 – THE NEUTRON-ELECTRON SCATTERING LENGTH.

Today there is a great effort to study the details of the hadronic structure by different experimental means. One important quantity is the mean square radius $\langle r_n^2 \rangle$ of the charge distribution of the neutron which is proportional to the slope of the Sachs form factor $G_E(q)$ at q=0 and can be deduced from low energy

neutron-atom scattering. The corresponding experiments are based on the coherent interference between neutrons scattered by the nucleus and the electron cloud of the atom. At low energies this process is described by the scattering amplitude

$$f(Q) = b_N + Z\, b_{ne}\, f(E,Q)\,,$$

where b_N is the nuclear scattering length, Z is the number of electrons and f(E,Q) is the known atomic form factor. Since the first proposal by Fermi and Marshall [3.57], many experiments have been caried out to determine $\langle r_n^2 \rangle$ and the neutron-electron scattering length b_{ne} which are related by

$$\langle r_n^2 \rangle = 3 \frac{m_e}{m_n} \alpha_0 b_{ne}$$

where a_0 denotes the Bohr radius and m_n and m_e are the masses of neutron and electron mass, respectively. In Table 3.5 a chronological list of the experimental results [3.57-3.71] is given which also shows the great variety of methods. Besides the angular correlation experiments of Krohn and Ringo [3.63,3.64], highest accuracies have been achieved by transmission measurements.

In recent years, the reliability of experimental values of b_{ne} has been discussed extensively [3.71]. Since $\langle r_n^2 \rangle$ and b_{ne} are interesting quantities of reference for theoretical models of the nucleon, new high precision experiments are required. Specifically, a determination of b_{ne} via angular scattering [3.65,3.66] should be performed. To achieve the high accuracy it is essential that these new measurements are accompanied by the development of an improved theoretical analysis.

3.D.1.A – ANGULAR SCATTERING : The low repetition rate of high intensity bursts combined with the 230 m flight path of the TOF facility provides ideal conditions for a remeasurement of the angular distribution of neutron scattering on noble gases, specifically on Xe. The use of gaseous sample avoids uncertainties due to solid state corrections. The concept of the measurement is similar to the pioneering experiment of Krohn and Ringo [3.63,3.64] and will make use of modern electronics and new methods of analysis. At low energies the differential elastic cross section is of the form

$$\sigma(E,\Theta) = b_N^2 + 2\, Z\, b_N b_{ne}\, f(E,\Theta) + [Z\, b_{ne}\, f(E,\Theta)\,]^2,$$

where we have ignored absorption, incoherent scattering and other small contributions. The angular distribution shows an anisotropy due to the known atomic form factor. Specifically the form factor of noble gases is well known. For Xenon the expected anisotropy is of the order of 1.5%. To achieve the best results scattering of neutrons in the energy range between 0.01 eV and 100 eV must be

considered. Special care has to be taken to account correctly for the rescattering of neutrons inside the setup. Because of the known form and the high intensity a relative accuracy of better than $5\ 10^{-4}$ should be within reach of this experiment.

Experiment	Target	b_{ne}	Year	Reference
Angular scattering	Ar	-0.1±1.8	1947	[3.57]
Transmission	Bi	-1.9±0.4	1951	[3.58]
Angular scattering	Kr,Xe	-1.5±0.4	1952	[3.59]
Mirror reflection	Bi/O	-1.39±0.13	1953	[3.60]
Angular scattering	Kr,Xe	-1.4±0.3	1956	[3.61]
Crystal spectrometer transmission	Bi	-1.56±0.05	1959	[3.62]
		-1.49±0.05	1976	in [3.66]
		-1.44±0.033	1997	in [3.71]
	Ne,Ar,Kr,Xe	±0.06	1966	[3.63]
Angular scattering	Ne,Ar,Kr,Xe	-1.34±0.03	1973	[3.64]
Angular scattering	^{186}W	-1.3±0.03	1975	[3.65]
Single crystal scatt.	Pb	-1.60±0.05	1975	[3.65]
Filter-transmission, mirror reflection	Bi	-1.364±0.025	1975	[3.65]
	Bi	-1.393±0.025	1986	[3.67]
Filter-transmission, mirror reflection	Pb,Bi	-1.55±0.11	1986	[3.68]
	thorog. ^{208}Pb	-1.32±0.04	1995	[3.69]
TOF transmission, mirror refl.		-1.31±0.03±0.04	1997	[3.71]
	Pb-isotopes,Bi		1995	[3.69]
Filter transmission, mirror reflection		-1.33±0.027±0.03		
TOF transmission		-1.32±0.03		
Filter transmission, mirror reflection				

Table 3.5 : Experimental results of b_{ne} in units of 10^{-3} fm

3.D.1.B – TOTAL CROSS SECTION : The highest accuracy so far has been achieved by the transmission method [3.69,3.70], where liquid thorogenic ^{208}Pb and ^{209}Bi targets have been used. A determination of the energy dependence of the total cross section of the ^{86}Kr isotope may be envisaged as complementary measurement. From the atomic form factor it is obvious that the energy range between 0.01 eV and 100 eV must be covered.

The concept of a transmission experiment is simple but its analysis becomes rather sophisticated when a level of accuracy of 10^{-4} should be reached. Besides the necessary experimental corrections for deadtime, background and overlap neutrons one has to perform a careful study of resonances, absorption, the Doppler effect and small interaction terms (e.g. Schwinger scattering, electric polarizability) which modify the energy dependence.

At the moment transmission experiments cannot be planned at the TOF facility because the expected rate during the burst is too high for available detector systems. Therefore in the beginning phase it is planned to study ^{86}Kr at GELINA and to combine the results with the angular scattering data obtained at the TOF facility at CERN.

3.D.2 – THE ELECTRIC POLARIZABILITY.

Another important structure constant of the neutron is its electric polarizability α_n which describes the response of the neutron to external electric fields. Because of the tight binding of the constitutents of a neutron, strong electric fields are required to obtain a measurable effect. Nowadays only the electric fields in the vicinity of heavy nuclei are strong enough to induce a significant electric dipole moment. This effect can be seen in neutron-nucleus scattering where a small but long ranged $1/r^4$ potential term must be added to the usual nuclear potential which is of short range. This difference in range shows up as a linear k-dependence in the scattering amplitude and consequently in the cross sections [3.72].

The simplest way to determine α is a measurement of the energy dependence of the total cross section. Such measurements have been performed by several groups [3.73,3.74]. Using a ^{208}Pb target of high purity, Schmiedmayer et al. [3.73] measured the total cross section in the energy range 100 eV to 500 keV with a precision in the order of 10^{-4}. The extracted value

$$a_n = (1.20 \pm 0.15(\text{stat}) \pm 0.2(\text{syst})) \cdot 10^{-3}\ \text{fm}^3,$$

is the best presently available. This measurement performed at ORELA was not optimized and allows only the determination of an upper limit of about 2×10^{-3} fm^3. There are strong indications that better results could be achieved. In particular it was claimed that accuracies of 10^{-4} fm^3 are within the reach of the experiment. This uncertainty would be smaller than the expected retardation effects and would allow the distinction betwen static and dynamical polarizabilities. Unfortunately it was not possible to repeat the experiment at ORELA because of organisational reasons. Therefore this important dynamical structure constant is still under discussion and a remeasurement with increased accuracy is required.

It is planned to perform this missing measurement at the TOF facility. However, as pointed out previously transmission experiments are not feasible at

the moment because there are no detectors available to handle the high flux during the burst. Actually the expected rate of 500 keV neutrons will be about 20 neutrons/cm^2 ns, far above the abilities of the fastest detectors. Although there will be increased effort in the development of ultrahigh rate detectors it is questionable whether such rates will be manageable in the near future.

As a way out of this difficulty we are considering scattering out of the forward direction which also contains the linearly k-dependent term proportional to α_n, however, at the expense of a more complicated theoretical analysis. Simulations are under way to find the optimal geometry for a high precision measurement. Similarly to transmission experiments an accuracy of 10^{-4} must be achieved. It must be emphasized, however, that we do not intend to measure the angular distribution which will be almost impossible with such uncertainties [3.75]. Such a scattering experiment on ^{208}Pb is scheduled for the next phase of the cross section measurement campaign. Its detailed design will depend on the current status of the development of high rate detection. Similarly to the experiment on the neutron-electron scattering length the method of analysis is an essential point which will be considered in detail by theoreticians .

It is also envisaged that a transmission experiment on the same target will be performed at GELINA to obtain a complementary data set.

4 – AVAILABILITY OF TARGETS AND SAMPLES.

The measurements of neutron induced cross sections at the CERN TOF facility require the availability of a pletheora of stable and radioactive targets of high purity.

Compared to radiochemical methods, considerably better purity can be achieved by mass spectroscopy. Such capabilities are available at the CSNSM Institute at Orsay [4.1] with a team having comprehensive experience in the isotopic separation and the production of monoisotopic targets through slowing-down of the ion beam and ion implantation. Enrichment factors of typically 10^3 and separated quantities of (300 mg x abundance) per six hours are presently possible. The yield can drop by a factor five for isotopes requiring chemical treatment, e.g. Sm. The ions can be implanted on very thin aluminum ($M\Omega/cm^2$) or carbon (1 μm) substrates with saturation values of 3 $\mu g/cm^2$. Thicker targets can be produced by slowing-down of the ion beam. The production of stable targets can start immediately, but the treatment of radioactive non-transuranic targets requires major modifications estimated to 500 kEURO [4.1]. The production of transuranic targets seems very difficult within the present regulations of CSNSM.

Significant quantities of actinides of good purity are available in the Analytical and Nuclear Chemistry Division (ANCD) at LLNL [4.2]. Nuclides available include ^{237}Np, ^{241}Am, ^{242m}Am, ^{243}Am, ^{243}Cm, ^{244}Cm, and possibly ^{245}Cm, as well as Pu isotopes. Also available are nearby accelerator facilities that can be used to produce long-lived radionuclides via charged particle reactions on separated stable isotopes. The ANCD has a full range of radiochemical and analytical capabilities for the purification of materials, the preparation and encapsulation of thin and bulk targets, advanced detector development, and the detection and analysis of radioactivity. Mass spectrometry capabilities are also available for use when appropriate.

The JINR as head organisation of the three Institutes FLNP, IPPE & IAT (Obninsk) and VNIIEF (Sarov) discussed [4.3] the availability of target materials, but the form, purity and conditions have to be clarified. Further clarifications are also needed for the determination of the capabilities of the Transuranium Institute at FZKarlsruhe [4.4] and of the IPN at Lyon [4.5]. The availability of target materials by the French CEA is also exploited in co-operation with GEDEON.

5 – THE EXPERIMENTAL PROGRAMME AND METHODS.

5.A – NEUTRON FLUENCE DETERMINATION.

At the TOF facility four important measurements have to be done in order to determine as precise as possible the cross sections from the data:

1) Monitoring of the proton beam.
2) Calibration and monitoring of the time-energy relation.
3) Determination of the absolute neutron fluence.
4) Monitoring of the neutron intensity.

5.A.1 – MONITORING OF THE PROTON BEAM : In the TARC experiment [5.1] the accurate measurement of the intensity of the proton beam was of special concern. Two beam tranformers were used to measure the number of protons from the signal induced by the beam charge in a coil mounted around a vacuum pipe. One beam transformer will be placed ~few meters beam-upstream from the lead target, whereas the other one will be situated immediately in front of the target. These beam transformers have been improved and developed by industry [5.2] for the TARC experiment. The design of the induction loop, through which calibrated charges simulating the beam are injected, allows a more linear behaviour of the calibration system [5.3].

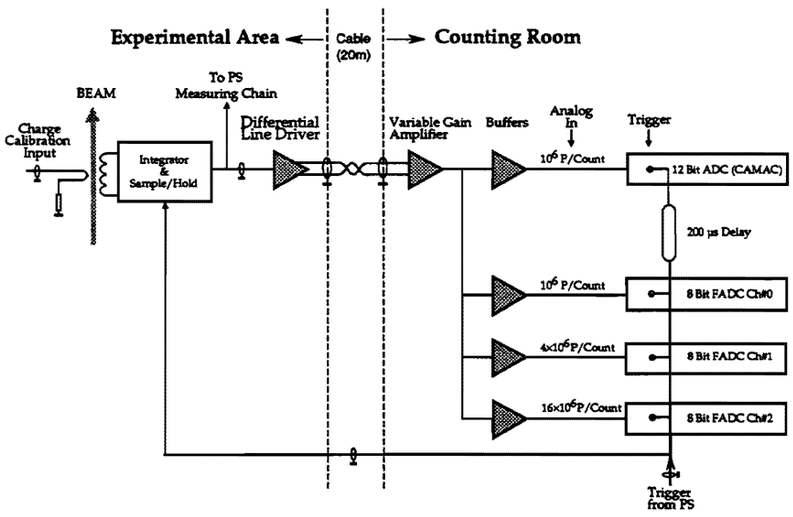

Figure 5.1: Beam Transformer Read-out and Calibration Block diagram.

The readout scheme is shown in figure 5.1. The beam transformers measure the beam intensity of each PS shot (figure 5.2) providing the detailed history of the experimental runs.

Since the beam intensity measurement is a key to ultimate accuracy of the experiment, cross-check measurements will be done by comparing the results of the two beam transformers which, according to beam simulation, should record the same beam intensity. These two measurements should agree very well, <1 %, and can be used as diagnostic for beam quality. The beam tranformers will be calibrated by injecting calibrated charge pulses through a wire simulating the beam [5.3].

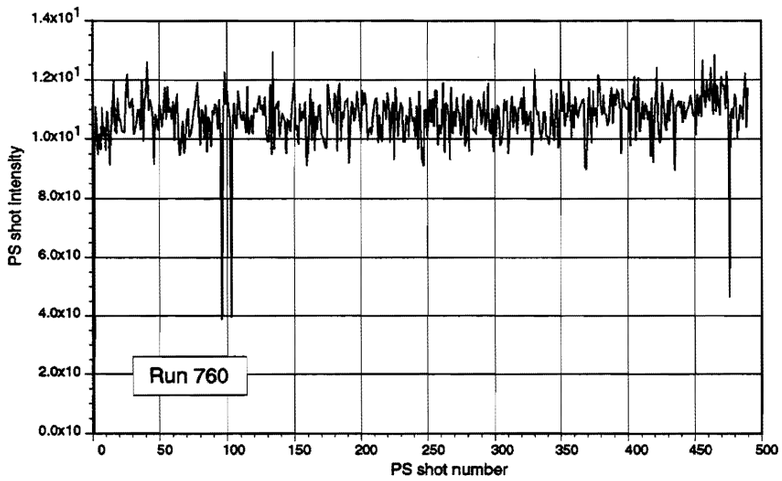

Figure 5.2: Example of measurement of the beam intensity (TARC run 760) showing the number of protons for each PS shot.

The absolute calibration of the transformers is usually performed by bombarding aluminium foils with beam, counting the ^{24}Na produced [5.4] and comparing to the response of the beam transformers. The irradiation of aluminium foils is a classic technique, involving the formation of ^{24}Na by the reaction $^{27}Al(p,3pn)^{24}Na$, ^{24}Na being detected via its 1368.45 keV gamma ray emission. The dominant uncertainty in the absolute calibration arises from the ^{24}Na production cross section amounting to 4%.

CALIBRATION AND MONITORING OF THE TIME-ENERGY CALIBRATION :
In TARC, the energy-time relation was measured [5.5] with the help of a CeF_3 crystal mounted in front of a photomultiplier equipped with a quartz window to record the time distribution of the fast (5 ns and 30 ns decay times) CeF_3

scintillation UV light produced by prompt γ's associated with radiative neutron captures on thin samples of elements with known capture resonance energies, i.e. ^{181}Ta, ^{197}Au, ^{109}Ag, ^{99}Tc, ^{115}In and ^{55}Mn. The measured time-energy relation from thermal energies to 300 keV is shown in fig. 5.3.

Given the extremely small sensitivity of CeF_3 to the incident neutrons, we intend to apply the same technique to determine and monitor the time-energy calibration of the Flash ADC's by taking data with the CeF_3 crystal in the beam at the measuring stations. Moreover, a permanent installation of such a counter is envisaged at the periphery of the beam tube, e.g. at the place where the neutron beam tube reduces from 60 to 40 cm, without influencing the neutron beam and the measurements.

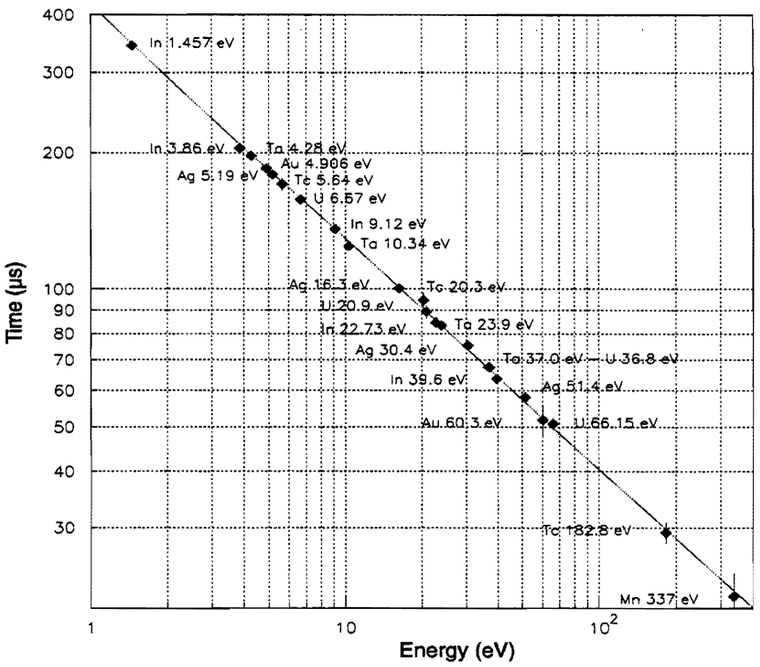

Figure 5.3: Experimental relation from the TARC experiment between time and energy from the multiplier measurements. The curve is a fit to the function $K/(t + t_0)^2$

5.A.3 – DETERMINATION OF THE NEUTRON FLUENCE : In the TARC experiment [5.5] several techniques were used to measure neutron fluences over the desired energy range from thermal to MeV neutrons, i.e. $^6Li/^{233}U$ sandwich detectors and ^3He detector in the scintillation mode covered the neutron energy range from thermal up to above 200 keV and ^3He ionization detector covered the higher energy range from 10 keV to 2 MeV. These measurements were complemented by measurements using fission reactions in ^{232}Th, ^{237}Np and

^{238}U. In all cases, the measurements were found to be in good agreement with the simulation (fig. 5.4).

We intend to use similar detectors to measure the neutron spectrum at the TOF facility. During data taking and in case the samples are "transparent" these detectors can be mounted in the end of the neutron beam tube. An additional information during data taking will come from detectors of the same type but this time permanently mounted on windows at the steps of the vacuum tube, monitoring in this way the halo of the neutron beam in relation to the incoming protons.

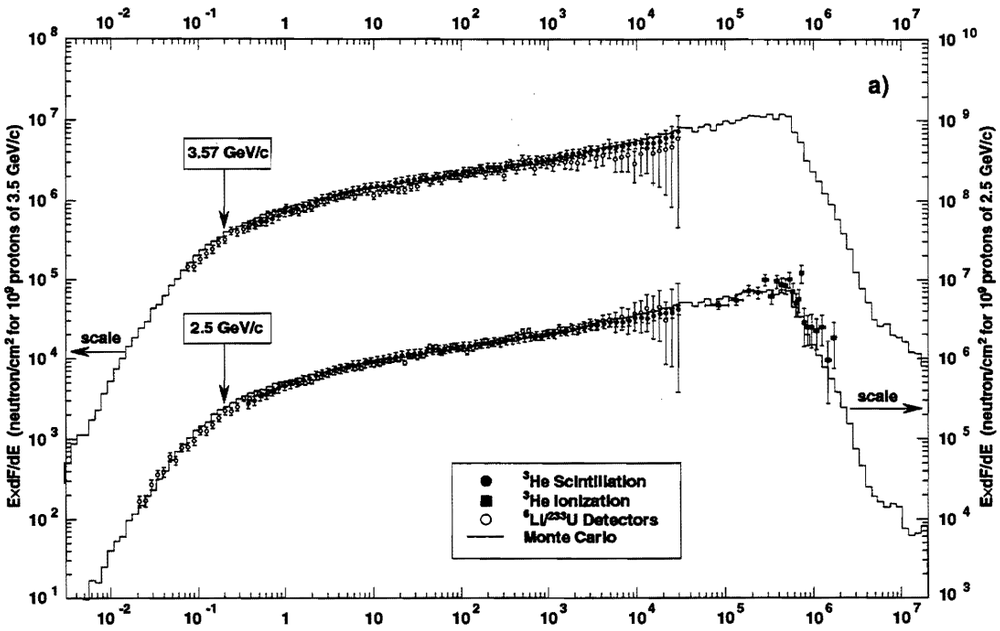

Figure 5.4: Example of TARC measurements of the neutron fluence. E´dF/dE is shown as a function of neutron energy, from 2.5 and 3.57 GeV/c protons in hole number 10 (Z = 7.5 cm, at a distance of 45.6 cm from the centre of the lead volume). The Monte Carlo predictions are shown as histograms. The data are from 6Li/233U detectors (open circles), 3He in the scintillation mode (full circles) and 3He in the ionization mode (full squares). The error bars include both statistical and systematic errors added in quadrature;

Neutron detectors make use of the three following reactions having very well known cross sections :

$$^{10}_{5}B + {}^{1}_{0}n \rightarrow {}^{7}_{3}Li + {}^{4}_{2}\alpha \qquad \text{(Q-value = 2.792 MeV)}$$

$$^{3}_{2}He + {}^{1}_{0}n \rightarrow {}^{3}_{1}H + {}^{1}_{1}p \qquad \text{(Q-value = 0.764 MeV)}$$

$$^{6}_{3}Li + {}^{1}_{0}n \rightarrow {}^{3}_{1}H + {}^{4}_{2}\alpha \qquad \text{(Q-value = 4.78 MeV)}$$

In the first two cases ionization detectors can be made with BF_3 gas and ^3He gas measuring the neutron energy, but they are limited by the slow charge collection time. In neutron time of flight spectroscopy, the detector needs register only the arrival time of a neutron and a new 1 MHz ^3He ionisation chamber, described in details in 5.A.2, has evolved for this application. In the third case one uses normally lithium-containing scintillator materials. e.g. the standard NE 421 or the low-background NE912. In addition to the high enriched ^6Li, equivalent scintillators are also available with depleted lithium for background determination. The latter are neutron insensitive and can be used to measure separately the gamma contribution in a mixed neutron-gamma irradiation.

In the case of ^3He one can build a detector working in the scintillation mode [5.5] as used in the TARC experiment, showing apart from the excellent time resolution an energy resolution of ~10%. The decay time of the scintillation is only few nanoseconds, leading to very fast risetime of the output pulse, this advantage in timing being mostly suited in neutron time of flight spectroscopy. Another possibility is the use of the $^6Li/^{233}U$ sandwich detectors [5.5], where two thin silicon detectors are facing respectively a ^6Li and a ^{233}U layer. Both type of these detectors have been used in the TARC experiment.

In addition to the above methods, the detection of fast neutrons can be also based on elastic scattering of neutrons by light nuclei. Organic scintillators contain carbon as well as hydrogen and are standard commercial detectors commonly used in the Neutron Research. The neutron flux at the higher energies will be monitored by the standard liquid scintillation GEEL detectors (NE-213), the CERN ^3He gas scintillation counter and the ^{232}Th, ^{237}Np and ^{238}U fission gas detectors used in the FEAT experiment [5.6], as well as the Grenoble $^6Li/^{233}U$ sandwich detectors.

Parallel to these existing detectors, the groups of Coimbra and Delft will develop position–sensitive neutron detectors based on ^3He gas. Moreover, integrating and counting monitors will be developed using electrode structures for observing the *electron-charge-cloud signals*. Furthermore application of neutron-sensitive inorganic scintillators is considered. Systems will be optimized for the required position resolution, sensitivity and time-energy information.

5.A.4. - ^{3}HE IONIZATION DETECTOR.

The neutron detection is based on the ionisation produced by the ^{3}He(n,p)T reaction in a gas mixture ^{3}He-CF_4 (90-10 %). For events induced by slow neutrons, the Q-value leads to oppositely directed reaction products with energies of 573 keV and 191 keV for proton and triton, respectively. The (n,p) cross section has a 1/v energy dependence up to 1 MeV and does not present any resonance. In fig. 5.5 the simulation of the (n,p) event rates (dn/dE) for a PS shot of 0.75×10^{13} protons is represented.

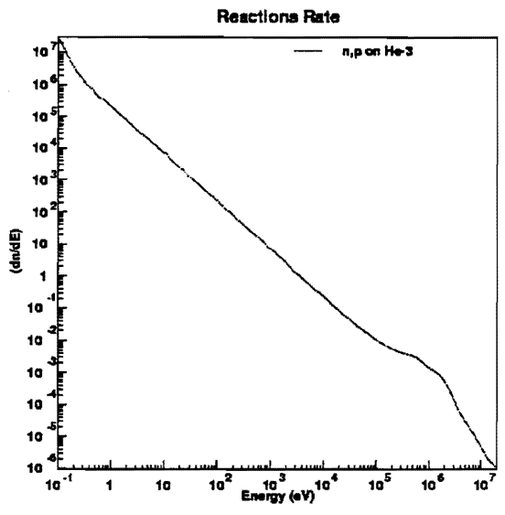

Figure 5.5: Event Rates versus Energy for (n,p) reaction in ^{3}He (1.7 mm, 3 bar)

The expected rates are calculated for a gas volume of ~ 0.22 l corresponding to a surface of 1256 cm^2 (ø = 40 cm) and a thickness of 1.7 mm. The dimensions and the working pressure are defined by the constraints discussed in the next chapter. Looking at the large ratio between the reaction rate in the nominal energy range, the first guess is that this dynamic range is too large. The situation becomes acceptable if we consider the rates versus time, as reported in fig. 5.6.

By implementing a detector with a moderate segmentation (20 to 30) and an appropriate signal shaping, it is possible to achieve a pile-up free rate on a single channel. In the energy region above 10^6 eV the reactions are significantly affected by the elastic scattering and, therefore, the detection could be implemented using the ionization produced by this interaction. The energy distribution of recoil protons has a theoretical rectangular shape comprised between zero and 75 % of

the energy of the incident neutron. Since in a TOF environment, the neutron energy is given by the time at which the interaction takes place, this behavior is not a problem for our purposes. Nevertheless a further R&D is necessary to better evaluate the possibility to use the proton recoil in ^{3}He to monitor the neutron flux for energies above 10^6 eV.

The detector design takes into account two main constraints: the time response and the minimization of the wall-effect. The detector time response must be maintained within 5 ns to be compatible with the accuracy of the neutron spill. To achieve this speed one possibility would be to use the signal generated by the current induced in a Parallel Plate Ionization Chamber (PPIC). Since the current amplitude is directly proportional to the number of free electrons produced by the ionization and inversely proportional to their drift time, the plates must be as close as possible to have the max. signal. Assuming a drift time of ~40 ns, a minimum ionization of 764 keV and an average energy of W =30 eV to produce an electron-ion pair, the peak current becomes ~ 100 nA.

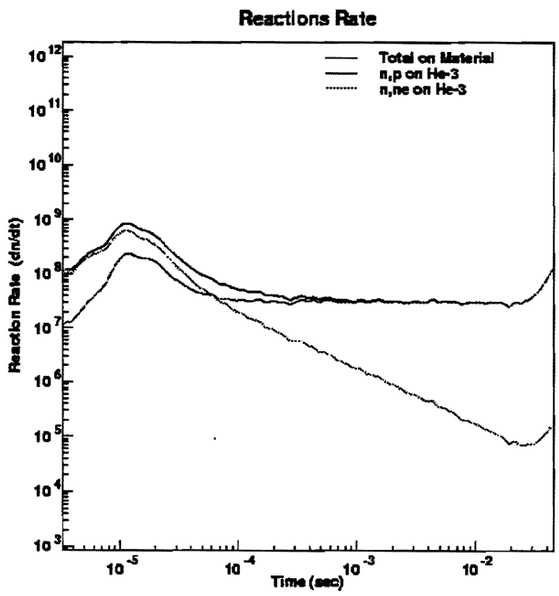

Figure 5.6: Event Rates for (n,p) and elastic reaction in ^{3}He (1.7 mm, 3 bar)

This figure is sufficiently large to produce a signal above noise even using a commercial transimpedance amplifier with a spectral noise of 1.8 pA /√Hz, corresponding to 10 nA r.m.s. noise in a bandwidth of 35 MHz (t_r = 10 ns). The wall-effect consists in the loss of ionisation for protons hitting the detector walls.

The proposed design claims a significant reduction of such effect. In fig. 5.7 the detector lay-out is sketched.

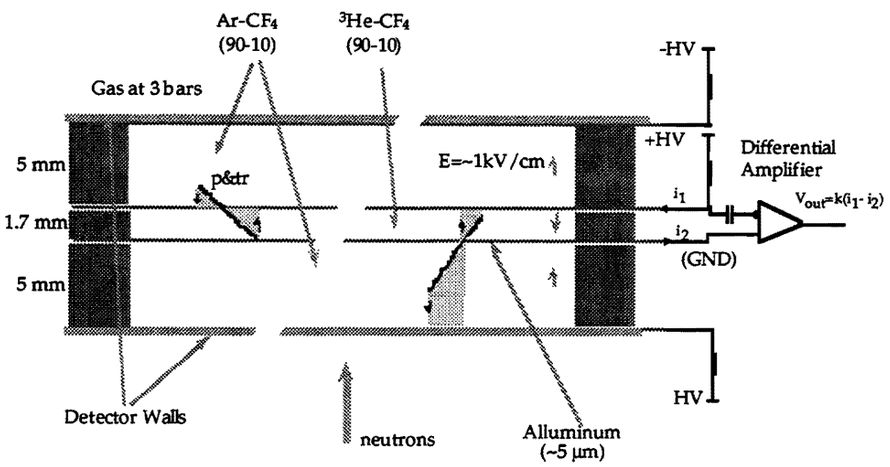

Figure 5.7: Detector lay-out.

The detector has a circular shape with a diameter ø ≥ 40 cm and a thickness of ~ 12 mm. The inner volume is divided in three parts physically separated by two very thin walls made out of metallised Mylar. The two outer volumes, facing the external detector walls, are filled with a gas mixture of Ar-CF_4 (90-10%) whilst the inner volume is filled with ^{3}He-CF_4 (90-10%). The pressure, identical for the two gases, is 3 bar. This relatively high pressure is required to minimize the proton absorption range and, therefore, the gap between the different electrodes. The typical range of a proton with 764 keV energy at a pressure of 3 bar is ~ 5.5 mm. The n,p reactions are taking place in the ^{3}He and a large number of protons are hitting the walls. The proton absorption length at the considered energy is $5x10^{-3}$ g/cm^2. Assuming the possibility to implement the walls facing the ^{3}He gas with a Mylar layer of ~1 μm metallized on both sides with 2 μm of Aluminum, the absorption in the wall is ~ 30% for a proton with a perpendicular trajectory. Under these conditions a significant absorption takes place in the Argon gaps. The electric fields are such that the electrons are drifting in directions producing induction currents of the same polarity on the two sides of the same wall. The electric field and the gaps are chosen to achieve the same drift time inside the ^{3}He and Ar gaps.

In fig. 5.8 are shown the total reaction rates in 10 mm of Ar at 3 bar where 90% are due to elastic scattering, 6.6% to inelastic scattering and 1.5% to capture. In the worst case the number of neutron interacting with Ar is always lower than

0.1% of the incoming flux. Concerning ^3He, these figures are one order of magnitude lower.

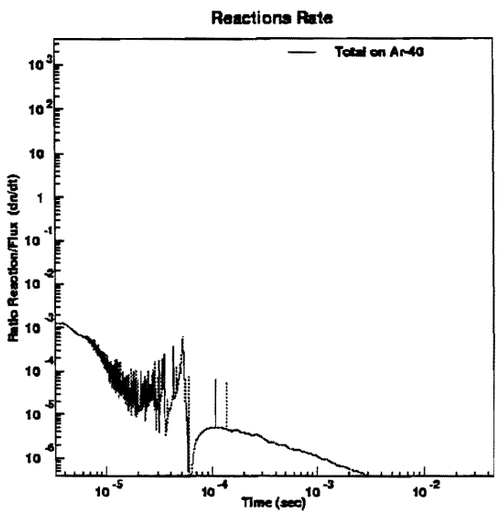

Figure 5.8: Relative reaction rate in 10 mm of Ar.

As usual the more significant effects are coming from the outer detector walls. Nevertheless, since this detector is foreseen to be installed at the end of the vacuum tube, their effect concerns only the back scattering. The possibility to implement the detector walls made out of Carbon and Mylar is always open, allowing a neutron flux contamination lower than 1% (see PPIC for fission-fragments).

5.B – NEUTRON INDUCED FISSION.

Between the different kinds of fission fragment detectors, we plan to use two well established counters: the Parallel Plate Avalanche Counter (PPAC) [5.7] and the Parallel Plate Induction Chamber (PPIC) [5.6].

5.B.1 – FISSION DETECTOR BASED ON THE PARALLEL PLATE AVALANCHE COUNTER (PPAC).

A target made with 1 mg actinide element spread on a 0.3 mg/cm^2 layer of 2 cm diameter is inclined at 30° with respect to the collimated neutron flux direction to offer a 1 cm^2 surface to the neutron beam. The target should be deposited on a thin substrate to allow the detection of the two FF in coincidence. On each side of the target are positioned two PPAC of 30 cm diameter able to detect and measure the position of the two FF emitted in coincidence by the

fissioning nuclei with almost 100 % efficiency. The solid angle covered by these PPACs is about 90 % of 4π. As PPACs work at very low gas pressure (7 mbar) the target and the PPAC will be placed in a stainless steel cylinder of 50 mm length with its axis perpendicular to the neutron beam direction (figure 5.9). The cylinder will be closed by 2 mm thick stainless steel flasks. This set-up is almost transparent to neutrons and γ-rays. This experiment could then be coupled with (n,γ) capture and (n,n') measurements for example.

PPACs have been known for many years as a precise timing instrument but were scarcely used before the considerable development of heavy ion physics, for which gas detector are better suited. A PPAC consists of two thin parallel stretched foils with a very low gas pressure in between. Particles traverse the detector perpendicular to the planes. The principle of operation is the same as a Multi Wire Proportional Chamber. The gap between the foils must be small, of a few millimeters, in order to maintain a high electric field, reduce the time spread and get a good time resolution. It has to be uniform to insure the same operating regime on the whole active surface of the detector. Copper coated epoxi resin for printed circuit board, on which thin aluminized plastic foils are glued, is very well suited for this purpose. The copper layer is used for electric connections.

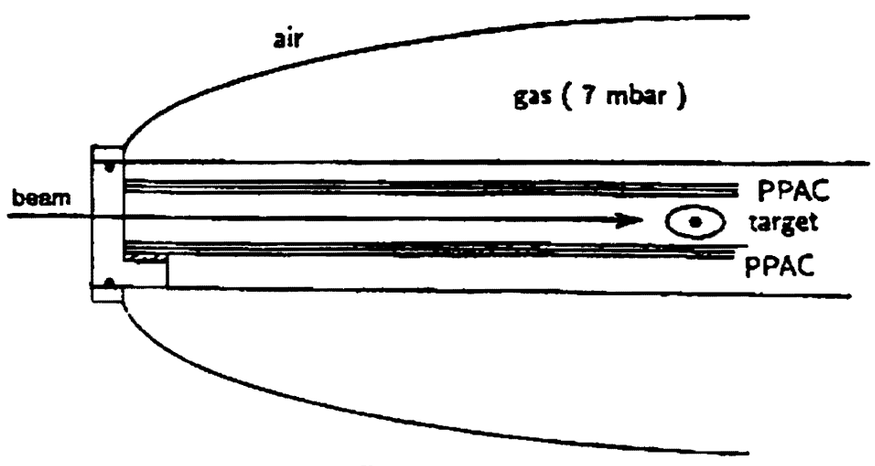

Figure 5.9 : Experimental set-up (half part)

These detectors are built to operate with pressures ranging from 1 to 20 mbars. In these low pressure conditions, a voltage of a few hundred volts applied between the plates, typically 300 V/cm/bar, is sufficient to insure the proportional regime. Released electrons gain enough energy to induce immediate secondary

ionization in the homogeneous electric field, and Townsend avalanche is formed. It seems that pure hydrocarbons are best suited for these detectors and higher gains can be reached with isobutane. Multiplication factors of thousands are obtained with 100 % efficiency in a wide domain of energy losses. For large energy losses like those obtained from FF, a pulse height saturation can occur, therefore, a relatively low voltage can be set making the detector very safe, far from sparking. A 2 to 3 ns rise time pulse is collected due to the high velocity of electrons and the good homogeneity of the electric field. Positive ions contribute very little because they are not very close to the anode, in comparison with what happens in a wire counter. Only the fast component of the signal due to the motion of electrons is used. The slow part from the positive ions is eliminated by differentiation of the signal. Best timing performances may not necessarily correspond to the fastest output rise time, since at very low gas pressure, pulse fluctuations can become important. Time resolutions of the order of 250 ps (fwhm) are obtained with such detectors even in large dimensions. Of course a delay of 40 to 50 ps/cm from the propagation time of a signal along the electrodes has to be taken in account. They could then be used as the stop signal to determine the TOF of the incident neutron.

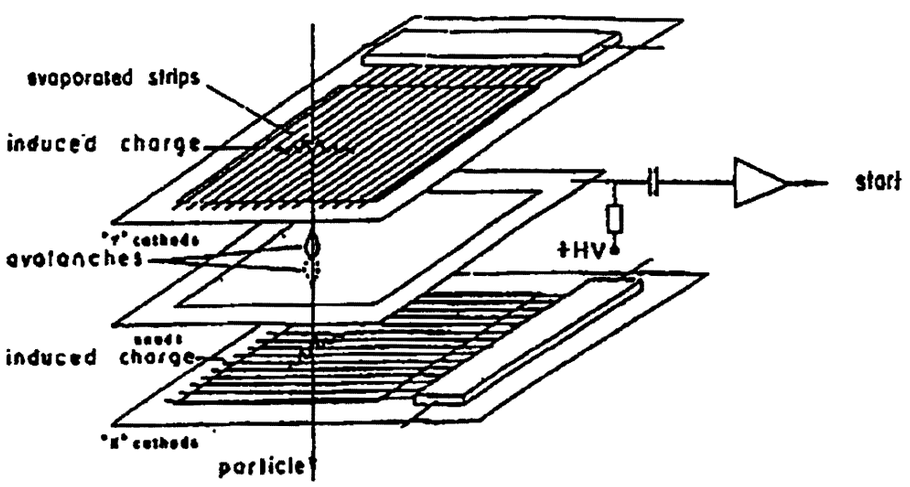

Figure 5.10: Parallel Plate Avalance Counter schematic diagram.

It is possible to achieve a very good spatial resolution with PPAC. The localization is realized by strips on cathodes. A detector could be made with strips every tenth of an inch by deposited Aluminum on 0.9 μm of Mylar foils placed on each side of an anode made of a similar foil aluminized on both sides as shown in figure 5.10. Due to the range of FF in Mylar (~12 μm), the limit angle for

FF detection in the first detection zone is 4.3° giving an X position determination only, and the limit angle is 10° with X and Y position measurements when the FF is able to enter the second zone.

Another configuration could be to have the neutron beam entering perpendicular to the PPACs. That way, the target could be parallel to the PPACs. The advantage would be that when a FF leaves the target tangentially, it reaches also the PPAC tangentially. The dead zone for target and PPACs coincide. There are two dead regions in the other configuration but this may be more convenient for γ-ray or neutron detector settings.

If we assume that we can get 50 fissions in 20 μs, this represents 2.5 MHz frequency. It means that each of the 300 strips must be equipped with its own fast preamplifier and discriminator and the resulting code extracted. PPAC posseses a number of attractive features: they can be built in large dimensions, they are not sensitive to radiation damage, the fast removal of positive ions gives them a high rate capability as position detectors. PPAC are the thinnest available time and position sensitive detectors.

Concerning the counting rates, if one takes the average fission cross section of 1 barn in the whole energy range, one should detect about 50 fissions per 20 μs pulse, (actually almost all actinide averaged fission cross sections range from 0.1 to 3 barns). To cover the whole neutron spectrum, one would need to sample into 400 energy bins not uniformly distributed. Within 24 hours one gets about 4000 fission events in each bin, resulting in a statistical error of 2 % only. The larger errors would probably come from others effects: exact solid angle determination, neutron flux at a given energy, number of the atoms in the target.

5.B.2 – FISSION DETECTOR BASED ON THE ABSORPTION IN A GAS (PPIC).

The most relevant characteristic of a Fission reaction is the large amount of kinetic energy liberated in the fission process. The typical kinetic energy of 160 MeV is divided between the two FFs leaving the interaction point in opposite directions. The most used FF detectors are parallel plate ionization chambers made out of a thin target deposited on a metallic layer, facing a volume filled with a pressurized gas. Because the fragments start out stripped of many electrons, their very large effective charge results in a specific energy loss grater than that encountered for other competing ionizing particles. An important

feature of a FF track is that the specific energy loss ($-dE/dx$) decreases as the particle loses energy in the absorbing medium. This behavior is in contrast to the light particles like alphas or protons and is a result of the continuos decrease in the effective charge carried by the fragment as its velocity is reduced. For particles with much lower initial charge, such as the alpha particle, electron pickup does not become significant until near the end of the range. This behavior allows to imagine a detector in which the neutron induced fission reactions are expected to be of much larger magnitude than any other competing reaction and therefore use the amplitude discrimination to recognize the FF signature. The peculiarity of a detector, in a time of flight measurement, is the need to perform an instantaneous measurement to avoid, or minimize, the pile-up. Because the maximum amplitude expected from pulse pile-up is an inverse function of the detector resolving time, a fast detector is also required in case of targets made with fissionable materials in which the alpha activity is relatively high. The proposed design, based on the current measurement in a Parallel Plate Induction Chamber, allows the construction of a detector with a time occupancy in the range 30 to 50 ns and a time resolution in better than 2 ns.

The neutron "spot" available at the measuring station has a diameter of 40 cm. To avoid neutron scattering in the bulky flange closing the TOF tube, the detector is housed in the vacuum. The detail of the detector is sketched in figure 5.11. The flanges are holding the detector walls and a sandwich of two very thin metallized Mylar® layers acting as the Anode and Cathode of the PPIC. On the Cathode are implanted the fissile targets with the required geometry. The detector walls made out of Mylar® reinforced with Carbon, must sustain the inner gas pressure. This very light structure allows the possibility to consider the detector as the container of the target it-self.

We assume the possibility to build a fissile target having a total circular shape of ø=40 cm with deposits distributed following a hexagonal lattice (or other). The active surface of each cell is lined by a free space to allow the FFs escaping from the boundaries to be fully absorbed in the active volume. The Anode, set at a positive voltage, has the same segmentation as the target. The detector dimensions and its pressure are chosen to achieve the full absorption of the FFs and, therefore, the clear separation to alpha background by simple amplitude discrimination.

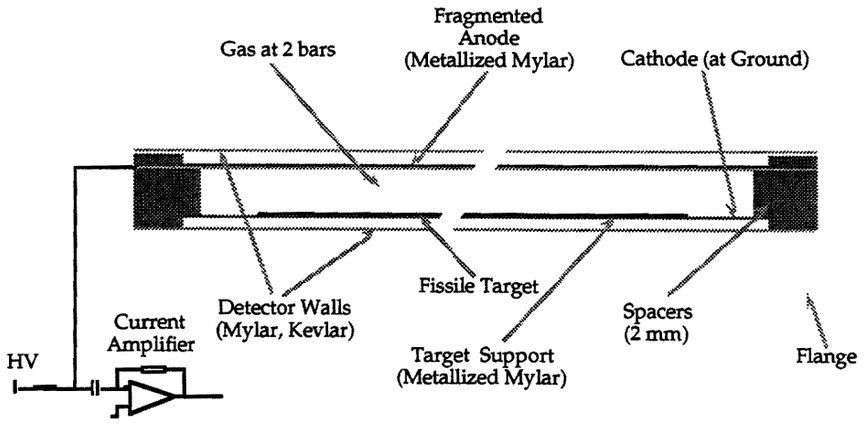

Figure 5.11 : Detector geometry

According to the measurements reported in [5.8] it is possible to build chambers producing pulses with 10 ns width and an unambiguous separation of alpha particles from the fission product pulses. Efficiencies as large as 98% were obtained with sources of ^{252}Cf of 1 mCi corresponding to a FF rate of 1 MHz and an alpha activity of 37 MHz. Independently from the detector time occupancy achieved and assuming that the front-end has a sufficiently large dynamic range, the simulations are showing the possibility to sustain an alpha activity of 5 mCi with good particle discrimination.

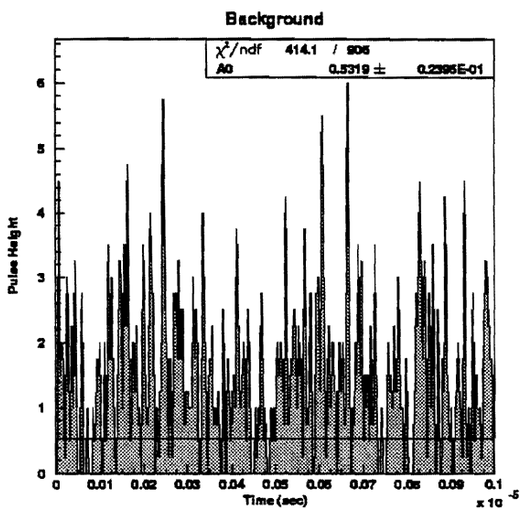

Figure 5.12: Simulation of 5 mCi background pile-up.

In figure 5.12 is reported the simulation to evaluate the background. The "physical quantum noise", normalized to 1, is a triangular pulse with 4 ns rise-time and 4 ns fall-time representing the clipped wave form of the detector current. Assuming a detector with dimensions and gas pressure such that the FF

with the minimum energy of 40 MeV leaving the target in any direction is fully absorbed, the ratio $E^{FF}_{min}/E^{\alpha}_{max}$=~8 for a typical alpha of 5 MeV. This figure is compatible with the max. pile-up of 6 given by the simulation and in agreement with the probability distribution.

Since the active volume of the detector is physically mounted on the neutron path, we must consider the effects of the detector structure on the neutron flux. The points to be considered are the "pollution" of the neutron flux, essentially due to elastic scattering, and eventually the gamma flash production due to captures. Concerning the gas used to absorb the FF, a reasonable choice is represented by an Argon mixture with ~5 % of CF_4, showing an absorption length at 1 bar of 22 mm for alphas and 8 mm for FF. According with the data reported in [5.9], the drift velocity for this mixture is 105 mm/μs that gives a detector time occupancy of ~40 ns for a gap of 4 mm and a pressure of 2 bars. Under these conditions and assuming an active detector surface of 1000 cm^2, the total reactions are equal to ~$1.5x10^4$, over the energy range between 0.1 and $2x10^7$ eV for a single PS shot of $0.7x10^{13}$ protons. The largest contribution is given by elastic scattering (90 %) and only ~ 250 events are due to capture. If we compare these numbers to the neutron flux the simulations are showing a flux contamination lower than $3.5x10^{-4}$ for energies higher than 10^5 eV and $1x10^{-6}$ in the rest of the spectrum as reported in figure 5.13. In case the capture events are giving a too large background to the neighboring detectors, the Argon mixture could be replaced by CD_4 showing very similar characteristics.

Since the required pressure to reach the detector response time is 2 bar and the detector is operating in vacuum, the nominal working pressure becomes 3 bars. The simulations are showing that in these conditions of pressure any metallic window is producing a strong effect on the neutron flux and must therefore be avoided. An interesting solution is provided by composite windows (Carbon, Kevlar® and Mylar®). The precise definition of the detector walls needs a very accurate mechanical design, nevertheless we can reach some conclusions based on calculations and measurements reported in [5.10]. The study was made on windows of Mylar® reinforced with Kevlar®. The most interesting conclusion is that the composite window has a mass of only 15% of that made with pure Mylar® to support the same pressure. Using an approximate formula for Mylar® windows the thickness required for a pure Mylar® window becomes 753 μm. Since the density for the two components is 1.4 g/cm^3, the mass for the window can be reduced to 0.21 g/cm^3.

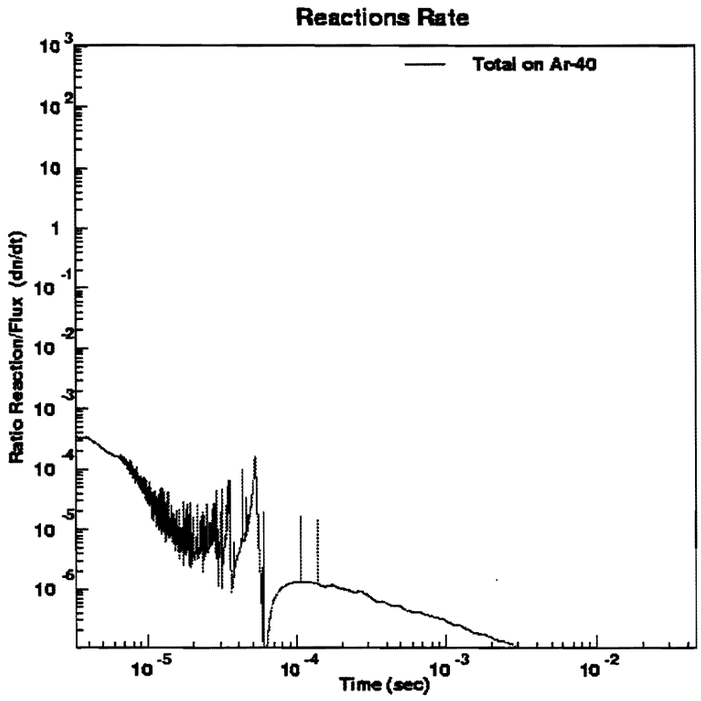

Figure 5.13: Relative Event Rates in 4 mm Argon at 2 bars over 1000 cm² surface.

Unfortunately the composition of the two materials being $C_5 H_4 O_2$ for Mylar® and $C_{14} N_2 H_{14} O_2$ for Kevlar®, the large quantity of Hydrogen will produce more than 1% events due to elastic scattering. To avoid this problem the Mylar® can be purchased in a form where the Hydrogen is replaced by Deuterium and the reinforcement could be made with Carbon fibers showing the same mechanical properties of Kevlar®. The total mass budget of materials, others than the gas, introduced on the neutron path can be fixed as follow: the Carbon fibre walls (2 x 0.75 mm), the Mylar® supports (4 x 10 μm) and the Aluminum metallization (15 μm). In figure 5.14 are reported the insertion losses produced on the neutron beam by the two Carbon walls of 0.75 mm.

Being the contribution of the Mylar® (Deuterium loaded) < 0.2% and that of the metallization < 0.1%, we can conclude that the insertion losses are around 1% of the neutron flux and are produced only by the Carbon walls. This situation is very satisfactory because the assumption to implement a counter with an active circular surface of ø=40 cm is probably only an academic exercise because a so large detector could not be built for reasons others than those concerning a stand alone FF detector.

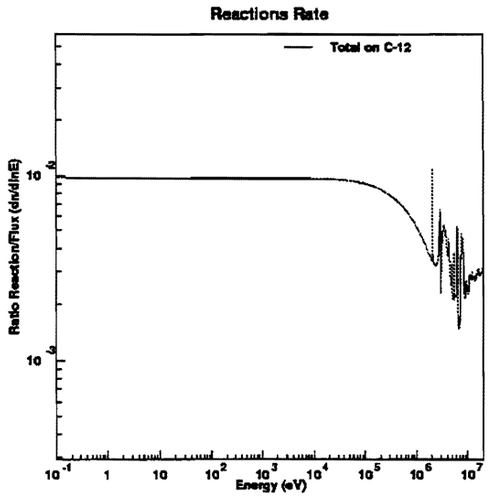

Figure 5.14: Absorption losses in Carbon walls (ø=40 cm)

We have now to evaluate the induced signal available on the chamber electrode. The high voltage is applied to the Anode through a resistor of several MΩ. and the decoupling to the Amplifier input is made with a high voltage capacitor. In response to the ionisation produced by the FFs in the gas, the current rises immediately to a value proportional to the ionisation while its shape and duration are depending on the track angle with respect to the electric field. For the detector filled with Argon, the instantaneous peak current for a FF of 40 MeV becomes:

$$I_{max}=\{(e_{FF}/w) \times q\}/t_d\} =\sim 5.3\ \mu A$$

where: e_{FF} = FF energy = 40 MeV, w = energy necessary to produce a free electron =~ 30 eV, q =electron charge = 1.6×10^{-19} C, t_d = drift time = 40×10^{-9} s. This current is sufficient to produce a large noise-less signal after amplification.

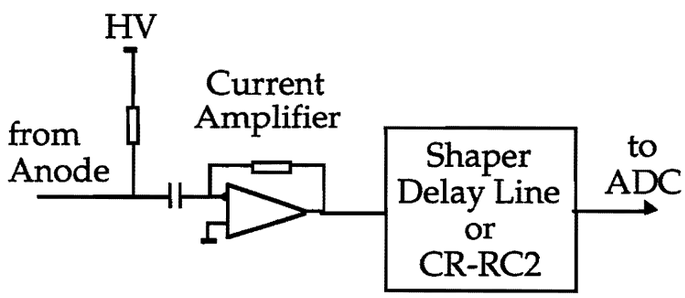

Figure 5.15: Front-end Electronics.

In figure 5.15 is presented a sketch of the front-end. The role of the Shaper is to subtract the base-line eventually introduced by the large background expected

for radioactive targets. The analog signal at the Shaper output can be sent to the Analog to Digital Conversion for digital storage. This information can be used, after discrimination, to veto the capture cross section detectors and, therefore, avoid the background induced by the gamma flash produced by the fission reaction.

As already mentioned it will be certainly necessary to fragment the detector surface to avoid a too large event rate for both fission reactions or back-ground. If we consider the problem of the detector fragmentation from a strict geometrical point of view, it appears that is possible to reach a fragmentation up to 128 cells with a detector surface occupancy of ~1000 cm^2 corresponding to 80 % of that of the nominal neutron spot.

Let's now consider the detector fragmentation from a physical point of view. The simulations reported in [5.11] [5.12] normalised to a single PS shot of ~ 0.75×10^{13} protons for the small lead target followed by a hydrogenous moderator, are helping to define the event rates. Following the results reported in [5.6] obtained on a detector used in a previous experiment and based on the same principle proposed here, the target density should not exceeds 0.3 mg/cm^2 to guarantee the clear separation of the FF from back-ground. In Table 5.1 are reported the expected yields for some interesting low radioactive elements. The high density of events appears, as expected, in the high part of the energy spectrum during the first 10-15 μs after the beam shot. A fragmentation of ~20 is sufficient to avoid the pile-up on a single channel.

Element	Max. Fission Rates [MHz]	Fission Reactions [per shot]	Fission Reactions [per day]
^{233}U	18	1.2×10^4	6×10^7
^{235}U	12	7.2×10^3	4×10^4
^{247}Cm	18	5.1×10^3	2.5×10^7
^{237}Np	15	1.6×10^2	8×10^5
^{239}Pu	18	2.3×10^4	1.1×10^8
^{242}Pu	14	1.3×10^2	6.5×10^5

Table 5.1 *Expected Yields for 1000 cm^2 Targets of 300 mg.*

The situation is completely different for highly radioactive elements reported in Table 5.2, for which the constraints are of two kinds: the max. background that allows the FF recognition in the counter and the radiation safety rules. Concerning the detector running, a radioactivity of 5 mCi seems the upper

limit for a single counter (see fig.5.12). The limitations given by the safety must be considered for each element and are depending on radioactivity other than alpha.

Element	Weight [mg]	Fission Reactions [per shot]	Fission Reactions [per day]
^{241}Am	1.46	1.5	$7.5x10^{3}$
^{242m}Am	0.47	$17x10^{2}$	$8.5x10^{6}$
^{243}Am	25	$1.2x10^{1}$	$6x10^{4}$
^{243}Cm	0.1	6.4	$3.2x10^{4}$
^{244}Cm	0.06	0.05	$2.5x10^{2}$
^{245}Cm	29.4	$1.5x10^{4}$	$7.5x10^{7}$
^{246}Cm	16.1	9.2	$4.6x10^{4}$
^{238}Pu	0.3	0.57	$2.8x10^{3}$
^{240}Pu	21.7	$1.4x10^{1}$	$7x10^{4}$
^{241}Pu	0.05	0.38	$1.9x10^{3}$

***Table 5.2** Expected Yields for 5 mCi Targets .*

For highly radioactive elements, the solution to reach a satisfactory statistic while keeping the total target radioactivity at reasonable levels, will be to measure these elements at a shorter distance. More generally all these parameters have to be carefully evaluated concerning the background produced by other ionizing particles than alphas and also concerning the spontaneous fissions that must be low compared to the neutron induced events.

To conclude, the proposed detector seems to be very well suited for measuring the shape of the FF cross section in the range 1 eV to 250 MeV. The time resolution of ~2 ns, consistent with the timing of the proton source and the $\Delta\lambda$ of the lead target, allows an energy resolution better than 10^{-3} at 1 MeV. The large signal produced by the ionization allows the use of a very simple front-end electronics and, therefore, the possibility to have a large detector fragmentation to enhance the statistics in case of highly radioactive elements. The low mass and the efficiency close to 100 %, are making this kind of detectors ideal as a part of a complex assembly for the measurement of the capture cross section.

5.B.3 – FISSION CROSS SECTION MEASUREMENTS IN YEAR 2000.

The groups of CERN and Orsay have proposed two types of detectors for fission (see 5.B.1 and 5.B.2). These detectors can be ready and calibrated at ILL-Grenoble by April 2000. They can perform the first cross section measurements on standard targets : ^{235}U and ^{233}U and possibly on ^{239}Pu. For neutron energies below 100 keV, they will serve to establish the overall perfomances of the

neutron beam, the energy resolution of the TOF and the background levels at the depths between the resonances. These elements will also serve to have the first spectroscopy of the resonances in the unresolved region above 100 keV. Fission measurements will be done also on some so called non fissile elements as ^{238}U, ^{232}Th, ^{237}Np, allowing to explore the higher neutron energy region through their threshold cross sections. Using 0.3 mg/cm^2 on 50 cm^2, the counting rate per day and per energy bin corresponding to a resolution of $2x10^{-4}$ are shown in Figure 5.16.

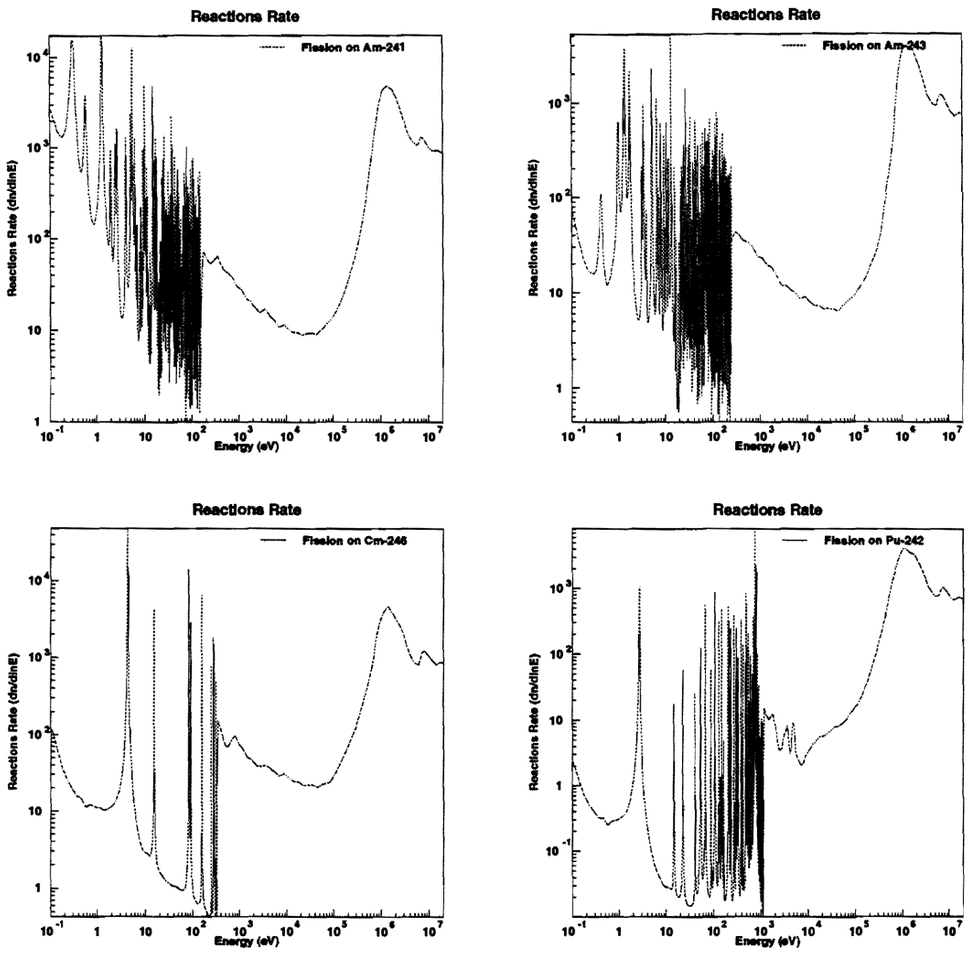

*Figure 5.16 : The simulated fission rates for a 10 days run and per energy bin corresponding to a bin-width of 0.05*E_n or 50 bins per energy decade.*

Neutron-induced fission cross sections of minor actinides like Am, Pu or Cm are important for justification of different ways of nuclear waste transmutation and deep burn-up strategies for modern fuel cycle. Those are also necessary as an input information for creation of complete fission cross section

systematics (FCS). Experimental data are available only in relatively narrow energy regions and have large discrepancies. The main part of the evaluations is based on statistical models tested with only low energy data. Therefore, any predictions of FCS cannot be done with satisfactory accuracy without special systematical measurements of FCS. There exist two measurements of ^{243}Am cross section below 50 eV, by Knitter et al [5.13] at GELINA and by Zamyatnin et al. [5.14] in Dubna. Fission widths extracted from these two measurements contradict with each other by a large factor. The background difficulties have been attributed to the spontaneous fission (SF) of the ^{244}Cm (0.05 atoms per cent) contamination and, mainly, to the characteristics of the IBR-30 booster, having permanent background between pulses (due to the multiplication of the delayed neutrons into the plutonium core of the booster). This type of background will be absent at the CERN-PS beam. The flight time of a 0.1 eV neutron for 200m is about 50 ms, resulting in a suppression of a factor of more than 300 of the background related to the ^{244}Cm contamination.

For ^{242}Pu there are no measurements below 50 eV, while data below 1 keV differ by an order of magnitude [5.15, 5.16]. In the ^{242}Pu measurements the main background will be caused by the fission of the ^{241}Pu (0.3%) contamination, but the very high resolution of the CERN-PS gives the possibility to separate the resonances of the two plutonium isotopes by time of flight.

EXPERIMENTAL METHOD	Multiplate/multisectional fast ionization chamber with alpha background suppression
ENERGY REGION	1 MeV — 200 MeV
TARGETS	Circular layers of high-purity Neptunium, Americium, Plutonium and Curium isotopes 10-100 μg/cm^2 thick, covered with 30 μg/cm^2 thick gold
ISOTOPES	^{237}Np, ^{241}Am, ^{243}Am, ^{242}Pu, ^{246}Cm (available in 2000-2001)
MONITOR	^{235}U or ^{239}Pu ; back-to-back geometry
CALIBRATION	Preliminary measurements at IPPE, Obninsk, EGP-15 accelerator with t(d,n) pulsed neutron source with energy up to 30 MeV; determination of numbers of nuclei in fissile targets with isotopic dilution method and alpha-spectrometry.

Like other even actinide isotopes, the fission cross sections of ^{242}Pu and ^{243}Am exhibit a threshold-type energy dependence, resulting to very small cross sections, typically barns for the strongest resonances. The high flux and the resolution of the CERN-PS source gives the possibility to study the level structure

in the sub-barrier region and extract the parameters of the levels in the second potential well.

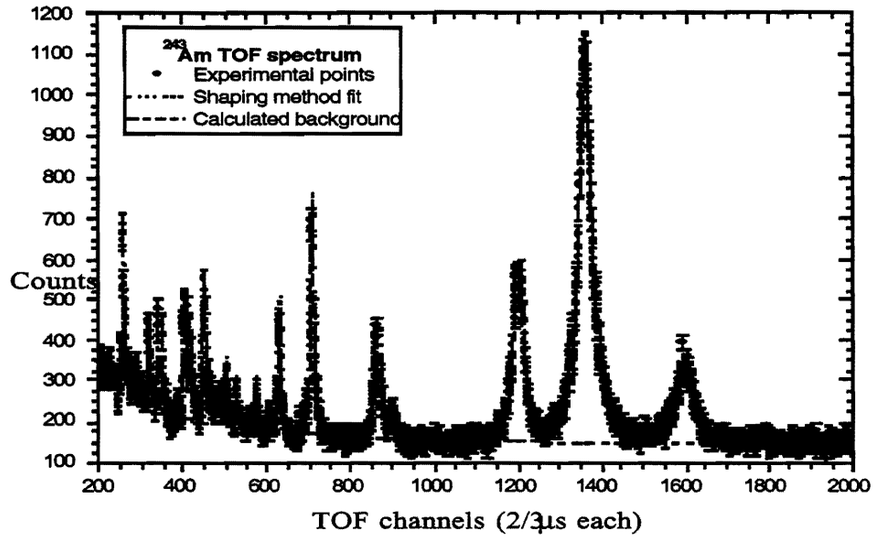

Figure 5.17. The ^{243}Am TOF spectrum measured at the IBR-30 booster in Dubna for a flight path of 15 m. The shown part of the spectrum covers the neutron energy interval from 0.8 to 50 eV.

The FLNP/JINR and the Obninsk groups intend to measure in the next 2 years the five nuclides listed below using an experimental technique developed already at IPPE and used in the measurements done at the IBR-30 reactor in Dubna for ^{243}Am [5.14]. In these experiments, the mass of the sample was about 2 mg and about 10^5 events in the energy interval from 1 eV to 10 eV were recorded (see Figure 5.17). "*Fresh*" targets will be prepared in 1999 and the experimental set-up will be adopted to better match the CERN TOF conditions. Moreover, they propose for the year 2000 to measure the fission cross sections ratio ^{237}Np/^{235}U in the neutron energy range 1-200 MeV. The experimental equipment will be tested using the ns-pulsed fast neutron sources of the IPPE in the energy range from 0.5 to 30 MeV and the IBR-30 resonance μs-neutron source of the Frank Laboratory of Neutron Physics. Target layers of ^{243}Am, with a total mass of 10 mg (5 layers of 2 mg each) are already available, while the ^{242}Pu sample has a mass of 30 mg.

5.C – NEUTRON CAPTURE REACTIONS.

When an (n,γ) reaction occurs, a cascade of gamma-rays is promptly emitted. Depending on the atomic mass of the nucleus, there can be from ~102 to ~104 possible de-excitation channels with gamma multiplicity averaging around 3 or 4. The cross section of the process can be determined by counting the number of cascades resulting from the target irradiated with a known neutron flux assuming that the detector efficiency is also known. The efficiency is usually measured in a calibration experiment with ^{197}Au as a target.

The most important feature of such measurements is that capture events have to be detected independent of the multiplicities of the repective gamma-ray cascades. Therefore, the following two extreme experimental approaches are possible: a) to use a detector with nearly 100% efficiency for all gamma-rays (total absorption detectors), and b) to detect only one gamma-photon from each cascade (then a detector with a very low efficiency, ~1%, is needed) but with the efficiency proportional to the gamma-ray energy (Moxon-Rae method [5.17]). An intermediate solution is also known. It assumes the use of a detector with ~10% efficiency and correction of each pulse amplitude with a weighting function [5.18].

Among other parameters, low sensitivity of the detector to neutron background is very important. This implies a careful choice of the detecting medium, as well as the capability to distinguish between (n,γ) and (n,f) reactions. The latter can be achieved, although not with a 100% efficiency, by measuring the cascade multiplicity (it is possible in some total absorption detectors that enable detection of the individual gamma-rays) or by anticoincidences with an additional fission fragment detector surrounding the target (see section on fission fragment detectors).

A time resolution better than ~10 ns and counting rate up to ~1 MHz are also desirable to profit from the high neutron flux and the good neutron TOF resolution. When radioactive target isotopes are investigated, the corresponding gamma-ray background will distort the measurements. However, it can be rejected if the detector energy resolution is good enough.

Among the existing capture detectors we consider the following :

1) For stable isotopes available in large quantities (~some mg to grams), those based on the Moxon-Rae principle ([5.19] is an example) seem to be

the most suitable due to the low sensitivity to neutrons and the potential possibility to operate them in current mode thus enabling high data acquisition rates.

2) For stable isotopes in small quantities or samples with low radioactivity, the liquid C_6D_6 scintillation detector with pulse height weighting can be used [Geel] as it enables, to some extent, rejection of gamma-ray background and is also very little sensitive to neutrons.

3) In the case of highly radioactive and fissile isotopes, the total absorption detectors, such as BaF_2 Crystal Ball [5.20] and NaI(Tl) "Romashka" [5.21,5.22] with good energy resolution would be the best choice. The HPGe 4π cluster detector with excellent energy resolution should also be considered [5.23]. New developments combining Micromegas photodetectors [5.24] with BaF_2 scintillators seem to offer a promising and rational path for the solution of high instantaneous rates, with the additional advantage of a low sensitivity to scattered neutrons.

Also new detection techniques may significantly contribute to improve the detector setup for neutron capture measurements. Far from pretending to mention all of them, we would refer new developments on a CeF_3 scintillator which has a very low sensitivity to neutrons [5.25] and total absorption liquid xenon gamma-ray detectors: a 4π segmented TPC with high position resolution or a very fast scintillation calorimeter with high energy resolution [5.26,5.27], especially advantageous for the experiments when a large detector is required.

5.C.1 – CAPTURE CROSS SECTION MEASUREMENTS IN 2000.

A neutron capture measurement to be performed in the first starting phase of the CERN TOF facility, i.e. in the years 2000 to 2001, should possibly comply with the following characteristics :

- The chosen isotope should be important for one of the research fields mentioned in Ch. 3. Since the funding of the detector station and associated infrastructure would be provided by the EC Fifth Framework Programme, the ADS field should be privileged.
- The measurement should emphasize the "added value" of the facility in comparison with the present ones.
- The gamma detectors should be the simplest of the existing detectors under operation at other TOF facilities.
- For checking purposes, at least part of the cross sections and/or resonance parameters of the chosen nuclide should already be rather well known.

- The measurement should be rather straightforward, thus avoiding the most difficult cases such as fissile or very radioactive isotopes .
- The sample should be readily available.

A possible candidate would be ^{232}Th, of interest for ADS and thorium fuel cycle in general. There are at least two reasons for this choice : first, the isotopes of interest for the Th fuel cycle have not received the same attention as those of the U-cycle. In the data files released in the nineties, the resolved region for ^{232}Th extends only up to 4 keV as compared to 10 keV for the case of ^{238}U, which however has a comparable level density. A capture measurement at 200 m flight path with a resolution of 1.5×10^{-4} would fill this gap. Secondly, there are even discrepancies up to 15% between the average ^{232}Th capture cross sections in the various data files above ~50keV.

The ^{232}Th (n,γ) reaction from thermal up to 200 keV is presently measured by a collaboration between FZK Karlsruhe and IRMM Geel. The CERN measurement, besides providing the better resolution as already stated, has also the advantage of being unaffected by the γ-activity of the sample which is a serious problem for the Geel measurement. Finally it should be noted that an extension of the resolved region up to 10 keV will probably require also a high resolution transmission measurement considered in section 5.E. Similarly, the capture cross sections for the elements ^{238}U, ^{237}Np, ^{99}Tc, ^{93}Zr, of interest for the ADS studies, are considered together with the well known targets used as standards, like ^{nat}Ag and ^{197}Au.

For these first measurements it is proposed to use "total energy" detectors, i.e. scintillators in which the proportionality of the detection efficiency to the total radiative energy emitted is achieved via a pulse-height weighting method. If the primary goal is a very low efficiency to scattered neutrons, the best choice is a deuterated hexabenzene (C_6D_6) based liquid scintillator : this kind of detector is currently used at the main existing TOF facilities, namely ORELA (Oak Ridge), LANSCE (Los Alamos) and GELINA (Geel). It is advisable to use scintillators canned in thin aluminium cylinders of 10 cm internal diameter and 7.5 cm height : for such a size, a pulse-height weighting function has been experimentally measured, and tested, at Geel.

The main experimental parameters would be as follows :

- Flight distance : 230 m.
- Beam and sample size : circular, 8 cm diameter corresponding to 50 cm^2.
- Sample thickness and type : ~10 mg /cm^2 .

- Detectors : four C_6D_6 scintillators of size as above, placed with their axis perpendicular to the neutron beam and with the entrance windows at ~6.5 cm from the sample centre.
- Neutron flux monitor in-beam, e.g. thin ^{10}B ionization chamber available at Geel, placed ~0.8m upstream.

The counting rates are estimated by simulation and compared to the results of a similar capture run performed at Gelina on a considerably shorter flight path, taking into account that in the year 2000 the proton pulse will consist of a single burst every 14.4s. Under this assumption, one can estimate (Fig. 5.1) that the total capture rate amounts to 7.5×10^6 and 17×10^6 per day for a 50 cm^2 and 100 mg/cm^2 sample of ^{232}Th and ^{233}U, respectively.

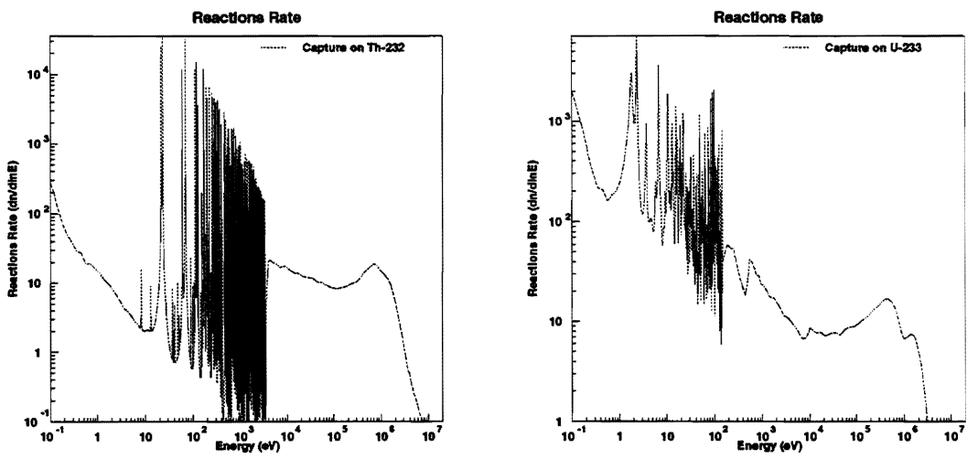

Figure 5.18: The simulated capture rates per day and per energy bin corresponding to a resolution of 2×10^{-4} or 12'000 bins per energy decade.

The instantaneous counting rate of the CERN TOF facility at 200 m flight path do not exceed 10 MHz for the example of ^{232}Th. The very fast decay time of the scintillator (3 ns) combined with fast photomultipliers and a standard Particle Physics FADC-VME data acquisition system allows this measurement without rate problems.

5.C.2 – SECOND PHASE MEASUREMENTS.

The desirable features of an ideal gamma ray detector for use in neutron capture cross section measurements, particularly by TOF techniques are :

- an efficiency for the detection of a capture event, which is independent of the particular gamma ray cascade emitted.
- low sensitivity to the scattered neutrons.
- fast response.
- low intrinsic background and ease of shielding.

In general, the main criteria in the choice of the type of such a calorimeter are its sensitivity to direct but also to scattered neutrons, its pulse rise time and the speed of the readout devices.

The best identification of neutron capture events is provided by the total energy of the capture γ-cascade. This requires a large solid angle (>90% of 4π) detector that operates as a calorimeter. With a γ-ray efficiency of better than 90% in the entire energy range below 10 MeV, capture events can be registered with almost 100 % probability. A typical example of such a detector is the design of the Karlsruhe 4π BaF_2 detector [5.20]. A similar large solid calorimeter, consisting of CeF_3 crystals, has been discussed by the Grenoble group [5.25]. The main arguments for the CeF_3 crystals are the faster decay time and the four times smaller sensitivity to the prompt neutron reactions.

New developments on particle detection techniques can contribute significantly to improve performance of the gamma-ray detection system. Liquid noble gases are very suitable for the detection of gamma-rays with high efficiency, especially liquid xenon due to large atomic number (Z=54), high density ($3g/cm^3$), excellent scintillation properties and the possibility to collect free electrons released by an ionising particle. Therefore, two types of a 4π liquid xenon total absorption detector are considered. First, a liquid xenon scintillation calorimeter with full direct light collection, similar to the one proposed in [5.27], can provide high energy resolution (about 4% at 1 MeV), time resolution better than 1 ns and counting rates up to several times 10^6 Bq. On the other hand, the experience accumulated on liquid xenon ionisation detectors self-triggered by xenon scintillation [5.26,5.28] allow also a highly segmented liquid TPC to be considered. Although limited in counting rate to ~10^5 Bq, its precise position resolution and the possibility of the whole event reconstruction makes the latter device a powerful tool for active neutron background rejection. Liquid argon should also be considered due to exceptionally low neutron capture cross section of its principal isotope, ^{40}Ar, that makes such a detector incomparably superior to any other 4π gamma-detector in terms of sensitivity to neutron background.

A key problem in the experiments with radioactive samples is the efficient detection of multiple gamma rays induced by neutrons in the presence of a large background of low energy gamma rays from radioactive targets. With values foreseen for the background intensity, like 10^9 Bq, we are naturally inclined to look into the potential opened by recent research on fast detectors for the high luminosity colliders. The application of fast photosensitive chambers, e.g. Micromegas, as massless photomultipliers has been considered by the group of G. Charpak for both crystal and liquid calorimeters. A combination of the Micromegas detector [5.24] as a photon detector with solid BaF_2 (CeF_3) or liquid noble gas scintillators seems to offer a promising and rational path for the solution of the problem, with the additional property of offering a low sensitivity to the background of scattered neutrons.

Concerning the gamma spectroscopy, the contribution of the ILL group [5.23] supplying a HPGe-detector array has been studied in relation to shielding and neutron background problems with encouraging results. The utilisation of this detector array would be particularly interesting for the gamma spectroscopy of fission fragments from (n,f) reactions, in particular for targets with small inherent gamma radioactivity.

Neutron capture studies on radioactive targets are hampered by the background from the sample activity. Although spallation neutron sources have not often been used for measurements of radioactive samples so far, their huge fluxes allow to reduce the sample mass by a factor of more than few 10^3 compared to the traditional facilities. In the case of a radioactive sample, the following background sources can be distinguished. a) Gamma-rays from the nuclear decay, typically with energies below ~1 MeV and fluorescent X-rays below 100 keV and b) Bremsstrahlung from beta activity (both internal, IB, and external due to passage of the beta particle in the surrounding materials).

Beta particles are slowed down by radiative processes as well as by collisional Coulomb interactions (ionisation and excitation). Radiative losses are always a small fraction of the energy losses due to ionisation and excitation and are insignificant in absorber materials of low atomic mass. The ratio of the specific energy losses of beta particles is given approximately by :

$$\frac{(dE/dx)_{Brems.}}{(dE/dx)_{Coll.}} \cong \frac{E \times Z}{700}$$

where E is in units of MeV. The cross section for radiative losses is given by

$$\frac{d\sigma}{dE_\gamma} \approx 5\frac{e^2}{\hbar c} Z^2 \frac{1}{\beta^2} \frac{r_e^2}{E_\gamma} \ln \frac{m_e c^2 \beta^2 \gamma^2}{E_\gamma}$$

where β (γ) is the velocity of the incident electron and Z is the charge of the nucleus. Note, that the cross section falls off with increasing photon energy roughly as 1/E. For the majority of the radioactive elements of interest, the maximum energy of the electrons does not exceed 1 MeV and therefore the bremsstrahlung in the sample is not expected to contribute significantly to the background rates seen by the calorimeter. On the other hand, the detector can be easily shielded from beta-particles with a low mass material without taking a risk to produce bremsstrahlung (for example, 2 mm of Be is enough to stop 1 MeV electron).

In respect to radioactive samples with inherent gamma emission, the mass of the sample depends on the specific activity of the isotope under study and the pileup rejection of the detectors and readout electronics. The probability that a given count is formed from the pileup of x+1 gammas is :

$$P(x) = e^{-R\tau}(1-e^{-R\tau})^x \approx \frac{x}{x!} R\tau \cdot e^{-R\tau}$$

where R and τ are the rate and the scintillation decay time, respectively. For a pileup level of 3%, each calorimeter module would accept a rate of ~10 MHz, ~0.5 MHz, ~50 kHz and ~25 kHz for a $(BaF_2)_{fast}$, a CeF_3 or LXe, a BGO and a $(BaF_2)_{slow}$ scintillator, respectively. Taking the BaF_2 Crystal Ball as an example of the 4π detector design reference, one can estimate that for a capture event with the average multiplicity of 3 about 7% of the individual detectors are hit. This allows the maximum sample activity to be estimated to ~4 mCi, ~200 μCi, ~20 μCi and ~10 μCi for the equivalent scintillator materials.

MATERIAL	Density [g/cc]	Attenuation length, AL, at 6 MeV [cm]	Decay time [ns]	Rel. light output	n-captures in 5 AL per pulse / cm^2 at 200 m
$PbWO_4$	8.28	2.98	5 - 15	0.01	28'833
BaF_2	4.89	6.01	0.7 (20%,fast) 620 (80%,slow)	0.05 0.20	8'613
$Bi_4Ge_3O_{12}$	7.13	3.59	300	0.15	4'145
CeF_3	6.16	4.77	10-30	0.10	2'138
LXe	2.95	9.18	27	0.90	

Table 5.1: *Properties of several inorganic crystal scintillators. The number of captures correspond to an energy range between 0.1 to $2x10^7$ eV according to the neutron spectrum at the CERN TOF Facility.*

However, the well known pulse-shape of the two slow scintillators BGO and a $(BaF_2)_{slow}$ can be off-line reconstructed, once the first part of the pulse is free of pileups and measured at several points. The utilisation of flash ADC's with 10 ns

clock allows to have 10 points in the first 100 ns of each pulse. By fitting the known pulse shape the corresponding gamma energy can be extracted by resolving the pileup pulses. This off-line analysis would correspond then to a pileup resolution of ~100 ns. In particular the BGO and $(BaF_2)_{slow}$ crystals with long decay times would run with higher sample activity, i.e. 120 μCi, at the same 3% pileup level, which is determined now exclusively by the 100 ns pileup resolution of the electronics.

In conclusion, the intrinsic activity of the radioactive samples in the case of nanosecond fast calorimeters, as $(BaF_2)_{fast}$, can be 4 mCi, whereas for the BGO and $(BaF_2)_{slow}$ it should not exceed ~5 MHz or 120 μCi per detector module. This means that the total acceptable rate would increase with the granularity of the detector.

Most of the radioactive targets under consideration have appreciable yields only for gamma energies below 100 keV. For these cases the activity of the radioactive sample could be even higher than estimated above. Firstly, such low energy gammas can be absorbed by a set of appropriate adsorbers (filters), for instance 1 mm Cd and 0.25 mm Cu for 70 keV gammas. Secondly, it can be seen that the pileups of such low energy gammas will induce an overall baseline, which can electronically be eliminated, because its level is much smaller compared to the total gamma energy deposited in the calorimeter from (n,γ) events (ΣE_γ > 1-2 MeV). The total gamma energy of (n,γ) events equals the binding energy of a neutron in the compound nucleus being studied, plus the kinetic energy of the incident neutron. In such cases, the sample activity can reach the level of 30 mCi where the gammas of the ^{135}Cs with E_γ<30 keV arise from internal and external bremsstrahlung and the 662 keV gammas are due to the ^{137}Cs contamination amounting to 10^{-3} (see chapter 4).

Since the statistical fluctuations of the baseline appear at the lower frequency spectrum than the pulses of the true capture events, the use of a highpass filter would reduce and smoothen these baseline fluctuations. In conclusion, for radioactive targets with gammas below ~100 keV, pileups can be tolerated without deteriorating the measurement of neutron capture events by detecting the total energy of the capture gamma cascade (ΣE_γ > 1-2 MeV) in a large solid angle (90% of 4π) calorimeter.

In respect to the photosensitive readout device, recent tests at Saclay and Collège de France have shown that the Micromegas, with a He gas filling with 6% of isobutane at atmospheric pressure, permits to detect single photoelectrons,

with a gain of 10^7, and a good pulse height resolution - for single electrons in a proportional mode - which is reached by no other detectors. The timing of the detector has been shown to be of the order of one nanosecond. In particular, the combination of BaF_2 and CsI has already been studied by J. Seguinot et al. [5.29]. We will have to choose between two strategies:

a) Reflective photocathodes deposited on the outer side of the thin grid, of 4μm thickness, which limits the amplification volume of Micromegas.

b) CsI photo cathodes deposited directly on the exit face of the BaF_2 crystal.

The BaF_2 crystals have a fast emission of VUV light, peaked at 225 nm, with a yield of 560 photons per MeV. With a reflective photocathode the maximum observable signal is limited, by total internal reflection to about 11.6% per face, i.e. 4.6 photoelectrons per MeV per face. But an additional loss by a factor two due to transparency of the grid has to be taken into account. Notice that the face can be placed at a distance of 100μm from the entrance grid of the amplifying space. With crystals of 1x1cm^2 section practically all electrons ejected from the CsI photo cathode deposited on the grid are detected. We may then expect a 100% efficiency for gammas above 1 MeV and a reduced efficiency for photons with an energy of the order of 0.2 MeV from the radioactive targets. A transmission photocathode, deposited directly on the crystals surface, would avoid the problem of losses due to internal reflection, but it would not increase the detected signal because its quantum yield is only 10% of the reflective cathode yield.

We are then lead to the study of a well defined detector:

- Crystals of BaF_2 of 8 cm length and 1x1 cm^2 section with about 1 m^2 surface.
- A mosaic of Micromegas detectors of 20x20 cm^2 with a gas filling of He and 6% of Isobutane.
- The VUV light pulses have a duration of 0.6 ns and the Micromegas detector has a time resolution of about 1ns.
- For a gamma energy of 1 MeV there are 3 photoelectrons detected
- The counting rate per crystal and per pad, due to a 10 GHz background, is 100 kHz which is rather low and permits the use of low noise amplifiers for each of the 10^4 pads which are collecting the avalanche of the counters.

In this respect Micromegas offers rather unique properties, where the events are selected from the background through two physical effects :

- The efficiency of the BaF_2 crystals for the capture gamma rays is higher than the efficiency for the gammas rays emitted by the radioactive targets.

- The multiplicity of the gammas produced by neutron capture is measured with a time resolution of 1ns leading to a rejection of the background. The accidental rate will depend on the limit set for the multiplicity and on the time resolution of the detector.

Physicists at Saclay and Coimbra would participate in the development and the construction of this Micromegas counter.

5.D – NEUTRON INDUCED (n,X) REACTIONS .

Any ADS project relies heavily on the cross sections of the (n,n') and (n,xn) reactions, since these reactions govern largely the flux and the energy spectrum of the neutrons in any reactor. To avoid model-dependent analyses, such reactions should be investigated with the help of neutron detectors.

With white neutron beams, such reactions have mostly been investigated by detecting not the neutrons, but discrete γ-rays which are produced in the final nucleus. Technically, this method is relatively straightforward since γ detectors can have a good time resolution, which allows to measure precisely the TOF of the neutron projectile, and a good energy resolution which allows to identify the final nucleus and thus the number of emitted neutrons. Measuring the excitation function of any of these reactions consists experimentally in registering the γ-spectrum as a function of E_n. The basic assumption of this method is that the cross section for production of secondary neutrons without emission of any γ-ray is negligible.

However, this method cannot be generalised to all possible nuclei. The final nucleus should preferably be an even-even nucleus. Indeed, in this case the γ ray which is used to identify the reaction channel is the transition from the first 2^+ state to the ground state. For even-even nuclei, often more than 90% of the γ-cascade proceeds via this transition [5.30]. Thus Vonach et al. for example have investigated ^{207}Pb (n,xn) reactions and have given cross sections for (n,2n), (n,6n) and (n,8n) reactions on ^{207}Pb, and for (n,n'), (n,2n), (n,3n), (n,5n), (n,7n) and (n,9n) reactions on ^{208}Pb.

The method consists in detecting γ-rays in a large solid angle set of scintillator modules, and the neutrons in coincidence in a number of DEMON [5.32 -5.36] modules. The events are triggered by the detection of any γ-ray. The γ-detectors must have a good time resolution, so that the projectile energy is precisely determined. It must also have a high efficiency and a low threshold to allow the measurement of coincidences to be triggered by low energy transitions

which are important at the threshold. It may also have a good energy resolution, which would help identifying given channels and a low neutron sensitivity. The Total Energy Spectrometer which is being brought in operation at CERN by the Isolde collaboration [5.31] would be a suitable candidate. However, the first experiments will be performed with 9 modules of the BaF_2 Karlsruhe Ball, corresponding to 1π solid angle. The neutrons will be detected in about 24 DEMON modules, each consisting of a NE213 cell 16 cm in diameter and 20 cm deep, with the n-γ discrimination performed by pulse-shape analysis. They will be located at about 1 m from the target. This geometry allows the determination of the time of flight of the detected neutrons, and thus their energy. This energy information is essential for the knowledge of the detection efficiency. It would also allow to measure double-differential cross sections of emitted neutrons in a later stage.

The principle of the method is based on the fact that any reaction leads to the emission of at least one detectable γ–ray. Then the detection of this γ-ray can be used as a trigger for the reaction, providing in addition the time of the collision and thus the energy of the projectile and the start for the time of flight of the neutron detection. Fission reactions must also be included in the trigger, since they contribute to the cross section of (n,xn) reactions. The measurement will be more simple for the fissile targets, by replacing the gamma detectors by fission ones, triggering thus on fission fragments instead of the prompt gammas.

If only (n,xn) reactions contributed to the trigger, the neutron multiplicity would be :

$$\nu = \frac{\sigma(n,n') + 2\sigma(n,2n) + \ldots}{\sigma(n,n') + \sigma(n,2n) + \ldots}$$

For instance, just above the threshold for the (n,n') reaction, ν must be found equal to 1. The method can be checked with the elements having well known σ(n,n'). When the (n,2n) channel opens, ν will increase in proportion to the relative cross sections for the (n,n') and (n,2n) reactions. Therefore, the measurement of ν reveals the opening of each new channel. In the example of ^{208}Pb, the method can be checked until the threshold of the 4n channel, and then it would allow to measure the σ(n,4n) until the (n,6n) channel opens. At higher bombarding energies, where the (n,xn) channels with large values of x open, it is no more possible to separate the cross sections for the different values of x but the results are still valuable for the comparison of the different model predictions.

Up to now we have made the assumption that each collision will produce at least one γ-ray. This hypothesis has increasing validity when the mass of the

target becomes heavier, the neutron multiplicity larger and the bombarding energy higher, but is not valid in the vicinity of the threshold of any channel with two consequences. The first one is the shift of the threshold by the energy of the first excited level, being of the order of a few hundred keV in the most heavy nuclei but much larger for magic or double-magic nuclei. This effect clearly can be corrected from the known Nuclear Data. The second consequence is the decrease of the trigger efficiency for low excitation energies. This effect has to be corrected by statistical model calculations including the discrete level scheme of the nucleus.

The method is valid only for the trigger acting on the (n,xn) reactions. But gamma rays are emitted also by the capture and the fission reactions which, however, have very small cross sections as soon as the bombarding energy reach the threshold of the (n,xn) channels at few MeV. Such contaminating reactions will therefore contribute very little in the trigger rate. The cross sections of such reactions are either sufficiently well known or will be independently measured, allowing thus the correction, if necessary, of such contaminations.

A GeLi detector will also be included in the set-up in order to test the possibility to measure (n,n'γ) to the lowest excited state at TOF. The neutron background will determine the closest distance at which this detector can be placed, and thus the counting rate.

Despite the fact that this method is not universal, its simplicity is such that it should remain an essential tool at the TOF facility. The main limitations come from the thresholds of the detectors, which are around 100 keV for gamma detection and 1 MeV for the neutron one. Thus the possibility to place a GeLi detector close to the target at TOF should be checked immediately. This method based on n-γ coincidences may even extend the interest of the GeLi measurements. More precisely, it would:

- Fill in some of the gaps corresponding to non even-even final nuclei;
- Select a given channel, even in the case that γ-lines corresponding to other mechanisms like capture, overlap with the line of interest;
- Allow to test the different theoretical models by investigating directly the neutron multiplicity as a function of bombarding energy. Actually, one of the aims of measuring σ(n,xn) is to allow to calculate the neutron multiplicity ν , and the Strasbourg group proposes to measure it directly;
- Provide experimental informations on the angular distributions and possibly on the energy distributions of the γ– and n-emission. These

informations are of course of great interest in conceiving the ADS prototype.

The identification of charged particles in the reactions with charged particles in the final state is mandatory, i.e. separate protons from α particles, but also from ^{2}H's, ^{3}He's and ^{3}H's. Because the cross sections for charged particle production are generally less than 100 mb, the target must have a large total mass. The measurement of low energy particles, like protons at 1 MeV or α particles at 5 MeV, implies very thin (< 1 mg/cm^2) targets, which means that such targets must cover a large surface, i.e. have a radius of several tens of cm. Therefore, the CERN TOF facility is of importance for such measurements.

The method for charged particle identification consisting in the measurement of the energy or the energy loss and the particle velocity is not possible at the TOF beam, since the time measurement is just used to determine the projectile energy. Combinations of gas detectors, thin and thick scintillators etc., have been used in other laboratories, but the probability to produce several particles in a single collision makes tracking indispensable. Moreover, It seems quite difficult to meet all these requirements with one single detector set.

It seems reasonable to define two regions for the energy of the detected particles. The one region extends from 1 to some tens of MeV for protons, and from 5 to ~100 MeV for the α particles. In this region, detectors must obviously be placed in vacuum. The second region will cover the higher energies. Classical nuclear physics detectors are, indeed, not suited for the time structure of the TOF beam, at least at high bombarding energies. Identifying the charged particles implies several measurements of their energy loss. The angular distribution for the charged particle emission is sometimes strongly forward peaked, implying the exposition of the detector to the neutron beam. The use of a combination of high-energy tracking detectors (MWPC, MSGC, drift chambers) seems to be mostly adequate. In particular, the use of radiation resistant Si-microstip detectors is very promising mostly for the charged particles produced with small angles. However, the decision on the final charged particle detector for charged particles requires more further discussion inside the collaboration.

5.E– ELASTIC AND INELASTIC NEUTRON SCATTERING.

Elastic scattering is a key process for understanding the great variety of nuclear reactions. Although it is the simplest collision process its study has yielded important insights into the nature of the nuclear many-body problem. Investigation of inelastic and reaction channels gives specific information on the structure of the collision partners. Before any of the below mentioned experiments can be performed a detailed characterisation of the beam of the TOF facility is required. Specifically the time energy correlation function, the spectrum of the beam, the absolute flux and the background at the measurement stations must be determined by standard measurements.

The study of elastic scattering below the first inelastic threshold can easily be performed with the white beam of the TOF facility because there is only one neutron exit channel and the TOF measurement directly gives the neutron energy. The measurements presented in 5.E.1 as well as elastic scattering in the resonance region, which is usually below the first inelastic threshhold, belong to this type of experiments.

Above the first inelastic threshold, there are several energy groups in the exit channels, and therefore the energy of the incident neutron cannot be extracted uniquely from the TOF. Additional information is needed to determine the energies of the incident and scattered neutrons. For instance a direct measurement of the energy of the scattered neutron can be perfomed with a neutron spectrometer. This technique, which can work only at sufficiently high energies (few tens of MeV), has been sucessfully used at the LAMPF/WNR facility and could be also implemented at the CERN TOF facility.

5.E.1 MEASUREMENTS ON THE ELECTROMAGNETIC STRUCTURE OF THE NEUTRON.

This section comprises measurements of the neutron-electron scattering length and the electric polarizability of the neutron. Two complementary experimental schemes are envisaged, i.e., angular scattering and transmission experiments. The following program of measurements is planned for the first phase of operation of the TOF facility.

- **MEASUREMENT OF THE NEUTRON-ELECTRON SCATTERING LENGTH BY ANGULAR SCATTERING:**

Recent measurements of b_{ne} by Kopecky *et al.* [3.69, 3.71] and Koester *et al.* [3.70] are based on transmission experiments on ^{208}Pb and ^{209}Bi. To end the ongoing discussion and to eliminate the discrepancies between these measurements and those of [3.66, 3.67] an independent determination using angular scattering techniques (similarly to Krohn and Ringo [3.62, 3.64]) is planned at the TOF facility in the beginning phase. A setup suitable for high precision angular scattering experiments is required [3.62, 3.64] using the modern techniques of data acquisition. The key parameters of the experiment are:

Proposed samples: Xe, Ar , thorogenic ^{208}Pb (liquid)

Sample position: at the 230m measurement station a beam collimation of a few cm^2 is necessary for the definition of the scattering volume and the scattering geometry.

Range of energies: 0.05 eV to 100 eV

Detectors: Neutron detectors (e.g. ^{3}He or ^{10}B loaded liquid scintillator detectors) at well defined angles.

Required accuracy: better than $5 \cdot 10^{-4}$

Expected use of beam time: starting with year 2000; this experiment is the first in a series of measurements concerning the fundamental properties of the neutron and could be scheduled in the group of first experiments at the TOF facility.

The challenge of this experiment lies in the precision which must be achieved. This implies that a detailed study of the background for the specific geometry of the setup is required. Small contributions which influence the q-dependence (e.g. nuclear resonances, effects due to the status of the target, etc.) must be taken into account carefully.

In the beginning phase complementary measurements of the neutron-electron scattering length via transmission experiments will be proposed. They will consider the energy dependence of the total cross sections of ^{208}Pb and ^{209}Bi to compare with the previous results at ORELA [3.71] but also of ^{86}Kr. In principle this experiment uses a standard setup for transmission measurements .

Again it is characterized by the challenging requirement of accuracy. The key parameters are:

Proposed samples: ^{86}Kr, thorogenic ^{208}Pb, ^{209}Bi

Range of neutron energies: 0.05eV - 100eV

Expected accuracy: about 10^{-4}

At present this transmission experiment (detector located in the primary beam axis) cannot be performed at the TOF facility because no adequate detection system is available which can handle the high peak flux. However, neutron peak fluxes of this magnitude will also occur in future spallation sources (e.g. AUSTRON, ESS) and therefore it is of great interest to develop the techniques of high rate neutron detectors. A possible direction might be based on current mode detectors (using fast scintillation materials) with segmentation of the detection volume and ultra-fast data acquisition electronics. With the availability of such a detector system the feasibility of transmission experiments at such high peak rates should be demonstrated first at the TOF facility.

- **MEASUREMENT OF THE ELECTRIC POLARIZABILITY BY SCATTERING OUT OF THE FORWARD DIRECTION:**

The determination of the electric polarizability requires experiments typically of accuracy 10^{-4}. This can be achieved in transmission experiments but is beyond the limits of angular scattering experiments nowadays. Therefore the best available data on the electric polarizability of the neutron have been obtained by transmission [3.73]. As already mentioned it appears now feasible to perform measurements which reduce the uncertainty in a_n to 10^{-4} fm^3.

It is the goal of the TOF collaboration to achieve this accuracy. The experiment, however, has not to be designed as a standard transmission experiment because of the high peak flux of about 20 neutrons/cm^2 ns at 500 keV (an energy which has to be included in these experiments). Positioning the detector out of the forward direction at a well defined angle will yield a similar information, i.e., a linearly k-dependent term of the cross section. Because of the high intensity of the beam the statistics can be optimized by the design of the setup. In particular it will depend on the status of the development of the high rate detector. The key parameters of the experiment are:

Proposed samples: thorogenic ^{208}Pb (compensated with radiogenic ^{206}Pb)

Sample position: at the 230m measurement station; a beam collimation of a few cm^2 at the sample is necessary for the definition of the scattering volume and the scattering geometry.

Range of energies: 100 eV to 500 keV

Detectors: Neutron detectors (e.g. ^{10}B loaded liquid scintilator detectors and plastic scintillators) at well defined angles.

Required accuracy: relative accuracy about 10^{-4}

Expected use of beam time: this experiment is scheduled as a follow-up experiment to the neutron-electron scattering length measurement by the angular scattering method.

At the accuracy required it will be of particular emphasis to have a good knowledge of all resonances and their parameters. Especially the occurence of resonances near the continuum threshold must be checked because they can influence the low energy behaviour. A good background determination is also required although they are expected to be smaller than in standard transmission experiments.

A complementary measurement of the electric polarizability via a transmission experiment on thorogenic ^{208}Pb will be proposed at GELINA in parallel. In principle it will be an adapted version of the ORELA experiment [3.C42] aiming an improved accuracy.

• **MEASURING THE PHOTO- AND MESON PRODUCTION IN np SCATTERING:**

As already mentioned there will be a considerable flux of neutrons up to energies of 1GeV at the CERN TOF facility. It is very promising that this unique feature of the CERN neutron source offers the possibility of direct measurements of the *np*-bremsstrahlung as well as of meson production. These experiments are challenging and are therefore envisaged as second phase measurements. The key parameters of these experiments are:

Proposed samples: H_2

Sample position: at the 230m measurement station.

Range of energies: 100 MeV to about 1GeV with emphasis on energies beyon the pion threshold

Scheduled start: 2002

In the beginning phase simulations will be performed to clarify the achievable accuracy at a given energy resolution. This can be followed by a detailed design of the detector structure. Particular attention will be focussed on the option of measuring the analysing power in *np*-bremsstrahlung experiments. In the beginning phase only preparatory works are planned within the collaboration.

6 – THE FIRST CROSS SECTION MEASUREMENTS.

6.A. – ASTROPHYSICS RELATED MEASUREMENTS.

In the first year of operation, the Astrophysics measurements of neutron capture cross sections at the CERN TOF facility will concentrate on a number of *tests* in order to verify the computer simulations of different experiments, to understand the backgrounds, and to master the data acquisition techniques as well as on *measurements* of resonance-dominated cross sections of stable light nuclei, which are important for the interpretation of isotopic anomalies in meteoritic material. All these experiments require a narrow beam with a diameter of 30 or less.

6.A.1. – BACKGROUND STUDIES AND DETECTOR TESTS.

These studies are of mutual interest for other groups as well and can, therefore, be carried out in close collaboration with Geel, Saclay, and Grenoble. The following measurements are planned for the period from May to July:

- **Conventional detectors** (C_6D_6 liquid scintillator and Moxon-Rae type) have to be tested with respect to sensitivity for scattered neutrons and for beam-induced backgrounds. A series of TOF measurements on different ^{197}Au samples with masses between 100 mg and 1 mg is proposed to investigate the achievable signal/background ratio and the count rate problem. These runs can be performed with rates between 10^3 and 10^6 true counts/day. Given the unavoidable backgrounds, the measurements have to be performed in a (sample in)/(sample out) mode using a low mass sample changer and will require acquisition times between 1 and 3 days, accumulating to a total duration of 2 weeks. The tests with gold samples have to be complemented by measurements of (n,γ) resonances in ^{27}Al and ^{19}F with different Γ_γ/Γ_n ratios. While the respective resonance

areas yield detailed information on the prompt sensitivity for scattered neutrons, the deep cross section minima between resonances indicate the general background level and the occurrence of delayed components. Since the small cross sections between resonances require longer runs, an additional period of 2 weeks is required for this part.

- **The test of a BaF_2 array** covering about 1π solid angle is planned for comparison with detailed simulations of (n,γ) experiments with this detector. The simulations will be carried out with the GEANT and FLUKA software, using a true model of the detector geometry and assuming different scintillator materials and different granularities. These simulations and the complementary measurements with the BaF_2 setup will subsequently be used for developing an improved 4π detector array for neutron capture studies by the end of 2000.

6.A.2. – CROSS SECTION MEASUREMENTS.

^{103}Rh : We propose to start in the fall of 2000 with a first TOF measurement on ^{103}Rh by using conventional techniques. This case has the following advantages:

(i) In the keV region, this (n,γ) cross section is well established by a number of independent data sets, where the results can be checked (and normalized if necessary).

(ii) The resonance region is poorly known. Therefore, the proposed experiment would provide new information at lower energies. Since Rh is a mono-isotopic metal, the preparation and definition of suited samples is straightforward. The required measuring time will, therefore, not exceed a period of one week.

$^{24\text{-}26}$Mg: Given the experience from the tests and from the ^{103}Rh experiment, the first actual measurement of immediate astrophysical interest is proposed for the stable isotopes of magnesium. This experiment is difficult because of the small cross sections of these nuclei, for which only rudimentary experimental data exist so far. The differential cross sections are dominated by few resonances, and the respective stellar averages are as small as a few millibarns. These cases could not be studied so far because of the limited fluxes at traditional neutron sources. The stellar (n,γ) rates of the Mg isotopes are important to analyze the isotopic composition of presolar inclusions in meteorites. Since a variety of such inclusions were found to represent pure s-process material, the isotopic pattern of s-process magnesium

provides insight into the role of the $^{22}Ne(\alpha,n)^{25}Mg$ and $^{21}Ne(\alpha,n)^{24}Mg$ reactions as neutron sources for the s-process. These measurements are estimated to last for about 3 weeks.

^{151}Sm : By summer 1999, a sample for neutron capture studies of about 300 mg ^{151}Sm is being prepared by a joint Oak Ridge/Karlsruhe effort. If the total activity of about $2.5x10^{11}$ Bq (7 Ci) can be accepted, the sample could also be used for a neutron capture measurement at the CERN TOF facility. This project would provide an important extension of the results from a planned experiment with the 4π BaF_2 detector at Karlsruhe in the energy range between 5 and 220 keV. The measurement – which is equally interesting for waste transmutation – would require beam time for about 10 days.

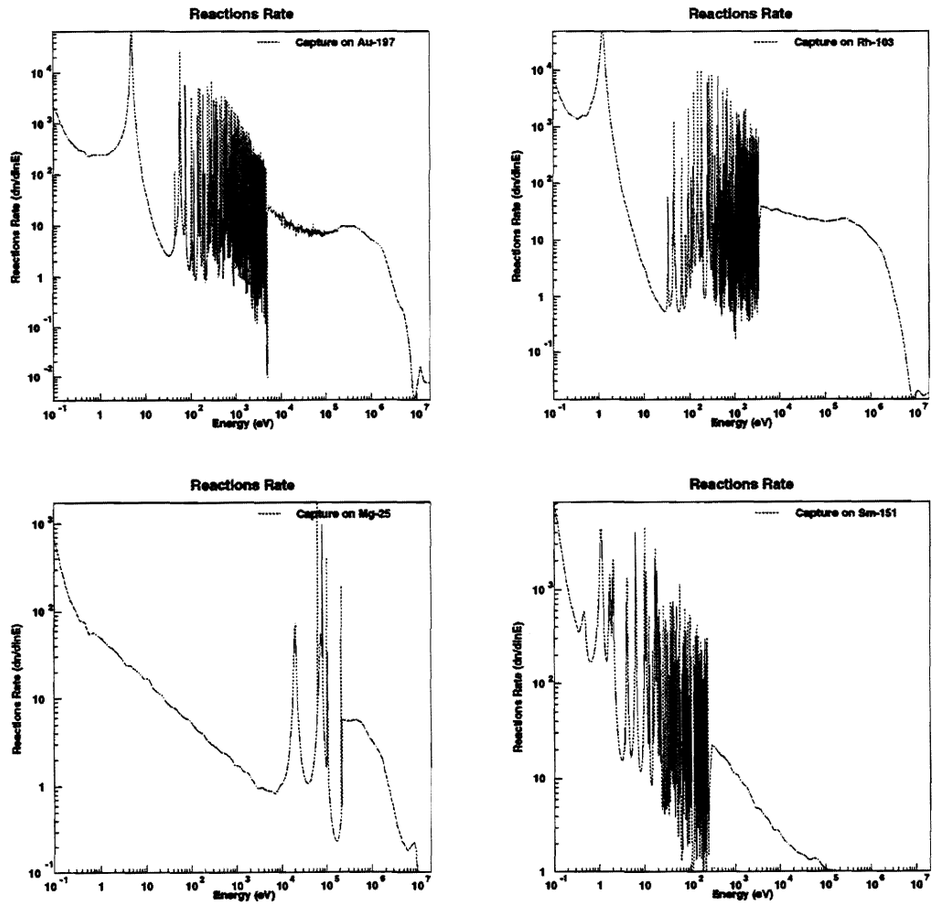

Figure 6.1. The expected capture rates per day and energy bin of $2x10^{-4}xE_n$ for a gamma detector efficiency of 10%.

6.B. – CROSS SECTION MEASUREMENTS RELATED TO ADS.

In the first stage of operation of the CERN-PS TOF Facility, cross section measurements should concentrate on the most important isotopes relevant to the Thorium fuel cycle and transmutation of long-lived radioactive waste from NPPs (Nuclear Power Plants). The measurements will rely on the use of standard techniques.

^{197}Au and ^{Nat}Ag: we propose to start in the fall of 2000 with a first **(n,γ)** measurements on the well known ^{197}Au and ^{Nat}Ag as a check of the reliability of the techniques used. The advantage of these elements is the well known cross sections in the resonance region. We have identified in the evaluated data files some 260 and 950 resolved resonances between 1 eV and 10 KeV for ^{197}Au and ^{Nat}Ag respectively;

^{238}U and ^{235}U: **(n,γ)** and **(n,f)** measurements for these two nuclides are necessary for normalization purposes. The resonace region is well known for both isotopes: for instance we have identified some 2000 resolved resonances up to 20 KeV for ^{238}U and some 3500 for ^{235}U up to 3.5 KeV. There is, however, some incentive to extend the resolved resonance region of ^{235}U beyond this value.

^{232}Th and ^{233}U: They are the base of the Thorium fuel cycle. The requirement for the nuclear data accuracy for these two nuclides are most stringent and include all types of neutron interactions.

(i) **(n,γ)** cross sections for ^{232}Th are badly known in the resonance region: only 300 resonance between 5 eV and 3.5 keV are resolved. We estimate some 40% discrepancy in the experimental data and 30% for the evaluated data.

(ii) For ^{233}U, **(n,γ)** measurements are badly needed: the resolved resonance region extends only to a few 100 eV and there is no direct experimental data. In the energy region between 0.1 and 1.0 MeV, the data are derived from α-measurements. Comparison between evaluated data show a considerable discrepancy between 100 eV and 10 keV, and above 1 MeV.

(iii) **(n,f)** measurements for ^{233}U are also required since the situation is similar to that of capture. The resolved resonance region has to be extended from 100 eV to a few keV. The comparison between experimental data shows some 5–10% discrepancy in the energy region between 0.1 and 10 MeV, where a target accuracy of about 1% is required for the EA. Furthermore, above 10 MeV, only one measurement exists. When comparing the evaluated data files, the discrepancy rises to ~ 10%.

(v) **(n,f)** measurements with ^{232}Th are required in the energy range between 6 and 20 MeV. Enough measured data exist below 6 MeV, however, above 6 MeV the discrepancy rises to values close to 15–30%.

(vi) **(n,2n)** measurements on ^{232}Th and ^{233}U are needed to estimate the production of ^{231}Pa and ^{232}U, which are the main nuclides responsible for the long-term and short-term radiotoxicity of the Th-based fuel cycle respectively. In thecase of ^{232}Th, experimental data exist in some energy intervals but with 15–20% discrepancy, where a target accuracy of at least 5% is required. For ^{233}U, they are no experimental data available and upto 8 MeV the discrepancy between the different evaluations reaches a factor 5. Therfore, reference experimental data are very much needed.

(vii) **(n,n')** measurements on ^{232}Th and ^{233}U will be also carried out since this reaction is important in estimating the average neutron flux spectrum in the fuel. Target accuracies for this reaction are of the order of 5–10%. Seldom data exist for ^{232}Th even though it is the dominant reaction (together with elastic scattering) after a few keV (i.e. 4 barn at 1 MeV versus 0.3 barn for capture). This is also true for ^{233}U, where both inelastic and fission processes are dominant above a few 100 keV, 1 barn versus 3 barn respectively.

Concerning the transmutation of minor actinide waste, important cross sections to be measured are **(n,γ)** and **(n,f)** for ^{241}Am, ^{243}Am, ^{244}Cm. **(n,γ)** measurements for ^{242}Pu and ^{246}Cm are also very interesting since these two nuclides are responsible for the production of a major part of Am and Cm isotopes in the case of ^{242}Pu and higher actinides such as Bk and Cf in the case of ^{246}Cm. Moreover, these two nuclides present abnormally small capture cross sections compared to the other actinides.

Regarding the transmutation of long-lived fission products, the **(n,γ)** cross sections of ^{99}Tc and ^{93}Zr should be remeasured with emphasis on the unresolved region above 1 keV.

Equally important to ADS studies, are the **(n,xn)** cross section measurements for structural and coolant materials such as ^{56}Fe, ^{208}Pb and ^{209}Bi.

7 – REFERENCES.

[1.1] C. Rubbia et al., "A Realistic Plutonium Elimination Scheme with Fast Energy Amplifiers and Thorium-Plutonium Fuel", CERN/AT/95-53 (ET); C. Rubbia et al., "Fast Neutron Incineration in the Energy Amplifier as Alternative to Geological Storage: the Case of Spain", CERN/LHC/97-01 (EET).

[1.2] C. Rubbia, J-A. Rubio, S. Buono, F. Carminati, N. Fiétier, J. Galvez, C. Gelès, Y. Kadi, R. Klapisch, P. Mandrillon, J.P. Revol and Ch. Roche, "Conceptual Design of a fast Neutron Operated High Power Energy Amplifier", CERN/AT/95-44 (ET); see also C. Rubbia, "A High Gain Energy Amplifier Operated with fast Neutrons", AIP Conference Proceedings 346, International Conference on Accelerator-Driven Transmutation Technologies and Applications, Las Vegas, 1994.

[1.3] Carlo Rubbia, "Resonance Enhanced Neutron Captures for Element Activation and Waste Transmutation", CERN/LHC/97-04 (EET).

[1.4] Data from the following nuclear data libraries have been compared:
JENDL-3.2, OECD NEA Data bank (1996);
JEF-2.2, OECD NEA Data bank (1996);
ENDF/B-VI, OECD NEA Data bank (1996);
BROND-2, OECD NEA Data bank (1996).
See also J. Cobo et al, "Notes on the Study of the Most Reliable Neutron Cross Section Data", CERN/AT/95-035 (ET).

[1.5] C. Rubbia and J.A. Rubio, "A Tentative Programme Towards a Full Scale Energy Amplifier", CERN/LHC/96-11 (EET).

[1.6] For the thermal neutron capture cross section of ^{90}Sr, the Atomic data and Nuclear data Tables, Vol. 29, Number 2, Sept. 1983, give a capture cross section of 0.9 barns, while M.A. Lone et al, NIM A332 (1993) 232-238 find 9.7 ± 0.7mb. There is essentially no data at other energies.

[1.7] S. Andriamonje et al., TARC Proposal, "Experimental Study of the Phenomenology of Spallation Neutrons in a Large Lead Block", CERN/SPSLC 95-17, SPSLC/P291, 5th May, 1995.

H. Arnould et al., "Experimental Verification of Neutron Phenomenology in Lead and Transmutation by Adiabatic Resonance Crossing in Accelerator Driven Systems", submitted to Phys. Letters B.

[1.8] C. Rubbia et al.,"A high Resolution Spallation driven Facility at the CERN-PS to measure Neutron Cross Sections in the Intervall from 1 ev to 250 MeV", CERN/LHC/98-02 (EET), Geneva, May 30, 1998.

[1.9] C. Rubbia et al.,"A high Resolution Spallation driven Facility at the CERN-PS to measure Neutron Cross Sections in the Intervall from 1 ev to 250 MeV: *a relative Performance Assessment*", CERN/LHC/98-02 (EET)-Add. 1, Geneva, June 15, 1998.

[2.1] S. Andriamonje et al., "Feasibility Study of a Neutron TOF Facility at the CERN-PS, CERN/PS 98-065 (CA), Geneva, 5 November 1998.

[2.2] MAD and BeamOptics description of the TT2/TT10 transfer lines. Part I: optics without emittance exchange insertion, G. Arduini, M. Giovannozzi, K. Hanke, J.Y.(Hémery, M. Martini, CERN/PS/CA/Note 98-14 (1998).

[2.3] C. Rubbia, "Relation between time and kinetic energy in a constant lethargy system", CERN/AT/ET/Internal Note 95-010, 2nd May, 1995.

[2.4] A.A. Bergman, A.I. Isakov, I.D. Murin, F.L. Shapiro, I.V. Chtranikh and M.V. Kazarnovsky, "Lead Slowing-Down Neutron Spectrometry", in Proc. 1st Inst. Conf Peaceful Uses At. Energy", vol. 4, 1955, p. 135.

[3.1] F. Kaeppeler, "Neutron Reactions in Astrophysics : Status, Further Needs and Technological Applications", in Proc. of the CERN-EC-GEDEON-OECD/NEA Workshop, 21-22 September 1998, CERN, Geneva.

[3.2] R. Gallino, M. Busso, and M. Lugaro, in Astrophysical Implications of the Laboratory Study of Presolar Material, edited by T. Bernatowitz and E. Zinner (AIP, New York, 1997), p. 115.

[3.3] G. Wallerstein et al., Rev. Mod. Phys. 69, 995 (1997).

[3.4] S. Amari and E. Zinner, Nucl. Phys. A 621, 99c (1997).

[3.5] F. Kaeppeler, Contribution to the Joint CERN-EC-GEDEON-OECD/NEA Workshop, CERN, 21-22 September 1998.

[3.6] M.B. Auferheide et al., Phys. Rev. **C53**, 3139 (1996) and references therein

[3.7] H. Leeb for the team from TU of Wien, Contribution to the Joint CERN-EC-GEDEON-OECD/NEA Workshop, CERN, 21-22 September 1998.

[3.8] "The NEA High Priority Nuclear Data Request List", Status in May 1998, OECD-NEA Nuclear Science Committee.

[3.9] JENDL-3.2, OECD NEA Data bank (1996); JEF-2.2, OECD NEA Data bank(1996); ENDF/B-VI, OECD NEA Data bank (1996); BROND-2, OECD NEA Data bank (1996). See also J. Cobo et al, "Notes on the Study of the Most Reliable Neutron Cross Section Data", CERN/AT/95-035 (ET).

[3.10] C. Rubbia, S. Andriamonje, D. Bouvet-Bensimon, S. Buono, R. Cappi, P. Cennini, C. Gelès, I. Goulas, Y. Kadi, P. Pavlopoulos, J.P. Revol, A. Tzima, V. Vlachoudis , "A high resolution Spallation driven Facility at the CERN-PS to measure neutron cross sections in the interval from 1 eV to 250 MeV", CERN/LHC/98-02 (EET)

[3.11] A. Arnould et al., "Experimental Verification of Neutron Phenomenology in Lead and Transmutation by Adiabatic Resonance Crossing in Accelerator Driven Systems", submitted to Phys. Letters. B

[3.12] S. F. Mughabghab, M. Divadeenam and N.E. Holden, Neutron Cross sections V. 1 Part A, Zz 1-60 (Academic Press Inc., 1981); S. F. Mughabghab, Neutron Cross sections V. 1 Part B, Zz 61-100 (Academic Press Inc., 1984)

[3.13] A. Mengoni et al, Phys. Rev. C 52, R2334 (1995).

[3.14] G.A. Miller, B.M.K. Nefkens and I. Slaus, Phys. Rep. 194 (1990) 1.

[3.15] C.R. Howell et al., Phys. Lett. B 444 (1998) 252.

[3.16] W. Glöckle, H. Witala, D. Hüber. J. Golak, Phys. Rep. 274 (1996) 107.

[3.17] T. Goldman et al., Few Body Systems 1992.

[3.18] V.R. Brown and J. Franklin, Phys. Rev. C 8 (1973) 1706; G.E. Bohannon, L. Heller and R.H. Thompson, Phys. Rev. C 16 (1977) 284.

[3.19] K. Michaelian *et al.*, Phys. Rev. D 41 (1990) 2689; P. Kitching *et al.*, Phys. Rev. Lett. 57 (1986) 2363; Nucl. Phys. A 463 (1987) 87.

[3.20] H.W. Fearing, nucl-th/9710061

[3.21] E. Grosse et al., Europhys. Lett. **2** (1986) 9; J. Stevenson et al., Phys. Rev. Lett. 57 (1986) 555; N. Alamanos et al., Phys. Lett. B 173 (1986) 392; K. Kwato et al., Phys. Lett. B 175 (1986) 125.

[3.22] M. Schäfer *et al.*, Z. Phys. A 339 (1991) 391; R. Heuer et al., Z. Phys. A 330 (1988) 315.

[3.23] K. Niita et al., Nucl. Phys. A 495 (1989) 91c.

[3.24] K. Niita, W. Cassing and U. Mosel, Nucl. Phys. A 504 (1989) 391.

[3.25] A. Bondar *et al.*, Phys. Lett. B 356 (1995) 8; H.O. Meyer *et al.*, Phys. Rev. Lett. 65 (1990) 2846; Nucl. Phys. A 539 (1992) 633.

[3.26] T. Ueda, Phys. Rev. Lett. 66 (1991) 297; Phys. Lett. B 292 (1992) 228; S.A. Rakityansky *et al.*, Phys. Rev. C 53 (1996) 2043; A.M. Green, J.A. Niskanen and S. Wycech, Phys. Lett. B 394 (1996) 253.

[3.27] H. Calen *et al.*, Phys. Rev. Lett. 79 (1997) 2642.

[3.28] H. Feshbach, Theoretical Nuclear Physics, Nuclear Reactions (New York, Wiley, 1992).

[3.29] L. Ray, G.W. Hoffmann and W.R. Coker, Phys. Rep. 212 (1992) 223.

[3.30] R.L. Varner, Phys. Rep. 201 (1991) 57.

[3.31] V.M. Strutinsky, Nucl. Phys. A95 (1967) 420

[3.32] P. Moller and J.R. Nix, Proc. Int. Conf. on physics and chemistry of fission, Rochester, 1973 (IAEA, Vienna, 1974) p. 103

[3.33] A. Bohr, Proc. Int. Conf. on peaceful uses of atomic energy, Geneva, 1955 (United Nations, New York, 1956) vol. 2 p. 220

[3.34] Blons et al, Nucl. Phys. A414 (1984) 1

[3.35] F. Osterfeld, Rev. Mod. Phys. 64, 491 (1992) and references therein

[3.36] C.D. Goodmann, in Intern. Symp. on "New facet of spin giant resonances in nuclei", SGR97, Eds. H. Sakai, H. Okurama and T. Wakasa, Tokyo, World Scientific p. 14 (1997) and references therein

[3.37] B.H. Wildenthal et al., Phys. Rev. C28, 1343 (1983)

[3.38] W.T. Chou et al., Phys. Rev. C47, 163 (1993)

[3.39] S.E. Koonin et al., Phys. Rev. 278 1, (1997)

[3.40] G. Martinez-Pinedo et al., Phys. Rev. C53 R2602 (1996)

[3.41] B.D. Anderson et al., Phys. Rev. C54, 602 (1996)

[3.42] T. Wakasa et al., Phys. Lett. B426, 257 (1998)

[3.43] W. P. Alford et al., Phys. Rev. C48, 2818 (1993)

[3.44] A. Richert in Lecture Notes on Physics, Proc. of the Int. Summer School, La Rabida (Springer, New York, 1995) and references therein

[3.45] K. Ikeda et al., Phys. Rev. Lett. 3 271 (1973)

[3.46] O.P. Sushkov and V.V. Flambaum, JETP Lett. 32 (1980) 352.

[3.47] V.E. Bunakov and V.P. Gudkov, Nucl. Phys. A401 (1983) 93

[3.48] S.K. Lamoreaux and R., Golub Phys. Rev. D 50 (1994) 5632.

[3.49] V.R Skoy, Phys. Rev. D 53 (1996) 4070.

[3.50] V.R Skoy et al., Nucl. Instr. Meth. A 402 (1998) 323.

[3.51] V.N.Bunakov and I.S.Novikov, Phys. Lett. B 429 (1998) 7.

[3.52] T.E. Chupp et al., Phys. Rev. C 45 (1992) 915.

[3.53] T. Maekawa et al, Nucl. Instrum. Methods A 366 (1995) 115.

[3.54] .J. Szymanski et al., Phys. Rev. C 53 (1996) 2576.

[3.55] V.R Skoy et al., Phys. Rev. C 53 (1996) 2573.

[3.56] M. Gatzke et al., Phys. Rev. Lett. 70 (1993) 690.

[3.57] E. Fermi and L. Marshall, Phys. Rev. 72 (1947) 1139.

[3.58] W.W. Havens, Jr., L.J. Rainwater and I.I. Rabi, Phys. Rev. 82 (1951) 345.

[3.59] M. Hamermesh, G.R. Ringo and A. Wattenberg, Phys. Rev. 85 (1952) 483.

[3.60] D.J. Hughes et al., Phys. Rev. 90 (1953) 497.

[3.61] M.F. Crouch, V.E. Krohn and G.R. Ringo, Phys. Rev. 102 (1956) 1321.

[3.62] E. Melkonian, B.M. Rustad and W.W. Havens, Jr., Phys. Rev. 114 (1959) 1571.

[3.63] V.E. Krohn and R.G. Ringo, Phys. Rev. 148 (1966) 1303.

[3.64] V.E. Krohn and R.G. Ringo, Phys. Rev. D 8 (1973) 1305.

[3.65] Yu.A. Alexandrov et al., Sov. J. Nucl. Phys. 20 (1975) 623.

[3.66] L. Koester, W. Nistler and W. Waschkowski, Phys. Rev. Lett. 36 (1976) 1021.

[3.67] Yu.A. Alexandrov et al., Sov. J. Nucl. Phys. 44 (1986) 900.

[3.68] L. Koester, W. Waschkowski and A. Klüver, Physica B 137 (1986) 282.

[3.69] S. Kopecky et al., Phys. Rev. Lett. 74 (1995) 2427.

[3.70] L. Koester et al., Phys. Rev. C 51 (1995) 3363.

[3.71] S. Kopecky et al., Phys. Rev. C 56 (1997) 2229.

[3.72] R.M. Thaler, Phys. Rev. 114 (1959) 827; G. Breit and M.L. Rustgi, Phys. Rev. 114 (1959) 830.

[3.73] J. Schmiedmayer *et al.*, Phys. Rev. Lett. 66 (1991) 1015.

[3.74] Y.A. Aleksandrov, Sov. J. Nucl. Phys. 38 (1983) 660; L. Koester, W. Waschkowski and A. Klüver, Physica 137 B (1986) 282.

[3.75] Y.A. Aleksandrov *et al.*, JETP Lett. 4 (1966) 134; G.V. Anikin and I.I.Kutukhov, Sov. J. Nucl. Phys. 14 (1972) 152;Y.A. Aleksandrov, Sov. J. Nucl. Phys. 37 (1983) 49.

[3.76] S. F. Mughabghab, M. Divadeenam and N.E. Holden, Neutron Cross sections V. 1 Part A, Zz 1-60 (Academic Press Inc., 1981); S. F. Mughabghab, Neutron Cross sections V. 1 Part B, Zz 61-100 (Academic Press Inc., 1984)

[3.77] M. B. Chadwick et al, Rad. Protection Dos., Vol 70 (1997), p.1

[4.1] R.Meunier, "Etude préliminaire à propos d'une éventuellement participation du CSNSM au projet TOF", Orsay, 15 January 1999.

[4.2] E. Henry, "Neutron Cross Sections for ATW Applications and Basic Science", in Proc. of the 1st TOF Colloboration Meeting, CERN, 7-8 January 1999.

[4.3] W. Furman, in Proc. of the 1st TOF Colloboration Meeting, CERN, 7-8 January 1999.

[4.4] J. Magill, private communication.

[4.5] N. Moncoffre, in Proc of the 1st TOF Colloboration Meeting, CERN, 7-8 January 1999.

[5.1] H. Arnould et al., "Experimental Verification of Neutron Phenomenology in Lead and Transmutation by Adiabatic Resonance Crossing in Accelerator Driven Systems", submitted to Phys. Letters. B

[5.2] Bergoz Instrumentation, 01170, Crozet, France. (address Web: www.bergoz.com

[5.3] J.-P.Revol et al., Baem transformer performance and calibration for the TARC Experiment, CERN/ET/Internal Note in preparation

[5.4] D. Brozzi, M. Embid and J.-P.Revol, Analysis of Aluminium foil activation to provide absolute calibration of proton intensities in the TARC Experiment, CERN/ET/Internal Note 97-25

[5.5] Neutron-Driven Nuclear Transmutation by Adiabatic Resonance Crossing, Final Report to the European Community

[5.6] F. Casagrande, P. Cennini, X. Li, "The Argon Gas Detectors for the Fission Measurement in the FEAT", NIM-A 372 (1996) 307-310

[5.7] C. Stephan in "Experimental Techniques in Nuclear Physics", edited by Dorin N. Poenaru and Walter Greiner, Walter de Gruyter, !997

[5.8] N. W. Hill, "Optimization of Nanosecond Fission Ion Chamber for Reactor Physics Application", IEEE Trans. Nuclear Science, Vol.NS-22, 1975

[5.9] F. Sauli, "Drift and Diffusion of electrons in Gases: a Compilation", CERN/EP 84-88

[5.10] W. J. Leonhardt et al., "Stress Rupture Considerations in the Design of Large Aperture Low Mass Composite Vacuum Windows" BNL-1998

[5.11] C. Rubbia et al., "A High Resolution Spallation Driven Facility at the CERN-PS to Measure Neutron Cross-sections in the Interval from 1 eV to 250 MeV" CERN/LHC/98-02 (EET)

[5.12] C. Rubbia et al., CERN/LHC/98-02 - Add. 1 (EET)

[5.13]H.-H. Knitter and C. Budtz-Jørgensen. Neutron-Induced Fission Cross-Section of ^{243}Am in the Energy Range from 1 eV to 10 MeV. NSE 99 (1988), p. 1-12

[5.14] M. Florek, V. Yu. Konovalov, Yu. S. Zamyatnin, Sh. S. Zeinalov. Neutron Induced Fission Cross-Sections of ^{243}Am in the Energy Region from 0.8 to 50 eV. In Proc. of XIV International Conference of Nuclear Fission, Obninsk, Russia, October 1998. (to be published)

[5.15] G.F. Auchampaugh et al. NP/A 171 (1971), p.31

[5.16] D.W. Bergen et al. LA-4420 (1970), p. 123

[5.17] M.C.Moxon and E.R.Rae, *Nucl. Instr. and Meth.* 24 (1963) 445

[5.18] F. Corvi et al.,Nucl.Instr.Meth.in Phys. Res.A265(1988)475; Nucl.Sci.Eng. 107 (1991) 272

[5.19] S.Jaag and F.Käppeler, *Phys. Rev*, C53 (1996) 2474 - 2485

[5.20] K.Wisshak e.a., *Nucl. Instr. and Meth.* A292 (1990) 595

[5.21] G.V. Muradian et al.,Nucl. Sci. Eng. 90 (1985) 60

[5.22] NIM v.A313(1992) p.256

[5.23] D. Habs e.a., Progress in Particle and Nuclear Physics, 38 (1996) 1-13

[5.24] G.Barouch et al, NIM-A 423 (99) 32

[5.25] A.Giorni, A CeF3 gamma detector, talk given at the First TOF Collaboration Meeting, CERN, 7-8 January 1999.

[5.26] V.Chepel et al, Nucl. Instr. and Meth. A367 (1995) 58; Nucl. Instr. and Meth. A392 (1997) 427.

[5.27] T.Doke and K.Masuda, Nucl. Instr. and Meth., A420 (1999) 62.

[5.28] E.Aprile e.a., *Nucl. Phys.* B32 (1993) 279.

[5.29] J.Seguinot et al, NIM in Physics Research, 297 (1990) 133-147

[5.30] H. Vonach et al., Phys. Rev. **C50**, 1952 (1994)

[5.31] Ph. Dessagne, private communication

[5.32] G. Guillaume et al., Nucl. Instr. and Meth. **A277**, 458 (1989)

[5.33] M. Moszinski et al., Nucl. Instr. and Meth. **A307**, 97 (1991)

[5.34] M. Moszinski et al., Nucl. Instr. and Meth. **A317,** 262 (1992)

[5.35] M. Moszinski et al., Nucl. Instr. and Meth. **A350,** 226 (1994)

[5.36] S. Mouatassim et al., Nucl. Instr. and Meth. **A359**, 530 (1995)